12-1991

The Sloan Sag: A Mid-Miocene Volcanotectonic Depression, North-Central McCullough Mountains, Southern Nevada

Hayden L. Bridwell
University of Nevada, Las Vegas

THE SLOAN SAG: A MID-MIOCENE VOLCANOTECTONIC DEPRESSION, NORTH-CENTRAL McCULLOUGH MOUNTAINS, SOUTHERN NEVADA

by

Hayden L. Bridwell

A thesis submitted in partial fulfillment
of the requirements for the degree of

Master of Science

in

Geology

Department of Geoscience
University of Nevada, Las Vegas
December, 1991

ACKNOWLEDGEMENTS

I would like to thank Dr. Gene Smith for keeping me enthused about this project. I feel as though he has taught me more about geology in the past two years than I have learned in all of my previous geologic studies combined.

Tracey Cascadden, Dan Feurebach and Terry Naumann also contributed substantially to this work. The countless converstions we shared added greatly to my understanding of volcanology and the dynamic geology of the Basin-and-Range province.

With great emotion, I thank my son Ian for helping me keep my perspective over the past two years.

ABSTRACT

In the Hidden Valley area of the north-central McCullough Mountains, southern Nevada, mid-Miocene andesite and dacite domes, flows and pyroclastic units (the Sloan volcanics) partially fill a sag in the underlying Hidden Valley volcanics. The 13.5 km diameter sag formed during and/or after the eruption of the Sloan volcanics. Sagging was accommodated by a combination of movement on the McCullough Wash fault system, and subsidence into evacuated chambers.

Major, trace and rare-earth element geochemistry suggests that the rocks of the Sloan volcanics belong to four groups, each of which were produced by partial melting of chemically distinct sources. With the exception of the Center Mountain dome complex, magmas rose rapidly without significant crystal fractionation or crustal contamination.

The Mount Hanna andesite member of the Sloan volcanics erupted as a hot, dry aphyric lava by a mechanism of fire-fountaining from a depth of up to 25 km, precluding a Plinian-style ash-flow event. Eruptions of felsic-to-intermediate lavas by a lava-fountaining event have been described in other areas, but the Mount Hanna andesite represents the first documentation of such an eruption in the southern Basin-and-Range.

CONTENTS

FIGURES

TABLES

INTRODUCTION

Location and Geography

Hidden Valley is in the north-central McCullough Mountains, Clark County, southern Nevada (Fig. 1). The thesis area covers 240 km^2 and is included on the Hidden Valley, Sloan, Sloan NE and Sloan SE 7.5 minute quadrangle maps. Dirt roads provide access to the western and central parts of the thesis area, however the eastern part must be approached by foot. Elevations in the thesis area range from 790 to 1292 m.

Previous Work

Because of its lack of economic mineral resources, little detailed geological mapping has been done in the McCullough Mountains. Hewett (1956) mapped the McCullough Mountains as part of the Ivanpah Quadrangle, but did not subdivide the Tertiary section. Longwell et al. (1965) did reconnaissance mapping for mineral resources in Clark County, but also did not differentiate the Tertiary volcanic rocks in the McCullough Mountains. Anderson et al. (1985) and DeWitt et al. (1989) mapped the South McCullough Wilderness Study Area in the southern McCullough Mountains for a study requested by the U.S. Bureau of Land Management, the U.S. Geological Survey, and the U.S. Bureau of Mines. Mapping for the wilderness study area, however, did not extend to the north into Hidden Valley.

Two masters theses were completed in the north-central McCullough

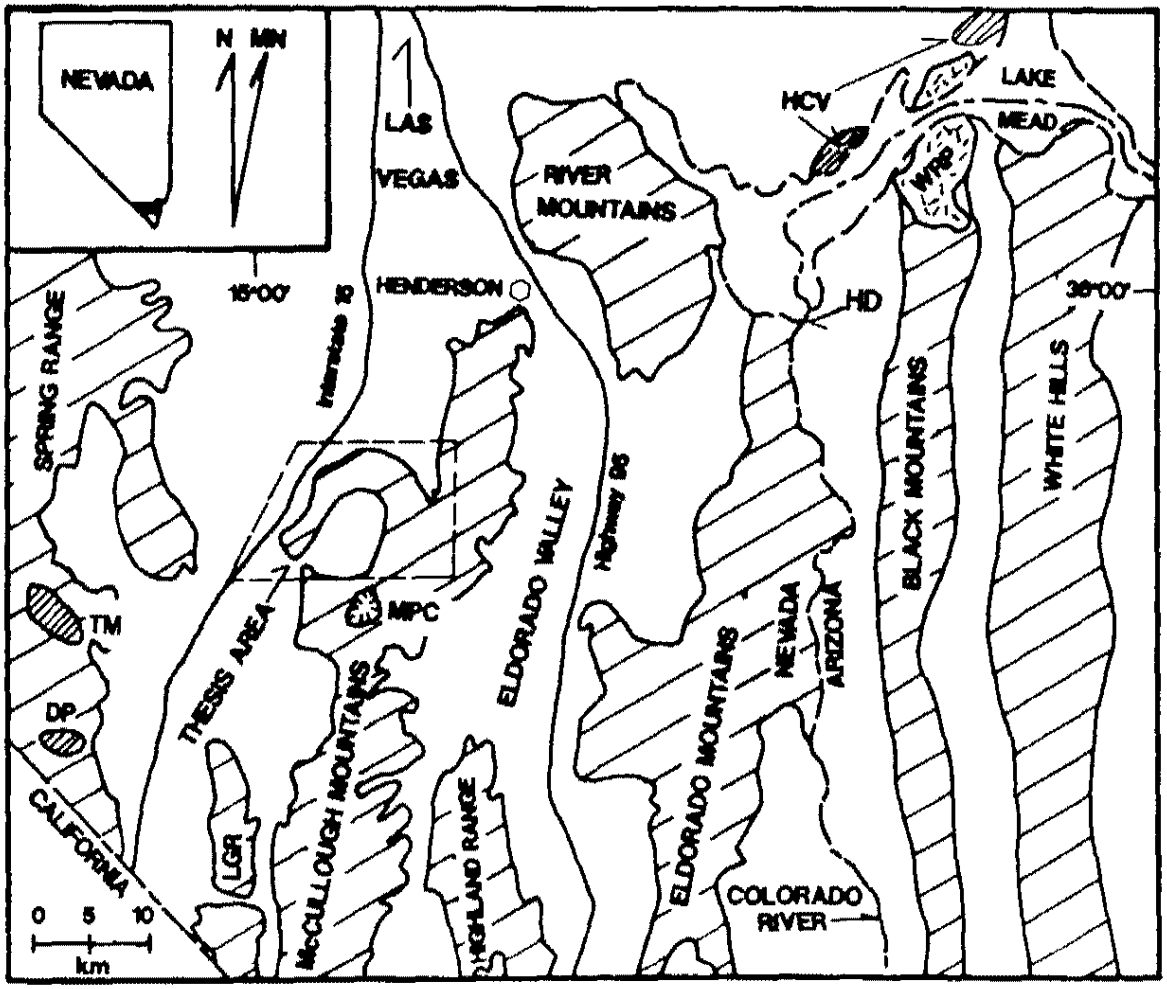

Figure 1: Location map of the thesis area and selected Tertiary igneous centers in the Las Vegas-Lake Mead vicinity. **MPC** = McCullough Pass caldera; **DP** = Devil Peak; **TM** = Table Mountain; **WRP** = Wilson Ridge pluton; **HCV** = Hamblin Cleopatra volcano; **HD** = Hoover Dam sag-graben caldera; **LGR** = Lucy Gray Range.

Mountains. Kohl (1978) studied the nature and source of carnotite in caliche deposits in Hidden Valley. Schmidt (1987) mapped and described a small (< 3 km diameter) caldera about 3 km southeast of Hidden Valley.

Purpose of Study

The Hidden Valley area contains andesite and dacite domes and flows, dacite and rhyolite pyroclastic units, and a late-stage hypabyssal dacite stock that partially fill a sag developed in the underlying basalt. This volcanic section is herein named the Sloan volcanics. In some areas, the contact between the Sloan volcanics and the underlying basalt is conformable, while in others it is not. Questions concerning the Sloan volcanics addressed in this thesis are: 1) Do the Sloan volcanics fill a volcanotectonic depression or caldera, or simply represent a dome field situated on the flank of an older stratocone? 2) How did the sag, now filled with the Sloan volcanics, form? 3) What is the petrogenesis of the andesites and dacites of the Sloan volcanics? 4) What is the internal stratigraphy of the Sloan volcanic section? 5) What is the absolute age of the Sloan volcanic section?

The purpose of this thesis is to present concise answers to the above questions.

I will demonstrate, using stratigraphic, lithologic and geochemical evidence, that the Sloan volcanics formed during volcanotectonic sagging caused by their eruption. I also suggest that the Mount Hanna andesite member of the Sloan volcanics erupted by a mechanism of lava fountaining, and may be the hot, dry analog of an ash-flow tuff.

Geologic Setting

The McCullough Mountains are in the southern Basin-and-Range province on the western border of the Colorado River extensional corridor. The north-south trending range extends from the New York Mountains in California to the city of Henderson in the Las Vegas Valley (Fig. 1).

The southern part of the McCullough Mountains consists of Precambrian igneous and metamorphic rocks (Longwell et al., 1965; DeWitt et al., 1989). The northern part consists of Precambrian basement overlain by a Tertiary volcanic section. Excellent exposure of the northern section is provided in a steep eastern escarpment.

In addition to the Sloan volcanic center, other volcanoes within 30 km of the thesis area include: 1) the McCullough Pass caldera approximately 3 km south of Hidden Valley (Schmidt, 1987); 2) Devil Peak, an intrusive rhyolite plug in the southern Spring Range (Walker et al., 1981); 3) Table Mountain, a dacitic (unpublished chemical data base, E.I Smith, University of Nevada, Las Vegas) eruptive center about 10 km north of Devil Peak; 4) The River Mountains stratovolcano complex (Fig. 1).

Structural Geology and Tectonics

The McCullough Mountains are a relatively stable block compared to ranges to the north and east. During Tertiary extension, the range was extended only about 20% (Weber and Smith, 1987). The west-dipping McCullough Wash normal fault is the only major internal structure in the McCullough Mountains.

This fault has a throw of at least 600 m, placing Precambrian basement against the Hidden Valley volcanic section in the central part of the range. Displacement decreases to the north to less than 50 m (Schmidt, 1987; Anderson et al., 1985). The Spring Range, to the west of the McCullough Mountains, displays minor Tertiary extension (Carr, 1983; Wernicke et al., 1988). The Eldorado Mountains, to the east of the McCullough Mountains, are highly faulted with regional dips varying from 30° east to vertical, and were extended over 100% (Anderson, 1971).

A model proposed by Weber and Smith (1987) suggests that the River and McCullough Mountains lie in the upper plate of the west-dipping Saddle Island detachment system. According to their model, the left-lateral Hamblin Bay and Bitter Spring Valley faults are transfer structures between the Saddle Island and Eldorado Valley normal faults (Fig. 2). The detachment system is at a shallow depth beneath the Eldorado Mountains resulting in a high degree of extension. The McCullough Mountains and Spring Range represent blocks overlying the detachment at a greater depth, and were transported in the upper plate without significant internal deformation (Fig. 2).

A more recent model by Smith et al. (1991) suggests that the Eldorado Valley fault may be a steep westward-dipping normal fault. Isostatic rebound caused footwall rotation resulting in flattening of the fault. The Eldorado Mountains experienced high degrees of extension in the footwall block, while the McCullough Mountains and the Spring Range remained relatively undisturbed in the hanging wall. Smith et al. (1991) also suggest that these types of deeply

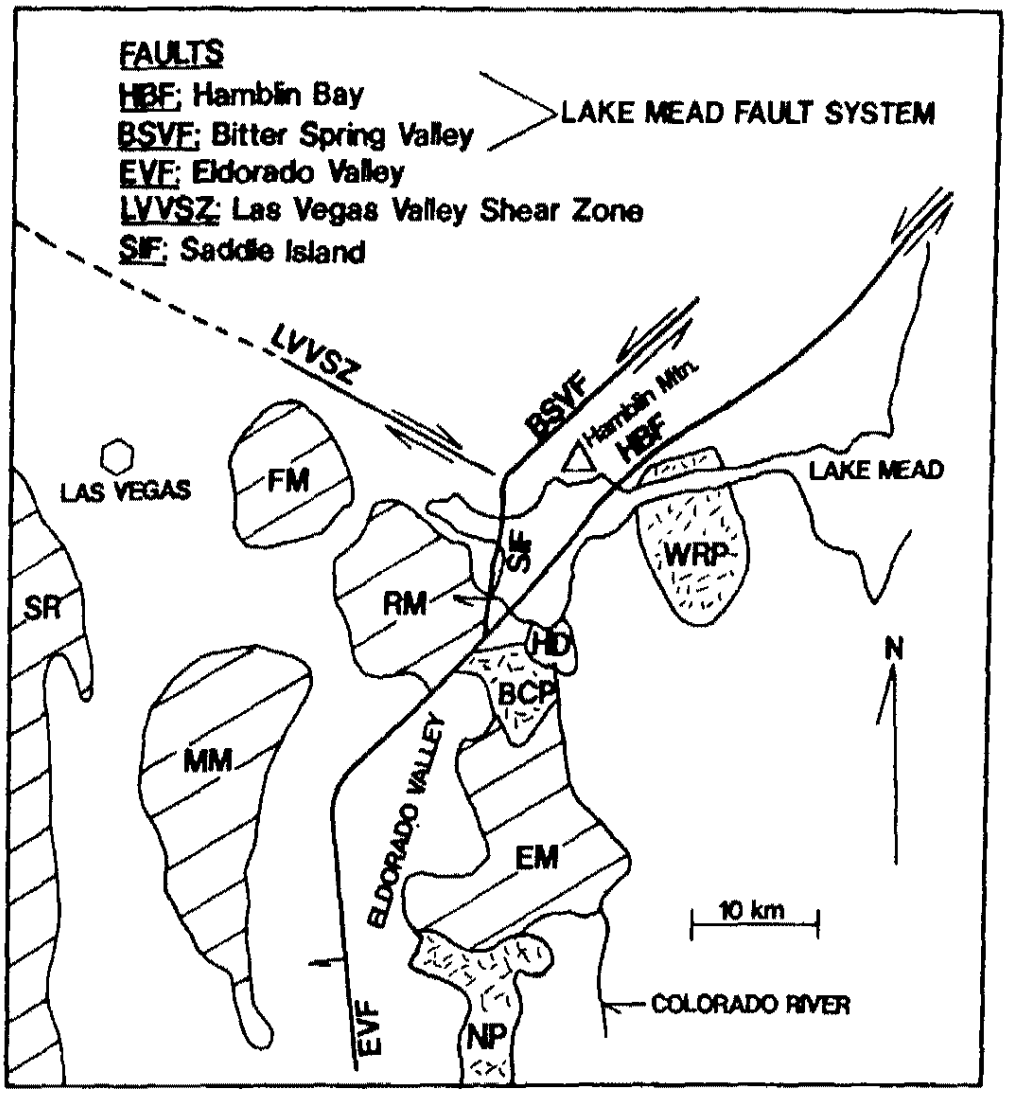

ROCK UNITS
FM: Frenchman Mountain
RM: River Mountains
MM: McCullough Mountains
EM: Eldorado Mountains
SR: Spring Range
HD: Hoover Dam Volcanics
NP: Nelson Pluton
BCP: Boulder City Pluton
WRP: Wilson Ridge Pluton

Figure 2: Location of major faults in the Lake Mead-Las Vegas area (modified from Weber & Smith, 1987).

penetrating high angle faults may provide conduits for magma migration. A model proposed by Duebendorfer and Wallin (1991) suggests that Frenchman Mountain and the River Mountains lie in a block that is bounded to the north by the Las Vegas Valley shear zone and to the southeast by the Saddle Island detachment system. The location of the Lake Mead fault system is not well constrained west of Hamblin Mountain. Bohannon (1979) suggested that this fault system may project through Las Vegas Wash, placing the River Mountains and Frenchman Mountain in separate structural blocks (Fig. 2). Sediments of the post 13.5 Ma Horse Spring Formation, however, crop out in the Rainbow Gardens area of Frenchman Mountain and are interfingered with volcanic rocks of the River Mountains. These sediments are not disrupted across Las Vegas Wash, suggesting that no post 13.5 Ma movement on the Lake Mead fault system occurred between the River Mountain and Frenchman Mountain blocks. If the Weber and Smith (1987) model is correct, the Saddle Island detachment is part of the Lake Mead-Eldorado Valley detachment system, thus placing the McCullough Mountains in the same structural block as Frenchman Mountain and the River Mountains (Fig. 2). No major strike-slip fault system has been documented between the McCullough and River Mountains (Anderson, 1977; Weber and Smith, 1987).

According to Duebendorfer and Wallin (1991), at 12 Ma, coeval movement on the Las Vegas Valley shear zone and the Saddle Island detachment moved the River Mountains-Frenchman Mountain block westward, opening the Red

Sandstone basin to the south of the Las Vegas Valley shear zone. Because the McCullough Mountains are in the same structural block, they were also transported westward; and because no major structure exists between the McCullough Mountains and the Spring Range, the Spring Range also must have been transported westward in the same structural block.

Intermediate Volcanism

Volcanic rocks erupted during Tertiary extension in the Las Vegas area are intermediate calc-alkaline suites with only minor amounts of basalt and rhyolite (Anderson, 1971; Smith, 1982; Mills, 1985; Feuerbach, 1986; Smith et al., 1990). The intermediate volcanic section in the McCullough Mountains is an example of such an occurrence. Proposed models for the production of intermediate suites during regional extension include: 1) assimilation of felsic crustal material and mafic mantle melts during magma ascent (Damon, 1971); 2) magma mixing of felsic and mafic end members (Glazner, 1989); 3) open system models utilizing the assimilation and/or mixing of felsic material with a fractionated mafic phase (Nielson and Dungan, 1985; McMillan and Dungan, 1986; Novak and Bacon, 1986; Smith et al., 1990).

The production of intermediate igneous rocks during Tertiary extension in the Las Vegas-Lake Mead area as a result of magma commingling of felsic and mafic end members has been documented by Naumann and Smith (1987), Naumann (1987), Larsen (1989), Smith et al. (1990) and Larsen and Smith (1991). The Sloan volcanic section lacks textural evidence of magma commingling. I will

suggest in this thesis, therefore, that intermediate volcanic rocks may also have been produced from partial melts of mid-to lower-crustal material without undergoing commingling and/or contamination from other sources.

CALDERAS: A GENERAL DISCUSSION

A caldera is a volcanic depression larger than the crater that caused its subsidence (Walker, 1984). There are three major types: shield calderas, summit calderas and ash-flow calderas (Wood, 1984).

Shield calderas result from subsidence along ring fractures following partial drainage of magma from shallow chambers by fissure eruptions on the flanks of the volcano. A classic example is the caldera system at the summit of Mauna Loa, Hawaii (Wood, 1984). Summit calderas form from the rapid emptying of a magma chamber beneath a stratovolcano resulting in cauldron collapse and the eruption of ash-flow tuff. Mount Mazama (whose summit cauldron is presently filled with Crater Lake) is an example of this rare caldera type (Wood, 1984). Ash-flow calderas are not associated with stratovolcanos and are much more common. They result from cauldron collapse following the eruption of large volumes (100-1,000 km^3) of rhyolitic to dacitic ash-flows. The Valles Caldera in New Mexico is such an example (Wood, 1984).

Caldera development associated with felsic, pyroclastic systems follows a general sequence described by Smith and Bailey (1968), and Lipman (1984). Felsic domes form over incipient ring fractures above a shallowly-emplaced magma chamber. Dome formation is followed by voluminous Plinian eruptions of ash-flow tuff from vents along the ring fracture zone emptying a large portion of the magma chamber. Collapse occurs as the caldera floor subsides into the evacuated chamber, either during or after the pyroclastic eruptions. Subsequent

erosion of the oversteepened walls causes enlargement of the caldera boundary and the formation of slump breccias within the crater. A resurgent dome forms when more magma enters the evacuated chamber causing upwarping of the caldera's floor. Volcanic domes may be emplaced along extensional faults on the resurgent dome or in the moat of the caldera. A typical caldera cycle ends with hydrothermal activity (Fig. 3). Not all calderas undergo complete collapse. Many calderas that erupt small-to-moderate volumes of ash-flow tuff (10-50 km^3) experience incomplete subsidence along horseshoe-shaped faults (Lipman, 1984). An example is the Three Creeks Caldera in the Marysvale volcanic field, Utah (Steven, 1981). Other calderas associated with low-to-modest volumes of ash-flow tuff appear to be unfaulted sags (Lipman, 1984; Walker, 1984), such as the Taupo volcanic center, New Zealand (Grindley, 1965; Cole, 1979). Factors that may contribute to downsagging or incomplete subsidence include: 1) a magma chamber at great depth (> 10-15 km); 2) structurally coherent roof rocks; 3) resurgence of magma into the chamber during eruption preventing emptying of the chamber; 4) a small volume of magma relative to caldera area (Steven and Lipman, 1976; Steven et al., 1984; Walker, 1984).

Ninety percent of the documented Tertiary-aged calderas in the Basin-and-Range province are greater than 15 km in diameter. Worldwide, only about ten percent of all Quaternary-aged calderas exceed this size (Walker, 1984). According to Walker (1984), this size difference may be attributed to crustal type. Basement in the Basin-and-Range province is largely Precambrian crystalline rock,

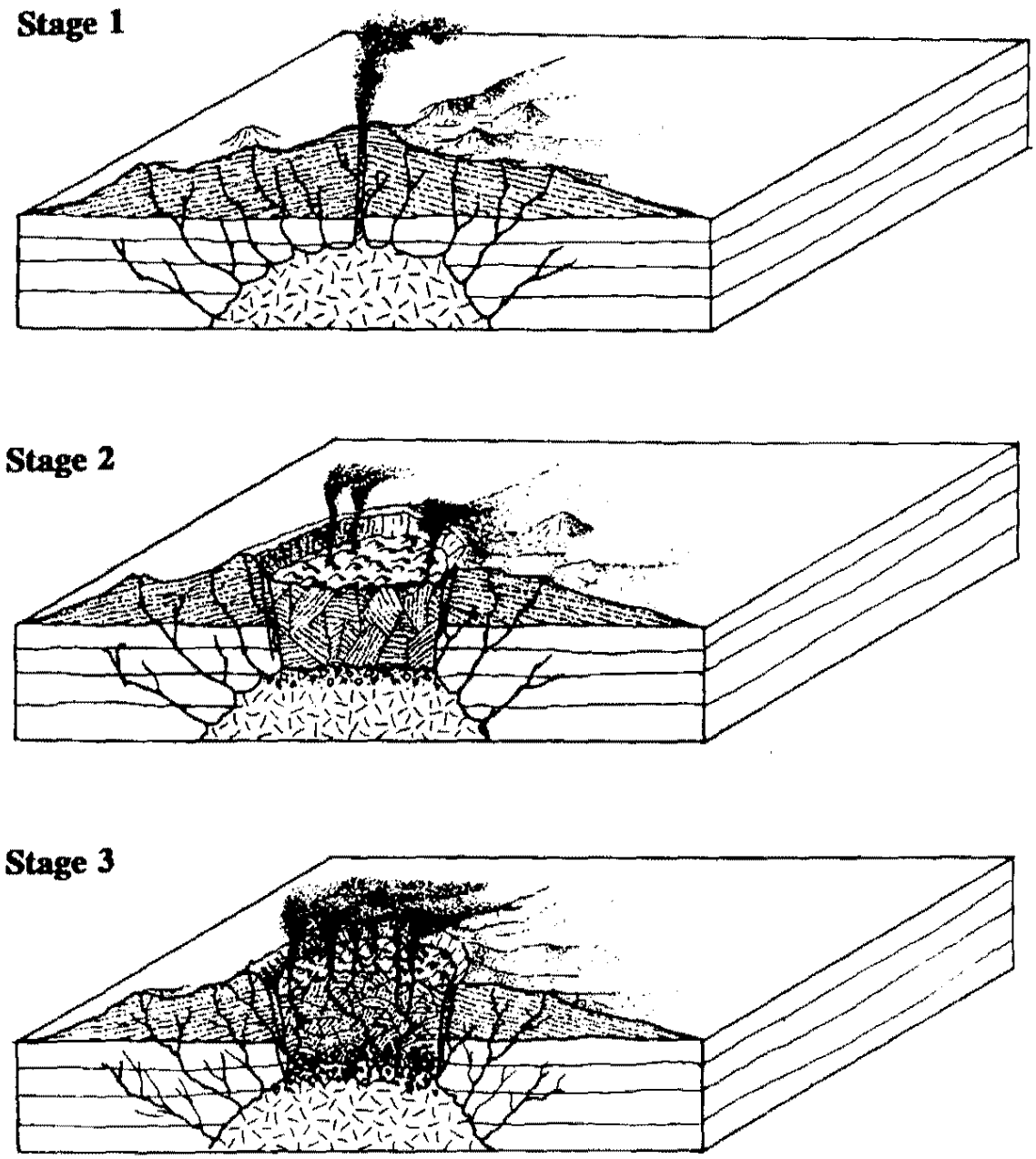

Figure 3: Collapse Caldera Sequence: **Stage 1:** Pyroclastic eruptions occur from vents above ring faults over a shallowly-emplaced magma chamber. **Stage 2:** Caldera collapse occurs during and/or after the pyroclastic eruptions. **Stage 3:** Erosion causes embayment and enlargement of the caldera margin. Slump breccias from the oversteepened walls form within the caldera. Resurgence of magma into the chamber may cause upward doming of the caldera floor.

whereas most Quaternary calderas are emplaced in young crust. Rigid crystalline basement rock may enhance complete separation and subsidence of the caldera floor resulting in larger collapse structures. Another factor contributing to the larger size of Basin-and-Range calderas may be enlargement due to extension.

Small ash-flow calderas in the Basin-and-Range province include the 3.5 km diameter Van Horn Mountains Caldera in the Trans-Pecos volcanic province in the Van Horn Mountains, Texas (Henry and Price, 1986), and the less than 3 km diameter McCullough Pass Caldera in the central McCullough Mountains, southern Nevada (Schmidt, 1987). The 13.5 km diameter Sloan sag discussed in this thesis is an example of a small volcanotectonic depression in the Basin-and-Range province.

ANALYTICAL METHODS

Fifty seven rock samples were analyzed for major element oxides. Forty six samples were analyzed for trace elements. Fresh, unweathered samples collected in the field were ground to -200 mesh using a Dyna Mill air suspended impact attrition mill and an agate mortar and pestal. Major element oxides were analyzed by X-ray fluorescence techniques on a Rigaku 3030 X-ray spectrometer at the University of Nevada, Las Vegas (UNLV). Trace elements were analyzed by instrumental neutron activation analysis at the Phoenix Memorial Laboratory at the University of Michigan. Kohl (1978) and Schmidt (1987) provided additional analyses of the Hidden Valley Volcanics and the Tuff of Bridge Spring.

One sample each of the Center Mountain dacite and the Tuff of Bridge Spring were dated using the K-Ar method on biotite separates. Mineral separations were done at UNLV. Approximately 10 pounds of fresh, unweathered sample was crushed in the attrition mill. The sample was then separated into six fractions of differing specific gravities on a number 13 Wilfley Table. Final biotite separation was done using heavy liquids (sodium metatungstate) and a Frantz magnetic separator. K-Ar dates were done by Krueger Enterprises in Cambridge, Massachusetts.

An $^{40}Ar/^{39}Ar$ sanidine date was obtained from the same sample of the Tuff of Bridge Spring. Sanidine separation was done at UNLV using the above methods. Sample irradiation was done at the Ford nuclear reactor, University of Michigan. $^{40}Ar/^{39}Ar$ dating was performed at the University of Maine, Orono.

GEOCHRONOLOGY

K-Ar dates from biotite separates were obtained from the Center Mountain dacite member of the Sloan volcanics and the Tuff of Bridge Spring from the north-central McCullough Mountains. An $^{40}Ar/^{39}Ar$ date from a sanidine separate was obtained from the same Tuff of Bridge Spring sample. These are the first age dates obtained from rocks of the north-central McCullough Mountains.

The K-Ar date for the Center Mountain dacite is 16.4 +/- 0.5 Ma, the K-Ar date for the Tuff of Bridge Spring is 16.6 +/- 0.4 Ma (Table 1). The $^{40}Ar/^{39}Ar$ date on the Tuff of Bridge Spring, however, is 15.23 +/- 0.14 Ma (Table 2; Figs. 4a & 4b).

The differences between the Tuff of Bridge Spring dates may be the result of excess argon retained by the biotite. Minerals may include argon in their crystal lattice by means other than the radiogenic decay of ^{40}K. Argon may be absorbed from the atmosphere or diffused into minerals from the outgassing of K-bearing minerals in the crust and/or mantle (Faure, 1986). The K-Ar dating method assumes that all of the Ar in the sample is radiogenic, produced by the radioactive decay of K in that sample. If excess Ar is present, the K-Ar method may result in an anomalously old age (Faure, 1986).

The $^{40}Ar/^{39}Ar$ dating method is based upon the production of ^{39}Ar by irradiation of K-bearing minerals in a nuclear reactor. It has an advantage over the K-Ar method in that only radiogenic Ar is measured. The irradiated sample

Table 1: New K-Ar Dates For The North-Central McCullough Mountains					
Sample	K%	Ar* (ppm)	Ar*/Total	K (ppm)	Date & Error
Center Mtn. Dacite	7.92	0.007578	0.1885	7.92	16.4 +/- 0.5 Ma
Tuff of Bridge Spring	6.323	0.007294	0.461	7.543	16.6 +/- 0.4 Ma

* Denotes radiogenic

Table 2: New Ar-Ar date for the Tuff of Bridge Spring, central McCullough Mountains

Temp C	40Ar/39Ar	37Ar/39Ar	36Ar/39Ar	Moles 39Ar	% Total 39Ar	%Radiogenic Ar40	K/Ca	Age and error (Ma)
750	6.461	0.0348	0.0189	127.8	1.9	13.1	14.09	12.96 +/- 0.82
830	3.156	0.0314	0.0073	181.7	2.6	31.1	15.60	15.01 +/- 0.53
900	1.753	0.0312	0.0026	252.2	3.7	55.9	15.72	14.99 +/- 0.47
960	1.291	0.0306	0.0010	356.7	5.2	76.0	16.01	15.01 +/- 0.29
1020	1.176	0.0299	0.0006	531.7	7.7	82.9	16.41	14.91 +/- 0.20
1080	1.180	0.0295	0.0006	811.9	11.8	83.6	16.63	15.09 +/- 0.20
1120	1.166	0.0297	0.0006	987.6	14.3	84.5	16.52	15.06 +/- 0.14
1160	1.148	0.0291	0.0004	1012.2	14.7	87.4	16.86	15.34 +/- 0.14
1200	1.136	0.0292	0.0004	1014.9	14.7	87.9	16.80	15.26 +/- 0.14
1240	1.143	0.0288	0.0004	888.4	12.9	87.8	17.00	15.34 +/- 0.20
Fuse	1.252	0.0292	0.0008	729.4	10.6	80.2	16.79	15.34 +/- 0.18

Plateau age = 15.32 +/- 0.16 Ma

Isotope correlation age = 15.23 +/- 0.14 Ma

4A

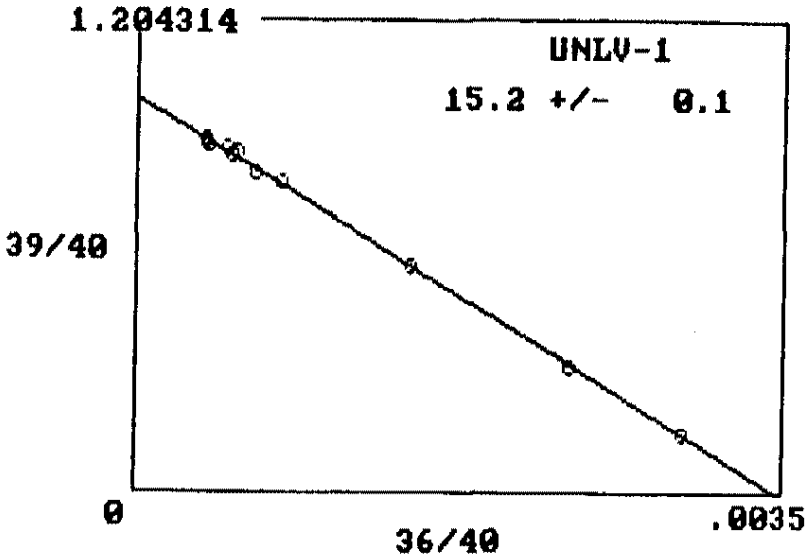

Y = B + MX
Y - $^{40}Ar/^{36}Ar$ = 289.5103 +/- 4.017002
B - $^{39}Ar/^{40}Ar$ = 1.003595 +/- 4.162581E-03
M - Slope = -290.5509 +/- 3.220593: Slope used in calculation of data
X - $^{36}Ar/^{40}Ar$ = 3.454109E-03 +/- 4.792633E-05
Intercept age = 15.23245 +/- 0.1388164 Ma

4B

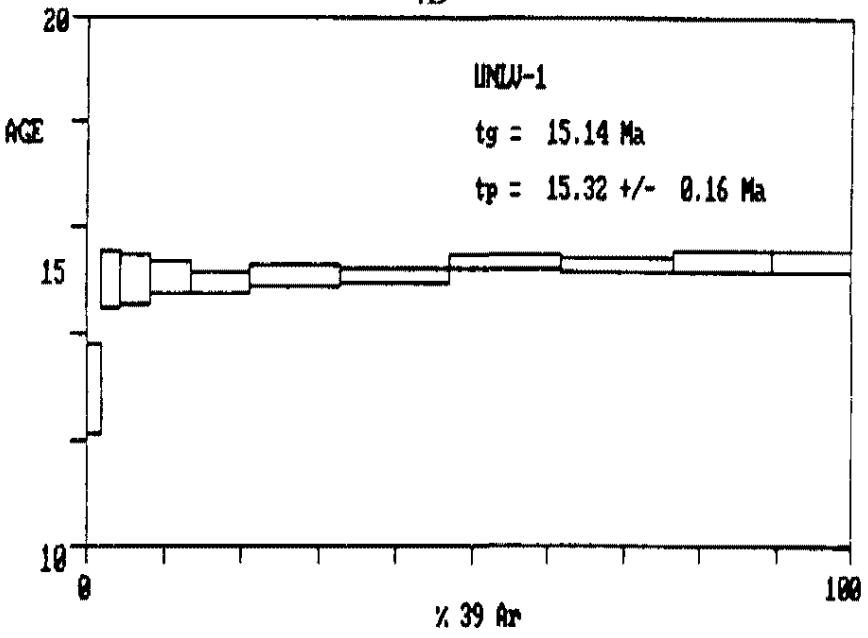

Figure 4: Ar-Ar age date data from the Tuff of Bridge Spring, central McCullough Mountains.

is heated incrementally and the $^{40}Ar/^{39}Ar$ ratio for each increment is determined. If the sample has not lost or gained Ar or K since the time of its initial cooling, the ratios at each temperature will be constant. This ratio will result in a "plateau" value that is used to calculate the age of the sample (Faure, 1986).

In $^{40}Ar/^{39}Ar$ dating, the isochron correlation method may also be used. A sample may also contain atmospheric ^{36}Ar. On a graph of $^{39}Ar/^{40}Ar$ versus $^{36}Ar/^{40}Ar$, values of these ratios determined for each increment of heating are plotted to produce an isochron. The slope of the isochron equals the value of ^{40}Ar (radiogenic)$/^{39}Ar$, which is used to calculate the age of the sample.

I accept the isotope correlation age of 15.23 +/- 0.14 Ma for the following reasons. The plateau values from the incremental heating of the Tuff of Bridge Spring sample have a small offset (Fig 4b). There is an initial plateau age of about 15.0 Ma, then it increases to about 15.3 Ma. The offset in the plateau suggests that the sample may be slightly altered. The plateau date of 15.32 +/- 0.16 Ma (Fig. 4b) for the sample was calculated using only the data from the higher plateau. The isotope correlation age (Fig 4a), on the other hand, takes into account all values of incremental heating, resulting in an average of the plateau ages (Faure, 1986). In this case, the isotope correlation technique has produced a higher quality date for the sample and will be accepted in this thesis.

Both of the K-Ar dates are suspect, therefore the actual age of the Sloan volcanics was not determined. I can only conclude that the relative age of the Sloan Volcanics is less than 15.23 Ma.

THE SLOAN VOLCANICS

Introduction

The Sloan volcanics consist of andesite and dacite domes and flows, dacite and rhyolite pyroclastic units, and a late-stage hypabyssal dacite stock. I suggest that they were erupted during and/or after the formation of a volcanotectonic sag in Hidden Valley.

The Sloan volcanics are the youngest volcanic rocks in the McCullough Mountains (< 15.23 +/- 0.14 Ma). They overlie the Hidden Valley volcanics, McCullough Pass volcanics, Pumice Mine volcanics, Tuff of Bridge Spring, and Eldorado Valley volcanics respectively. The entire section is underlain by Precambrian basement (Fig. 5).

Rocks were named using the chemical classification scheme of Irvine and Baragar (1971).

Pre-Sloan Volcanic Stratigraphy

Refer to Figure 5 for the stratigraphic column of the rocks described in this section.

Precambrian crystalline rocks crop out south of the thesis area and are composed of biotite monzogranite and biotite granitoid gneiss cut by pegmatite and aplite dikes (Anderson et al., 1985).

The Eldorado Valley volcanics are age equivalent to the Patsy Mine volcanics mapped by Anderson (1971) in the Eldorado Mountains. This unit is

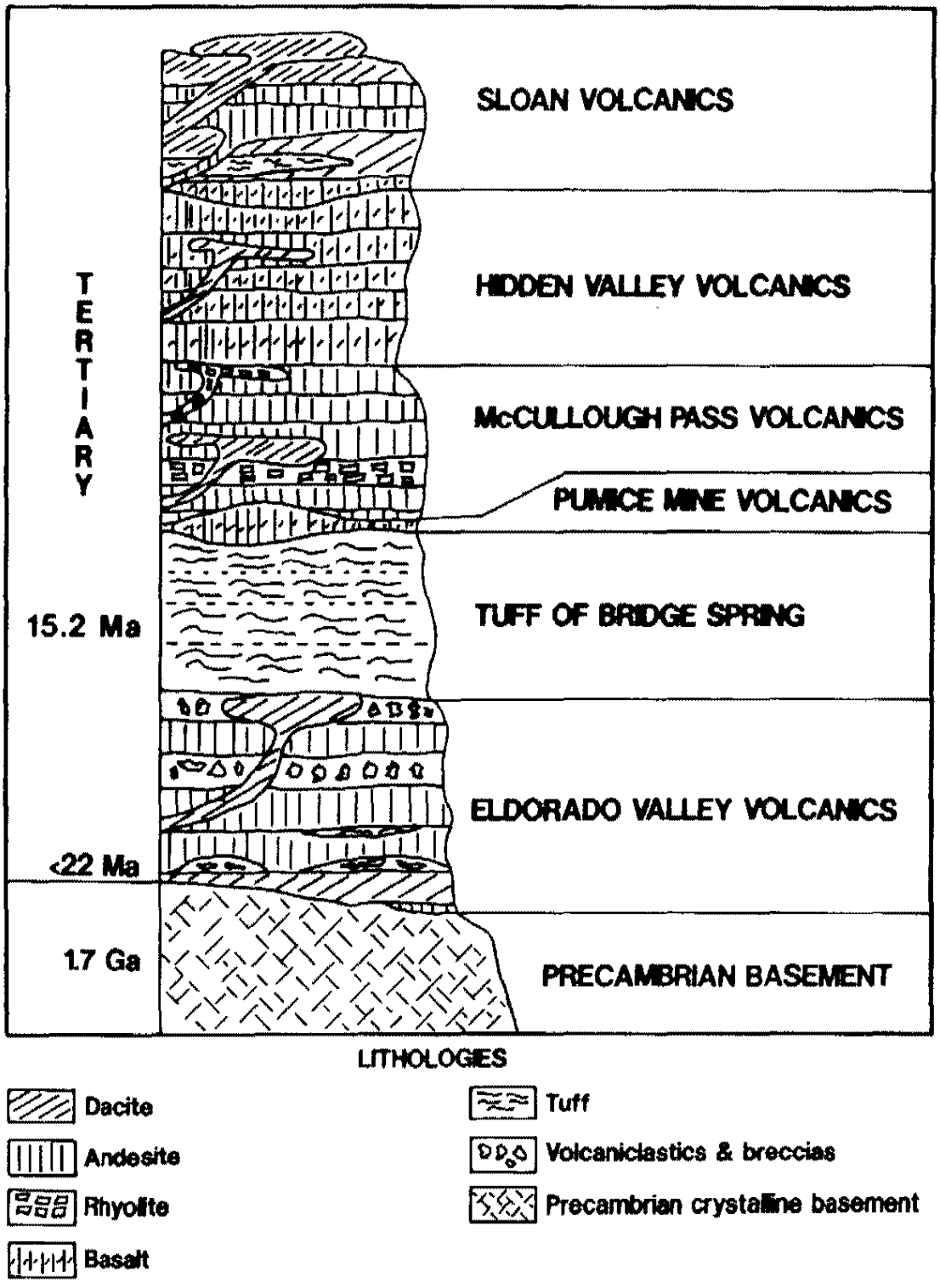

Figure 5: Stratigraphic column of the central McCullough Mountains.

almost 300 m thick on the eastern escarpment of the central McCullough Mountains. It thins rapidly to the west and does not crop out on the western margin of the range (Smith et al., 1988). Westward thinning of this and other volcanic units in the north-central McCullough Mountains may be due to a prominent buttress of Precambrian basement that prevented volcanic units from flowing to the west (Schmidt, 1987; Smith et al. 1988). Schmidt (1987) documented two members of the Eldorado Valley volcanics in the central McCullough Mountains. The lower member consists of thinly interbedded flows of hornblende andesite, olivine andesite and dacite. The upper member is composed mainly of volcaniclastic units.

The Tuff of Bridge Spring is a rhyolite to dacite ash-flow tuff of regional extent. The tuff crops out in the Eldorado Mountains (Anderson, 1971), the Highland Range (Bingler and Bonham, 1972), the McCullough Mountains (Schmidt, 1987), and the White Hills (Cascadden, 1991) and southern Black Mountains (referred to in Cascadden, 1991), Arizona (Fig. 1). In the McCullough Mountains, the Tuff of Bridge Spring consists of a single cooling unit up to 145 m thick (Schmidt, 1987). It crops out in the central part of the range and pinches out to the southeast of Hidden Valley. Scattered outcrops also occur to the west of Hidden Valley (Plate 1), and were mapped as the Erie Tuff by Kohl (1987). A sample of the Tuff of Bridge Spring from the central McCullough Mountains was dated at 15.23 +/- 0.14 Ma ($^{40}Ar/^{39}Ar$, sanidine).

The Pumice Mine volcanics consists of andesite and basalt flows and

breccia units up to 60 m thick (Smith et al., 1982; Schmidt, 1987). This thin unit is a marker bed separating the Tuff of Bridge Spring from the McCullough Pass volcanics.

The McCullough Pass volcanics are composed of rhyolite domes, dikes, flows and pyroclastic units, andesite flows and dikes, and volcaniclastic rocks that were deposited during and after the collapse of the McCullough Pass caldera (Schmidt, 1987). The outflow facies of the McCullough Pass tuff extends northward from its source into the Hidden Valley area.

The Hidden Valley volcanics are age equivalent to the upper Patsy Mine or lower Mount Davis volcanics in the Eldorado Mountains (Anderson, 1971). This unit is up to 245 m thick on the eastern escarpment of the north-central McCullough Mountains and thins to the west. The Hidden Valley volcanics consist of basalt and basaltic-andesite flows, cinder cones and scoria. Rocks contain clinopyroxene and olivine phenocrysts, and subordinate quartz xenocrysts. The Sloan volcanic section overlies the Hidden Valley volcanics in central and eastern Hidden Valley.

Stratigraphy of the Sloan Volcanics

The oldest rocks of the Sloan volcanics include the Mount Hanna andesite and the rocks of the Center Mountain dome complex. The Center Mountain dome complex is composed of the Cinder Prospect member, Tuff of the Sloan volcanics, Center Mountain dacite, and the Mount Ian andesite (Fig. 6). Since the Mount Hanna andesite member is not in contact with the Center Mountain dome

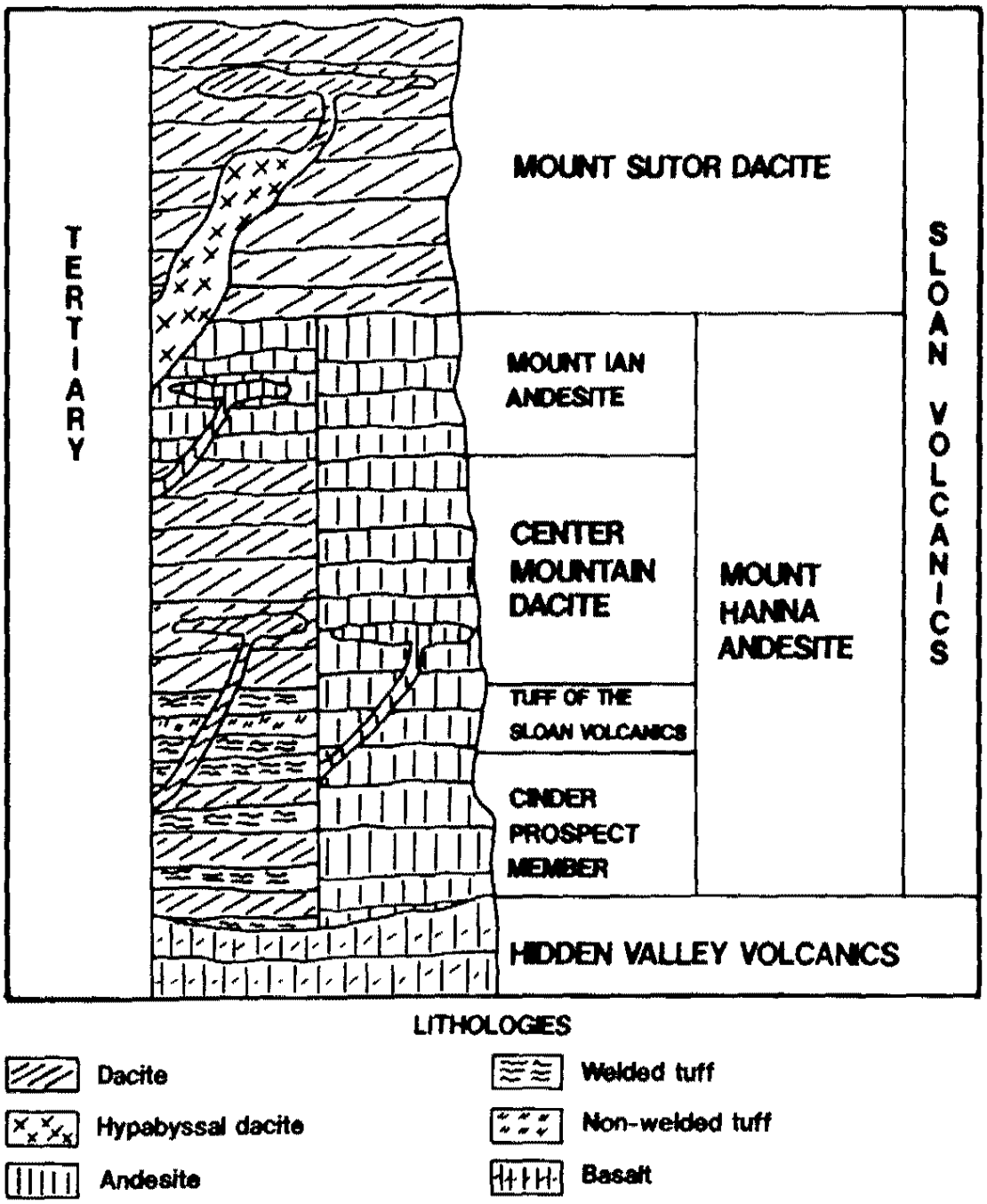

Figure 6: Stratigraphic column of the Sloan volcanics, north-central McCullough Mountains.

complex, the relative age of these sections cannot be determined (Plate 1).

Refer to Figure 6 for the stratigraphic column of the rocks described in this section. Refer to Appendices A and B for rock chemistry.

The Mount Hanna andesite is aphyric with SiO_2 contents ranging from 59.37 to 60.74 weight%. Flows are up to 5 m thick and are commonly platy and foliated on their surfaces.

The Cinder Prospect member consists of thinly interbedded dacite flows and rhyolite to dacite ash-flow tuffs with SiO_2 contents ranging from 61.31 to 69.88 weight%.

The Tuff of the Sloan volcanics consists of three cooling units, each approximately 2 m thick. From oldest to youngest the units are: 1) welded rhyolite ash-flow tuff (SiO_2 = 69.76 weight%); 2) poorly-welded dacite ash-flow tuff (SiO_2 = 64.87 weight%); 3) welded dacite ash-flow tuff (SiO_2 = 64.26 weight%).

The Center Mountain dacite is composed of flows of biotite dacite with SiO_2 contents ranging from 67.67 to 68.06 weight%.

The Mount Ian andesite intrudes and overlies the Cinder Prospect, Tuff of the Sloan Volcanics, and Center Mountain dacite members. Its SiO_2 content varies from 57.84 to 60.22 weight%.

The youngest member of the Sloan volcanics is the Mount Sutor dacite. It is a biotite dacite with SiO_2 contents ranging from 61.67 to 64.96 weight%.

Characteristics of the Sloan Volcanic Centers

The Mount Hanna andesite differs from other members of the Sloan volcanics in that it was erupted from a single vent. This unit is up to 307 m thick and has a maximum volume of 9 km^3. Other members erupted from numerous vents and domes. The Mount Hanna eruptive center is about 100 m across. The vent has been eroded and is occupied by a volcanic neck formed of resistant andesite, silicified by hydrothermal activity. Black and red oxidized autobrecciated andesite surrounds the vent (Fig. 7; Cross section C-C', Plate 1). Two small volcanic domes occur about 1 km southwest of the vent and are interpreted as parasitic vents on the flank of the Mount Hanna eruptive center. I suggest that the Mount Hanna andesite erupted at temperatures of approximately 1,000°C with a water content of less than 2% by a lava-fountaining mechanism. This eruption resulted in a lava flow analogous to a hot, dry ash-flow tuff. I will present evidence to support these observations later in this thesis.

The formation of the Center Mountain dome complex reflects the first two steps of four documented by Smith (1973) for the eruptive sequence at the Mono Craters, California. The complete sequence is: 1) creation of a tuff ring composed of ash, lapilli and ejecta, caused from hot rising magma contacting groundwater; 2) eruption of magma into the crater forming a dome; 3) cratering of the dome from explosions and/or collapse; 4) eruption of magma into the previously cratered dome. The interbedded ash-flow tuffs and dacite flows of the Cinder Prospect member and the Tuff of the Sloan volcanics were produced in

Figure 7: Photo of the Mount Hanna Andesite Vent Center

the early stages of pyroclastic and phreatomagmatic activity and reflect the formation of a tuff ring. The upper cooling unit of the Tuff of the Sloan volcanics contains blocky glass shards suggesting a hydroclastic eruption mechanism (Fisher & Schmincke, 1984). In a canyon in the southern part of the dome, (Sta.73, Fig. 8), the tuff contains armored mud balls and discontinuous stringers of dacite (Fig. 9) suggesting hydroclastic activity and lava fountaining. The Center Mountain dacite intruded the tuff ring, erupting thick, viscous dacite over the earlier units. The approximate volume of the dome complex is 0.44 km^3.

The Mount Ian andesite erupted from numerous domes and vents, many of which overlie tuff rings composed of black ash and cinder. One volcanic center (Sta. 120, Fig. 8) contains a volcanic neck of hydroclastic breccia of andesite clasts and bombs embedded in an ashy groundmass (Fig. 10). The deposit formed when hot, rising magma came in contact with groundwater. Clasts and bombs of quenched andesite were ejected from the volcano. Some fell back into the vent and became embedded in a fine-grained hydroclastic groundmass. Domes are characterized by platy andesite forming "onion skin" patterns. Foliation defined by platy slabs of andesite dip inward toward the conduit and become horizontal over the vent (Fig. 11). Single domes are less than 0.5 km in diameter, and up to 75 m high.

Both the southern and northern Mount Sutor dome fields are composed of flows of massive biotite dacite. Only two vents are exposed in the southern Mount Sutor field, but more may be buried by flows. A vent at station 91 (Fig. 8)

Figure 8: Sample Location Map

Figure 9: Photo of Hydroclastic Tuff at Station 73

Figure 10: Photo of Mount Ian Andesite Hydroclastic Breccia at Station 120

Figure 11: Photo of Platy, Foliated Mount Ian Andesite

consists of a tuff ring overlain by 3 to 4 m of explosion breccia overlain by 3 m of hydroclastic breccia, capped by dacite. This sequence suggests that an earlier dome was explosively disrupted by intruding magma creating a dacite breccia. Phreatomagmatic activity continued and resulted in the deposition of hydroclastic breccia. Viscous dacite covered these units. The northern Mount Sutor field contains a hypabyssal dacite stock that intruded its own volcanic cover (Fig. 12). The hypabyssal and volcanic rocks are chemically similar. I suggest that vents related to this shallow magma body were responsible for eruption of the dacites in the northern Mount Sutor field. Any volcanic domes and vents have since been stripped from the intrusion by erosion.

Petrography

Refer to Appendix C for detailed petrographic descriptions, and Appendix D for rock modes.

Tuff of Bridge Spring: The Tuff of Bridge Spring is a poorly-welded to welded rhyolite to dacite ash-flow tuff containing phenocrysts (10-33%) of sanidine, plagioclase, biotite, clinopyroxene and subordinate quartz, sphene, zircon and Fe-Ti oxides. The tuff includes pumice (1-12%), and basaltic and subordinate gabbroic and granodioritic xenoliths (1-10%). In welded units the pumice is flattened to fiamme. The groundmass consists of devitrified glass and glass shards. For further descriptions of the Tuff of Bridge Spring in the McCullough Mountains, see Kohl (1978) and Schmidt (1987).

Hidden Valley volcanics: Basalts are vesicular, subalkalic to transitional

Figure 12: Photo of Hypabyssal Stock in the Northern Mount Sutor Dacite Field

and contain phenocrysts (1-37%) of plagioclase, clinopyroxene and iddingsitized olivine. Some of the phenocrysts commonly occur in glomerocrysts. Two samples (Mc47 & Mc48) have phenocrysts (4-5%) of oxidized biotite or phlogopite. Some of the samples include up to 1% glass-rimmed quartz xenocrysts. The groundmass consists of microlites of plagioclase, clinopyroxene, iddingsitized olivine, and trace amounts of glass. For further descriptions, see Kohl (1978) and Schmidt (1987).

Mount Hanna andesite: The Mount Hanna andesite is fine-grained, hypocrystalline and commonly trachytic. Phenocrysts are rare (< 1%) and consist of highly embayed and pitted plagioclase and biotite. Andesite is characterized by microlites of subparallel plagioclase with subordinate Fe-Ti oxides, glass and highly birefringent cryptocrystalline grains (pyroxene & olivine?).

Cinder Prospect member: Ash-flows tuffs of the Cinder Prospect member contain phenocrysts (25-26%) of plagioclase, sanidine, biotite, Fe-Ti oxides and clinopyroxene with trace amounts of zircon. Subordinate basaltic, gabbroic and granodioritic xenoliths also occur. Plagioclase phenocrysts are commonly pitted and embayed. The groundmass consists of devitrified glass and glass shards, and trace amounts of granular hematite. Ash-flow tuffs are commonly vitrophyric. Biotite dacite contains glomerocrysts (4-6%) of plagioclase, biotite and Fe-Ti oxides, and phenocrysts (5-6%) of the same assemblage of minerals found in the glomerocrysts. The groundmass consists of microlites of plagioclase with subordinate oxidized biotite, zircon and glass.

Tuff of the Sloan Volcanics: Tuffs contain phenocrysts (17-36%) of

plagioclase, sanidine, biotite, clinopyroxene, Fe-Ti oxides, sphene and trace amounts of zircon. The basal rhyolite cooling unit (Mc59a) has trace amounts of monazite, epidote and allanite. The upper dacite cooling unit (Mc59c) has trace amounts of quartz. The tuffs also include devitrified pumice clasts (2-12%), and basaltic and gabbroic xenoliths (4-21%). The groundmass consists of devitrified glass shards. Shards from sample Mc59c are blocky.

Center Mountain dacite: The Center Mountain biotite dacite is holocrystalline and contains phenocrysts (6-9%) of plagioclase with subordinate oxidized biotite and Fe-Ti oxides. The groundmass consists of microlites of plagioclase with subordinate oxidized biotite, Fe-Ti oxides and clinopyroxene(?), and secondary calcite (1-5%) that coats fractures and partially replaces the groundmass. Rocks are commonly glomerocrystic and trachytic.

Mount Ian andesite: The fine-grained, hypocrystalline Mount Ian andesite contains phenocrysts (5-35%) of plagioclase, oxidized biotite and Fe-Ti oxides with subordinate orthopyroxene and iddingsitized olivine. Some phenocrysts occur in glomerocrysts. The groundmass consists of microlites of the phenocryst-phase minerals, dominated by plagioclase. Trace amounts of hematite and glass are also present.

Mount Sutor dacite: The Mount Sutor biotite dacite contains glomerocrysts (2-18%) of plagioclase, biotite and Fe-Ti oxides. Some glomerocrysts also contain orthopyroxene and/or clinopyroxene. Dacites include phenocrysts (2-6%) of the same assemblage of minerals found in the

glomerocrysts. One sample (Mc27) has less than 1% oxidized hornblende. Plagioclase is pitted, embayed, and displays oscillatory zoning. Biotite is commonly oxidized. The groundmass consists of microlites of plagioclase, biotite and Fe-Ti oxides, with subordinate orthopyroxene, clinopyroxene, zircon and glass. Two samples (Mc118 & Mc119) collected from the hypabyssal stock in the northern Mount Sutor field are coarse-grained but have an identical mineralogy to their volcanic counterparts.

GEOCHEMISTRY

Metasomatism

Tertiary igneous rocks in the Lake Mead-Las Vegas area are commonly metasomatized (Feuerbach, 1986; Smith et al., 1989; Larsen, 1989). During metasomatism rocks are strongly enriched in potassium and depleted in sodium, or vice versa. For example, some of the quartz monzonite samples from the Tertiary Wilson Ridge pluton (Fig. 1) have K_2O contents as high as 10.5 weight% and Na_2O as low as 0.75 weight% (Feuerbach, 1986).

Rocks of the Sloan volcanics appear not to have been appreciably affected by metasomatism. Similar K_2O and Na_2O contents (4 to 6 and 3 to 5 weight% respectively) suggest that potassium and/or sodium enrichment has not occurred. Harker variation diagrams show that K_2O and Na_2O increase with increasing SiO_2, but the data are scattered (Figs. 13A & 13E). The scatter may be due to minor remobilization of alkali elements.

Major Elements

Rocks of the Sloan volcanics are calc-alkaline (Fig. 14) and range from 58 to 70 weight% SiO_2 (Appendix A). MgO, Fe_2O_3, CaO, Al_2O_3, TiO_2 and P_2O_5 decrease with increasing SiO_2 (Figs. 13B, 13C, 13D, 13F & 13G). K_2O and Na_2O increase with increasing SiO_2 (Figs. 13A & 13E).

Harker variation diagrams divide the rocks of the Sloan volcanics into four chemically distinct groups. These are the: 1) Mount Hanna andesite and Mount

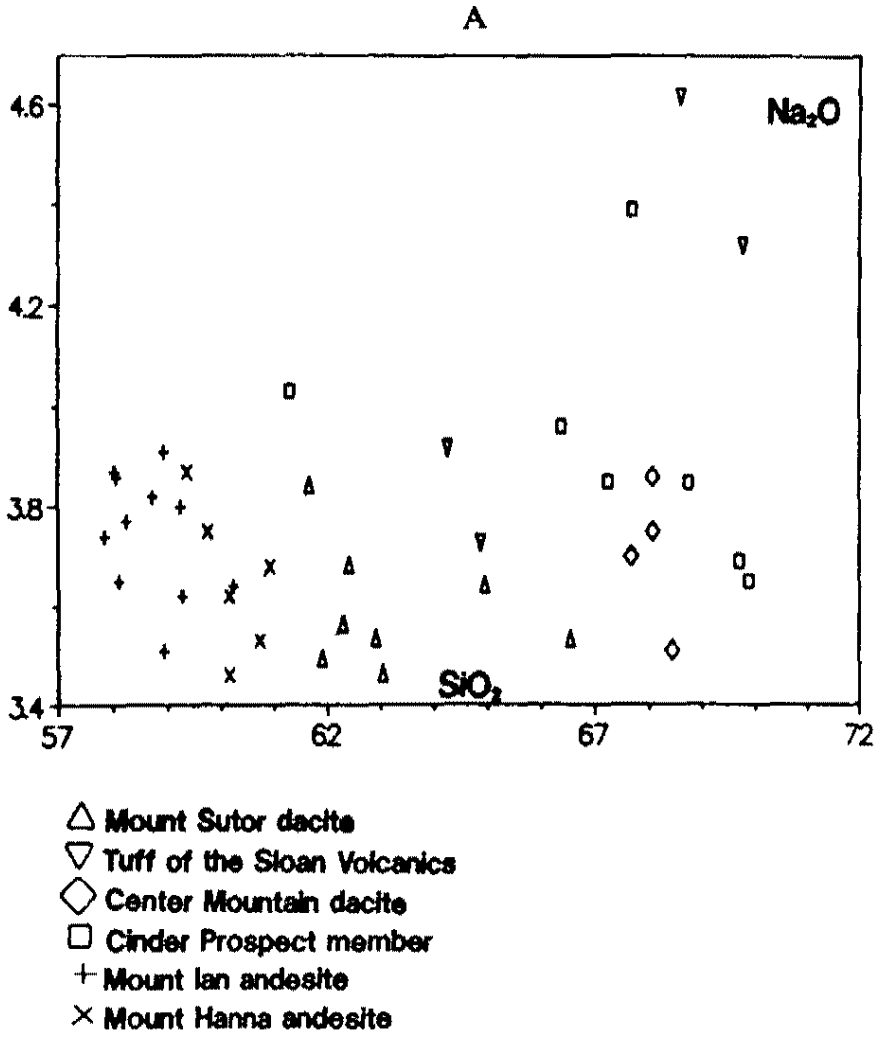

Figure 13: Harker variation diagrams

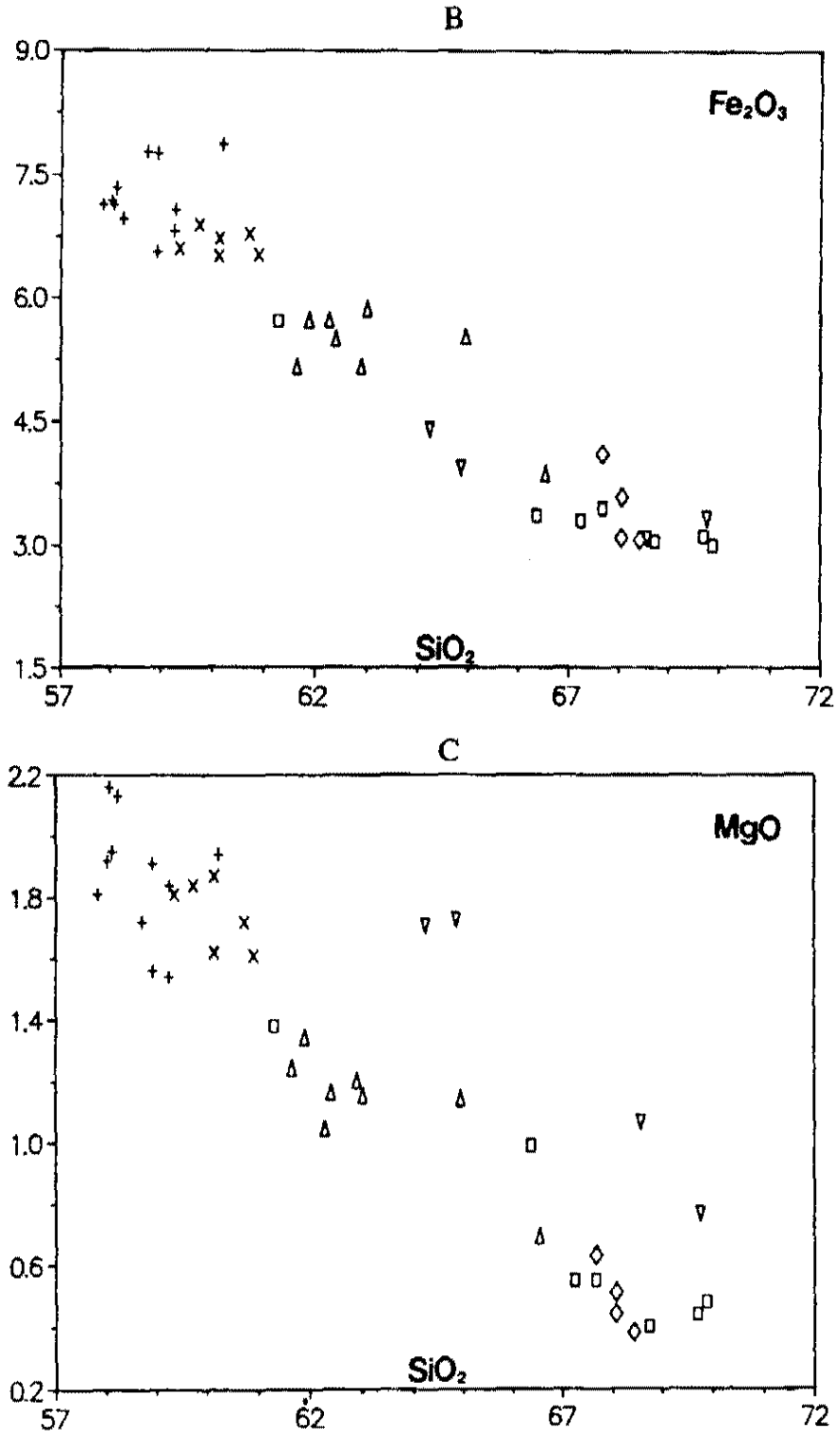

Figure 13: Continued

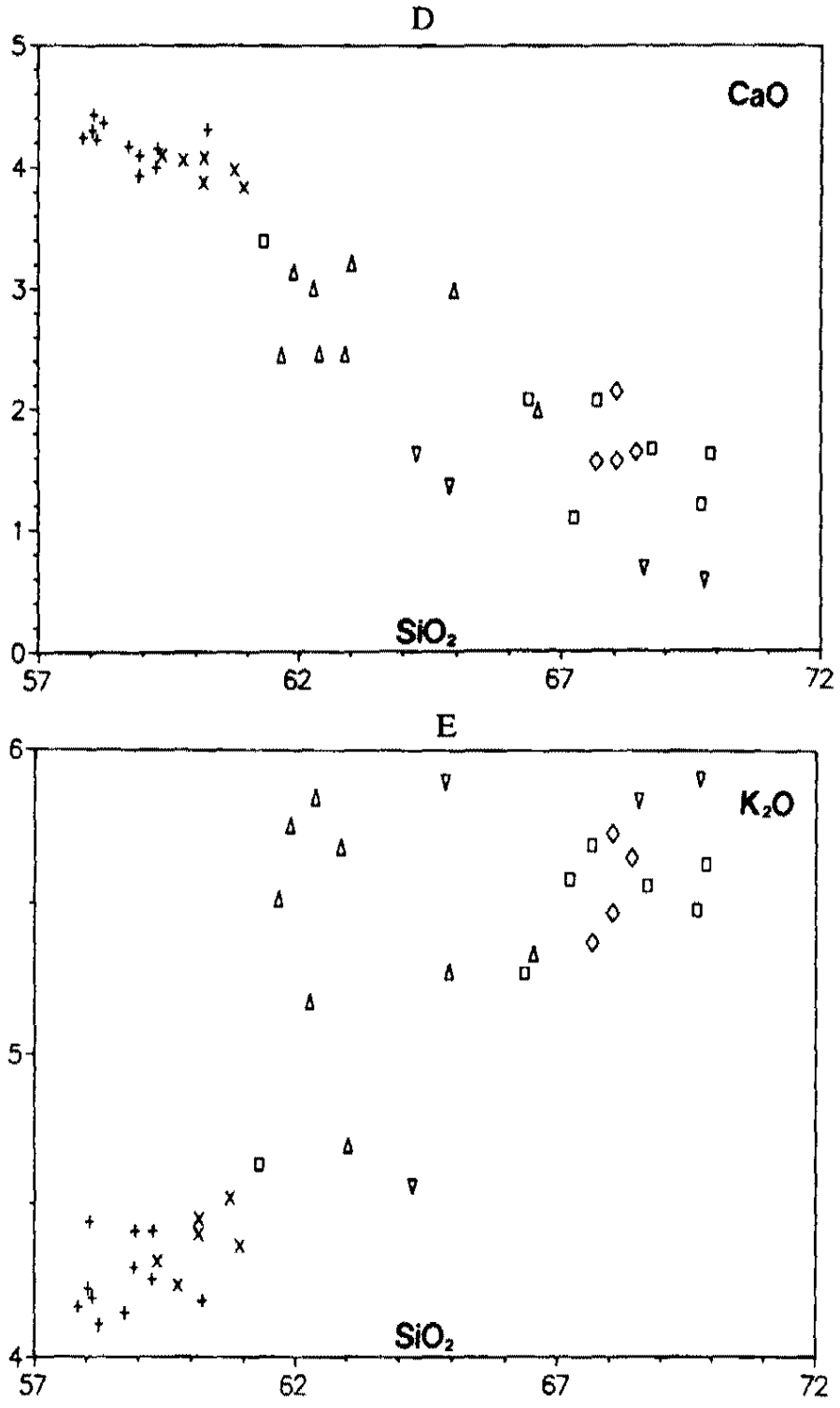

Figure 13: Continued

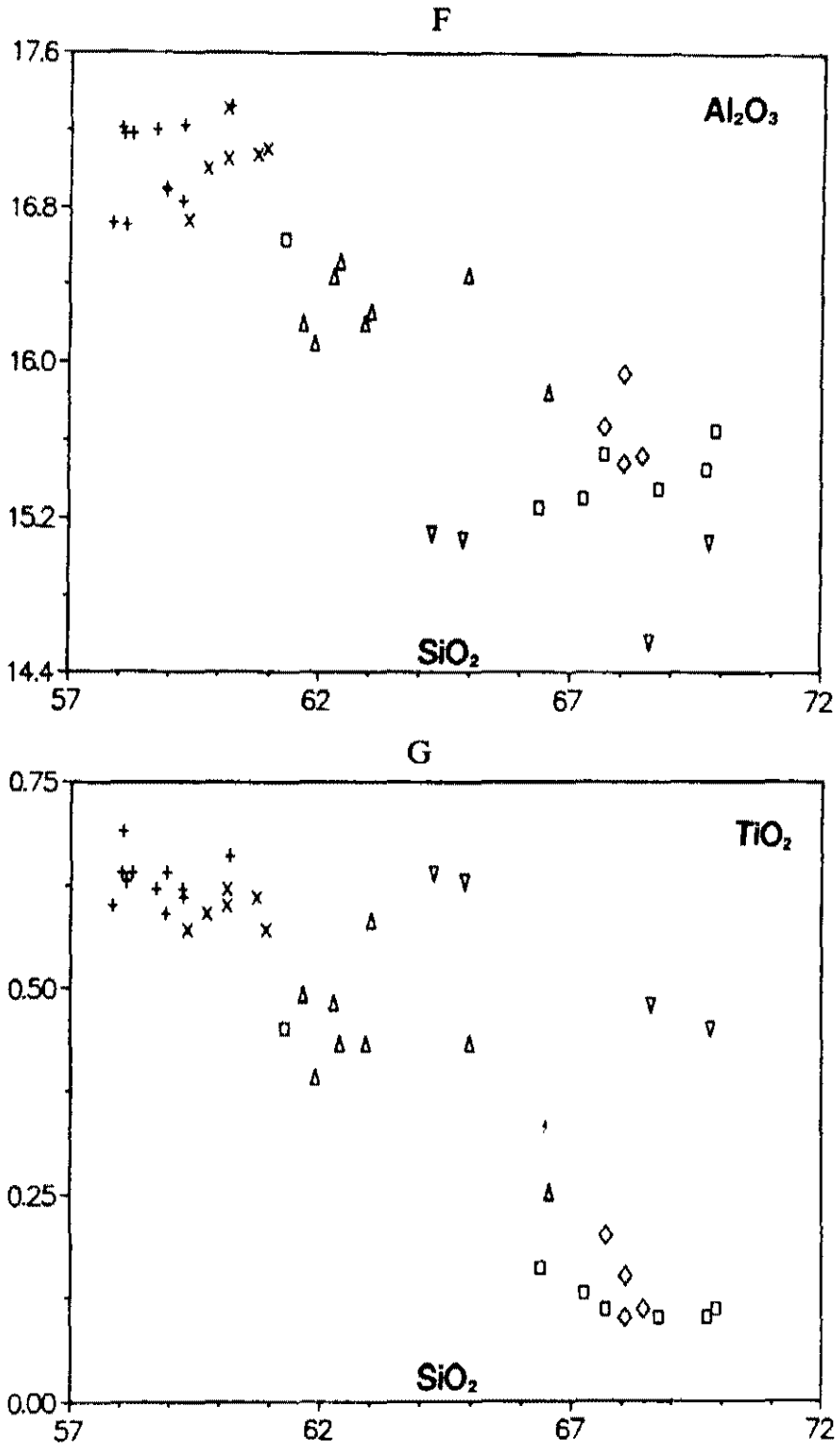

Figure 13: Continued

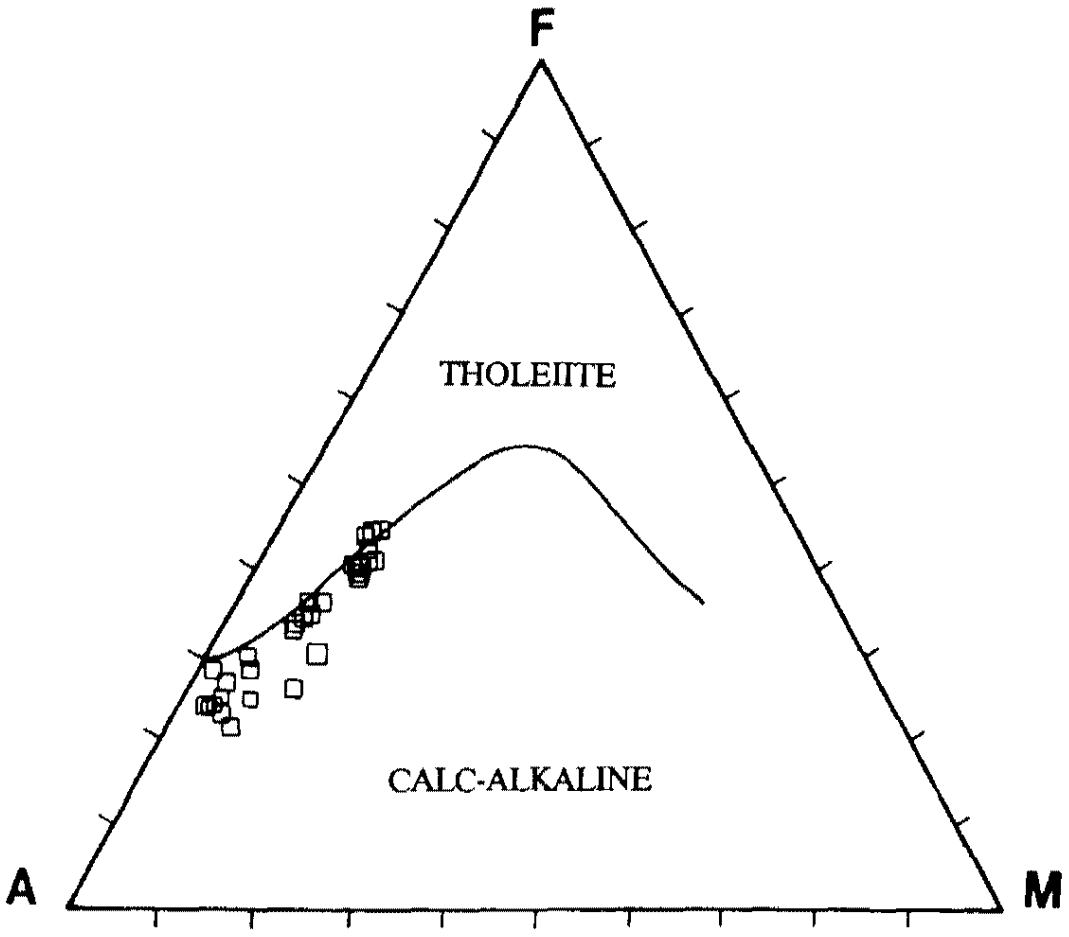

Figure 14: AFM diagram showing the calc-alkaline characteristics of the rocks of the Sloan volcanics. Diagram is after Irvine and Barager (1971).

Ian andesite (greater than 1.4% MgO, 0.55% TiO_2 and 16.7% Al_2O_3); 2) Mount Sutor dacite (0.6% to 1.4% MgO, 0.25% to 0.55% TiO_2, and 15.6% to 16.4% Al_2O_3); 3) Cinder Prospect member and Center Mountain dacite (less than 1.0% MgO, 0.20% TiO_2 and 16.0% Al_2O_3); 4) Tuff of the Sloan volcanics (similar range of SiO_2 as the dacites, but higher in MgO (0.8% to 1.8%) and TiO_2 (0.45% to 0.65%), and lower in Al_2O_3 (14.4% to 15.2%)) (Fig. 15).

Trace Elements

Compatibility of the trace elements in mineral phases is directly dependent upon rock type. For example, the large ion lithophile elements (LILE) Ba and Rb are incompatible in andesite, but compatible with biotite in dacite. The transition metals Co and Cr are compatible with olivine in andesite, but relatively incompatible in dacite. The LILE Th and the rare-earth element (REE) Ce are compatible only in accessory minerals such as monazite. Felsic rocks such as rhyolite and dacite contain a higher modal concentration of accessory minerals such as zircon, sphene, apatite and monazite than andesites and basalts.

In rocks of the Sloan volcanics, the concentrations of: 1) total REE (La, Ce, Nd, Sm, Eu, Tb, Yb and Lu) increase with increasing SiO_2 (Fig. 16A). 2) Th and the incompatible high field strength elements (HFSE) Hf and Ta increase with increasing SiO_2 (Figs. 16B & 16C); 3) the LILE Sr decreases with increasing SiO_2 (Figs. 16D & 16F); 4) the transition metal Co decreases with increasing SiO_2 (Figs. 16G & 16H); 5) Eu decreases with increasing SiO_2 (Figs. 16D, 16E & 16G).

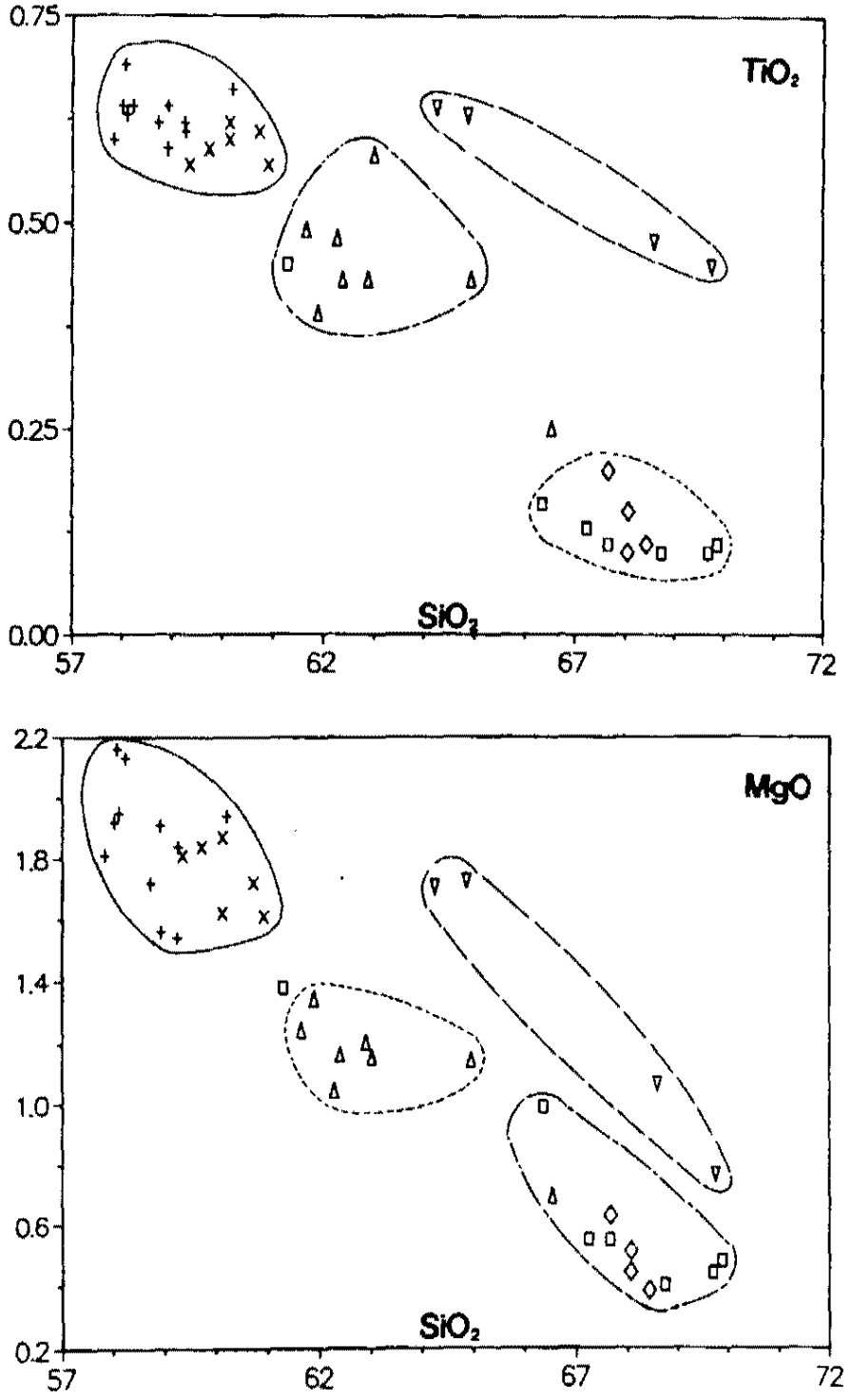

Figure 15: Harker variation diagrams showing the four chemically distinct groups of the Sloan volcanics. See Figure 13 for symbol explanation.

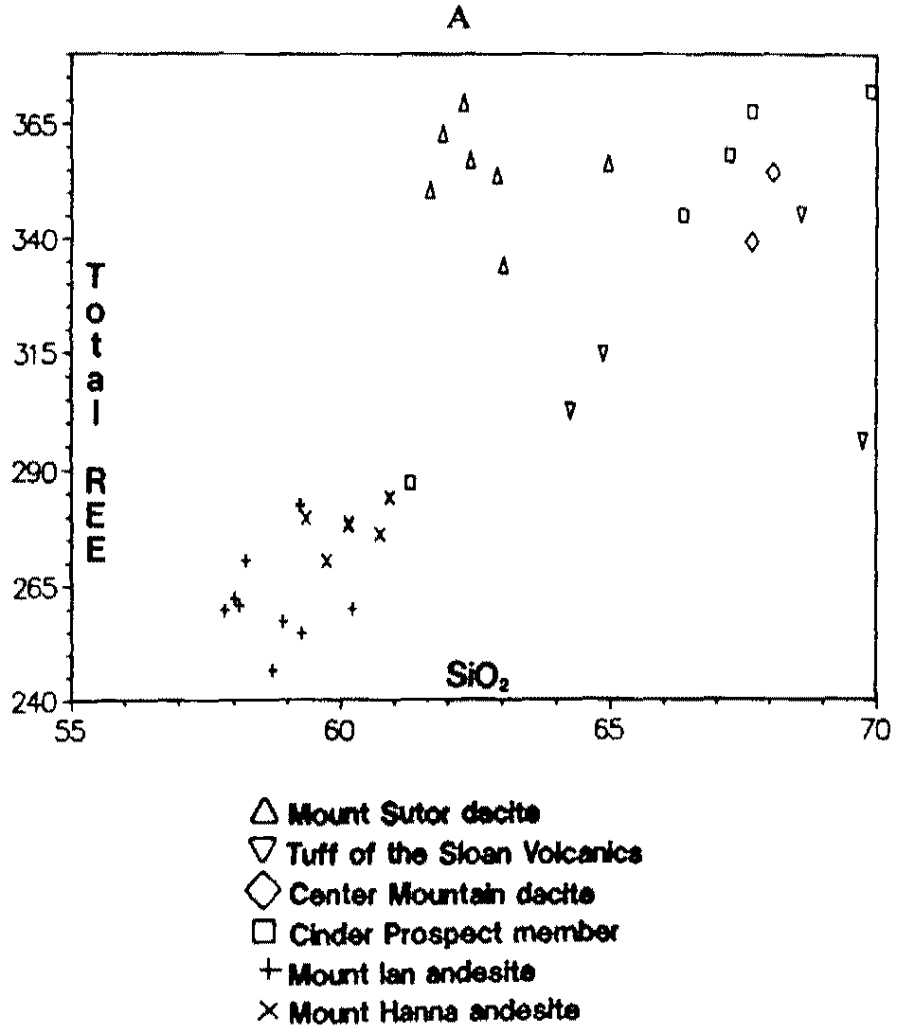

Figure 16: Trace element diagrams. Concentrations of SiO_2 and CaO are in weight percentage. Concentrations of trace elements are in ppm. Symbol in upper corner represents mean analytical error in ppm.

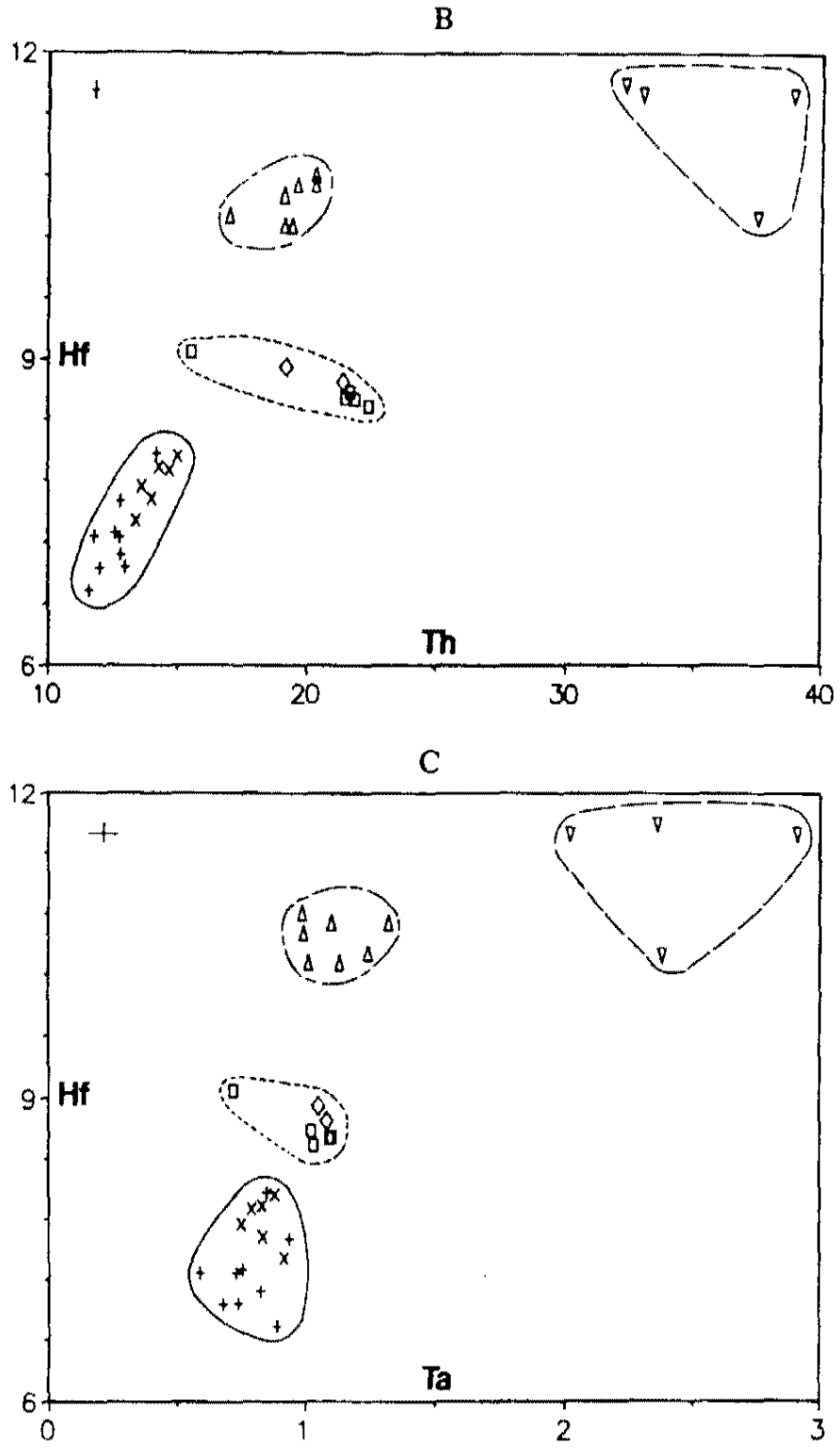

Figure 16: Continued

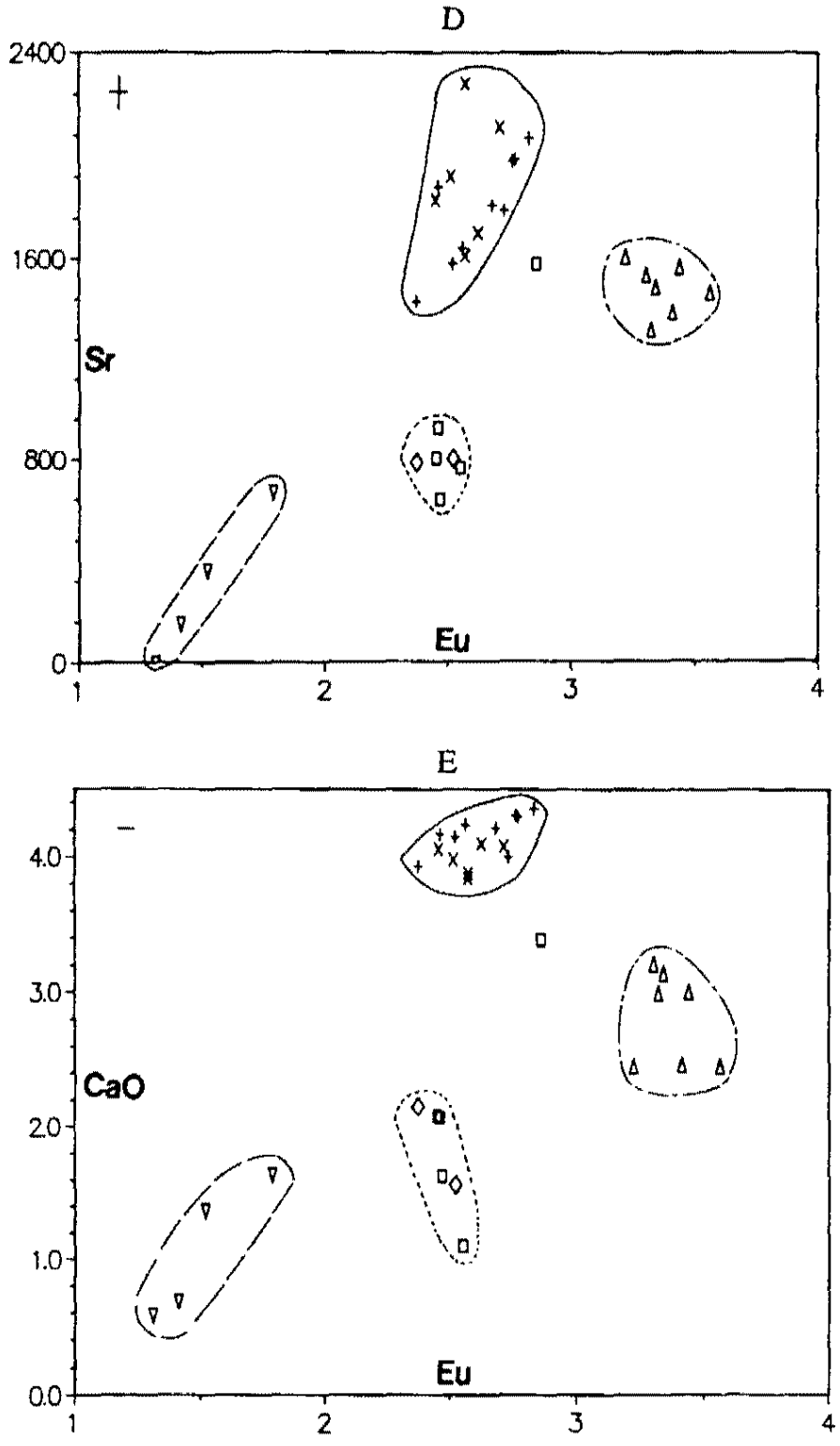

Figure 16: Continued

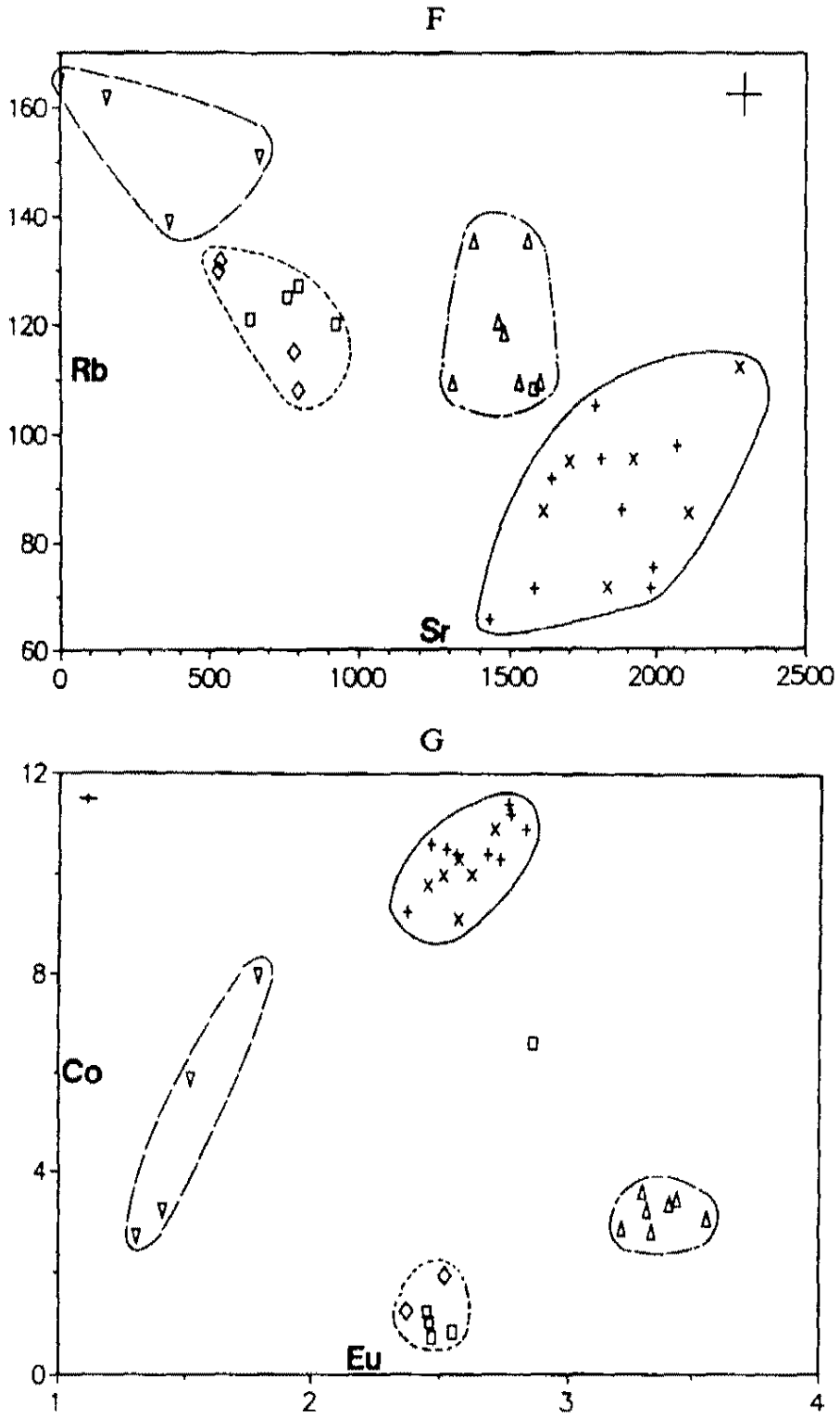

Figure 16: Continued

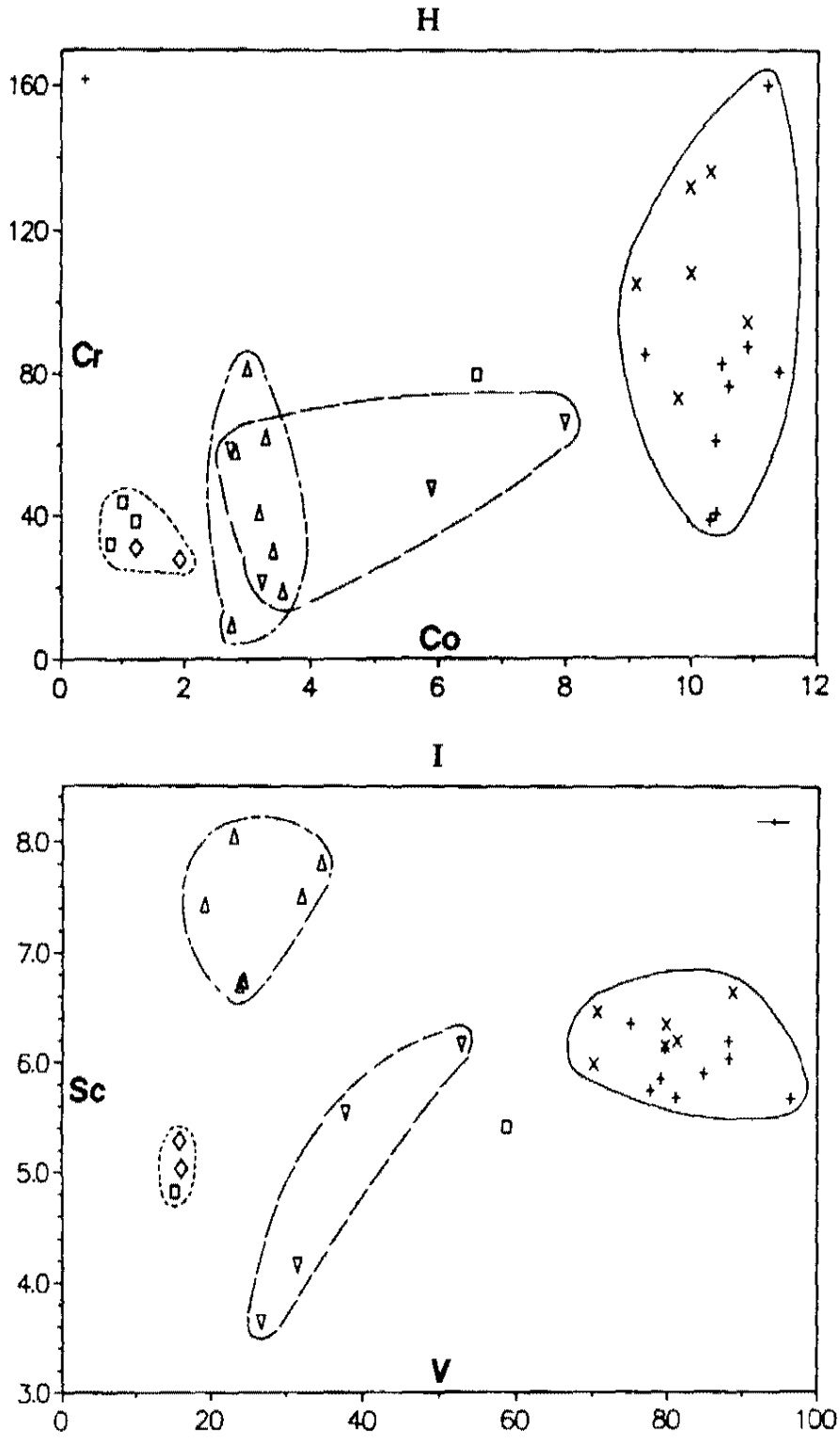

Figure 16: Continued

Chemical plots of trace elements distinguish the same four groups that are suggested by the Harker variation diagrams. For most elements, the differences between each group is greater than mean analytical error indicating that the differences between groups is statistically significant (Table 3). The andesites are more depleted in Hf, Ta and Th, and more enriched in Co than the other groups. The Mount Sutor dacite is enriched in Eu. The Tuff of the Sloan volcanics is depleted in Eu, and enriched Ta and Th. The Center Mountain dacite and the Cinder Prospect member are depleted in V.

If the rocks of the Sloan volcanics had a comagmatic relationship and were produced by a fractional crystallization or partial melting process, samples would plot on a continuous positive linear slope on an incompatible element diagram. Instead, incompatible element diagrams show four separate groupings of data (Fig. 16). A sampling bias could cause the gaps between groups. During sampling, however, I was careful to collect all the exposed compositional variations of volcanic and hypabyssal rocks. I suggest, therefore, that the four groups represent chemically distinct magma types and do not reflect incomplete sampling.

Spider diagrams may be used to distinguish the general chemical characteristics of rock suites, determine evolutionary paths and identify sources. Spider diagrams are constructed by normalizing trace element values to known concentrations and plotting them on a logarithmic scale. These diagrams minimize data scatter and emphasize general chemical trends and "signatures".

Caps

Table 3: Mean analytical error of trace elements used in chemical plots

Element	Error: +/- ppm	Error: +/- %Concentration
Sc	0.04	0.68
V	3.82	9.87
Cr	2.15	5.93
Co	0.16	3.94
Rb	8.33	7.62
Sr	114	14.7
Eu	0.07	3.23
Hf	0.21	2.32
Ta	0.11	9.53
Th	0.24	1.22

Normalized values used in this thesis are chondrite (Thompson et al., 1984) and MORB (Pearce, 1983).

Chondrite normalized REE diagrams (Thompson, 1984) show that the four rock groups have similar chemical signatures (Figs. 17A-17D). The Tuff of the Sloan volcanics differs only in that it is depleted in Eu (Fig. 17C). Rocks of the Sloan volcanics are enriched in light REE (LREE) and depleted in heavy REE (HREE). The LREE La varies from about 250 to 400 chondrite. The HREE Lu varies from about 10 to 25 chondrite.

Spider diagrams show a common depletion in P, Ti and Ta, and enrichment in Rb, K, La, Nd and Zr for the four rock groups of the Sloan volcanics (Figs. 18A-18H). The Tuff of the Sloan volcanics differs only in that it is depleted in Ba (Figs. 18C & 18G). Major and trace element diagrams are sensitive to small differences in source rocks and petrogenetic paths, while spider plots are not. The fact that the rocks of the Sloan volcanics are separated into four groups on major and trace element plots, but are not segregated on spider diagrams, suggests that the chemical differences between the groups are significant, but small.

Temporal and Spatial Variations in Chemical Trends

Spider diagrams indicate that the andesites of the Sloan volcanics have a chemically similar source as the older Hidden Valley volcanics, except that the Hidden Valley basalt is more depleted in the incompatible elements Ta, Th and La (Fig. 19). Its overall pattern is similar to the Sloan volcanics, suggesting that

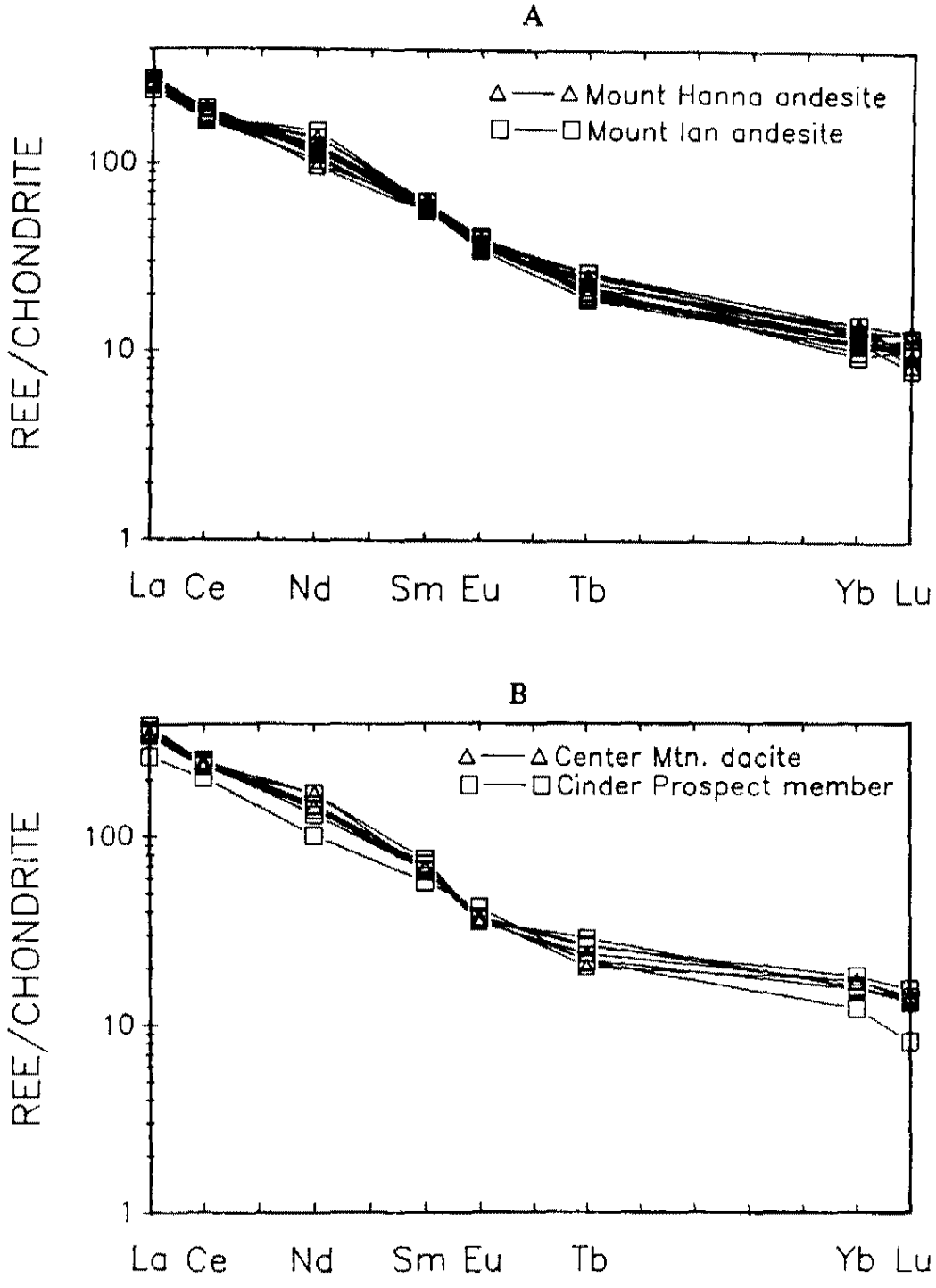

Figure 17: Chondrite-normalized REE diagrams

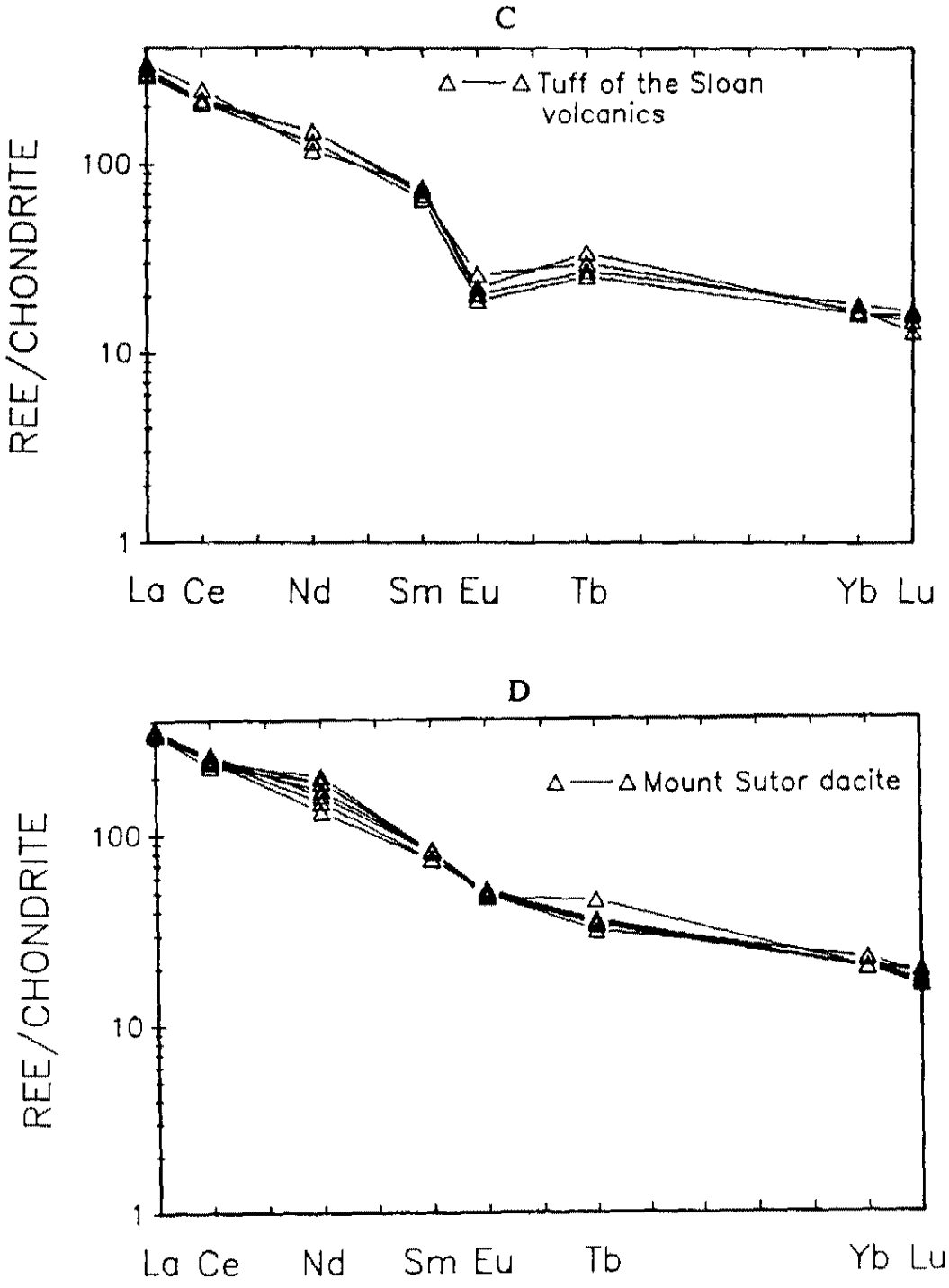

Figure 17: Continued

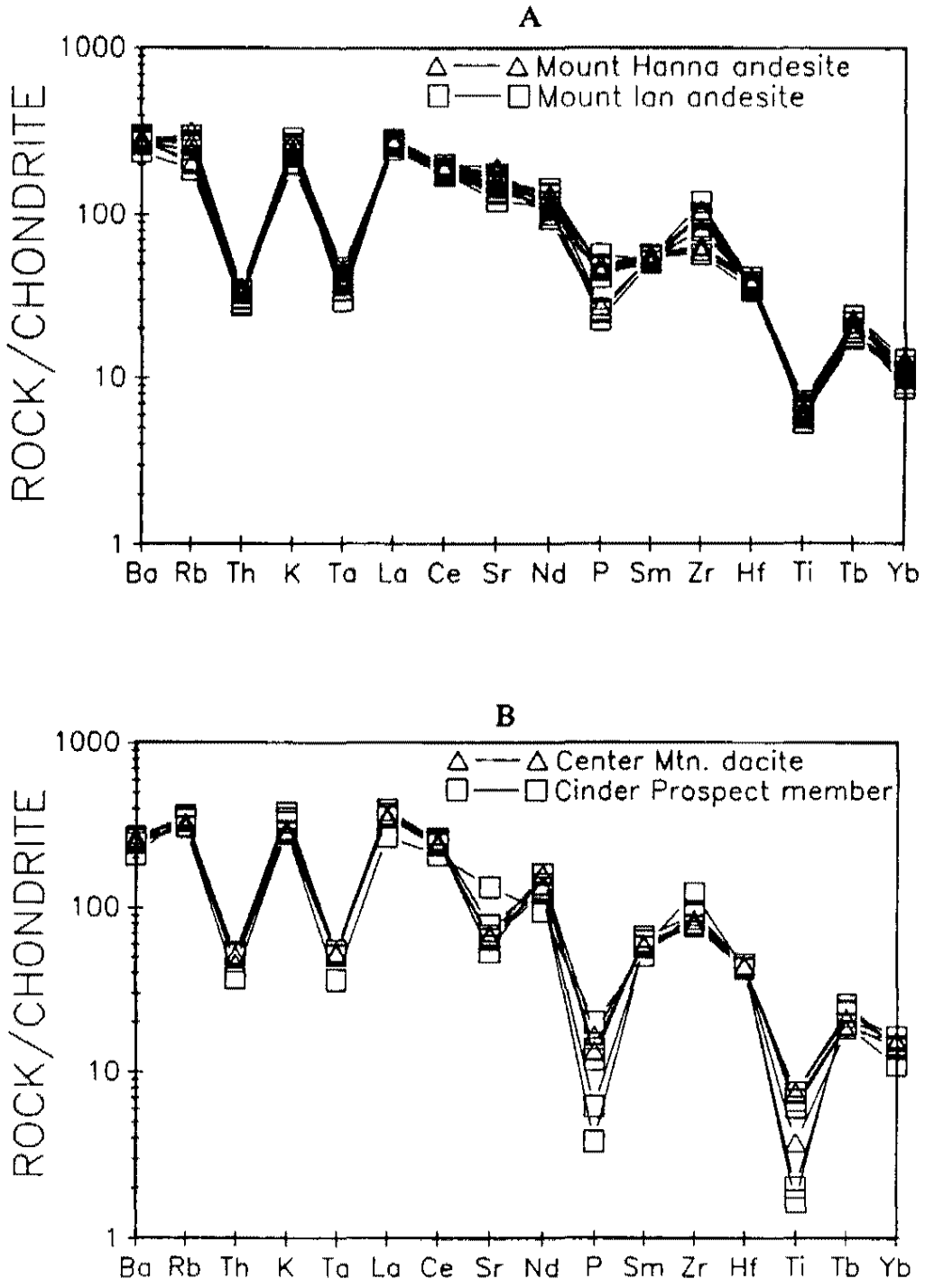

Figure 18: Chondrite and MORB-normalized diagrams for rocks of the Sloan volcanics.

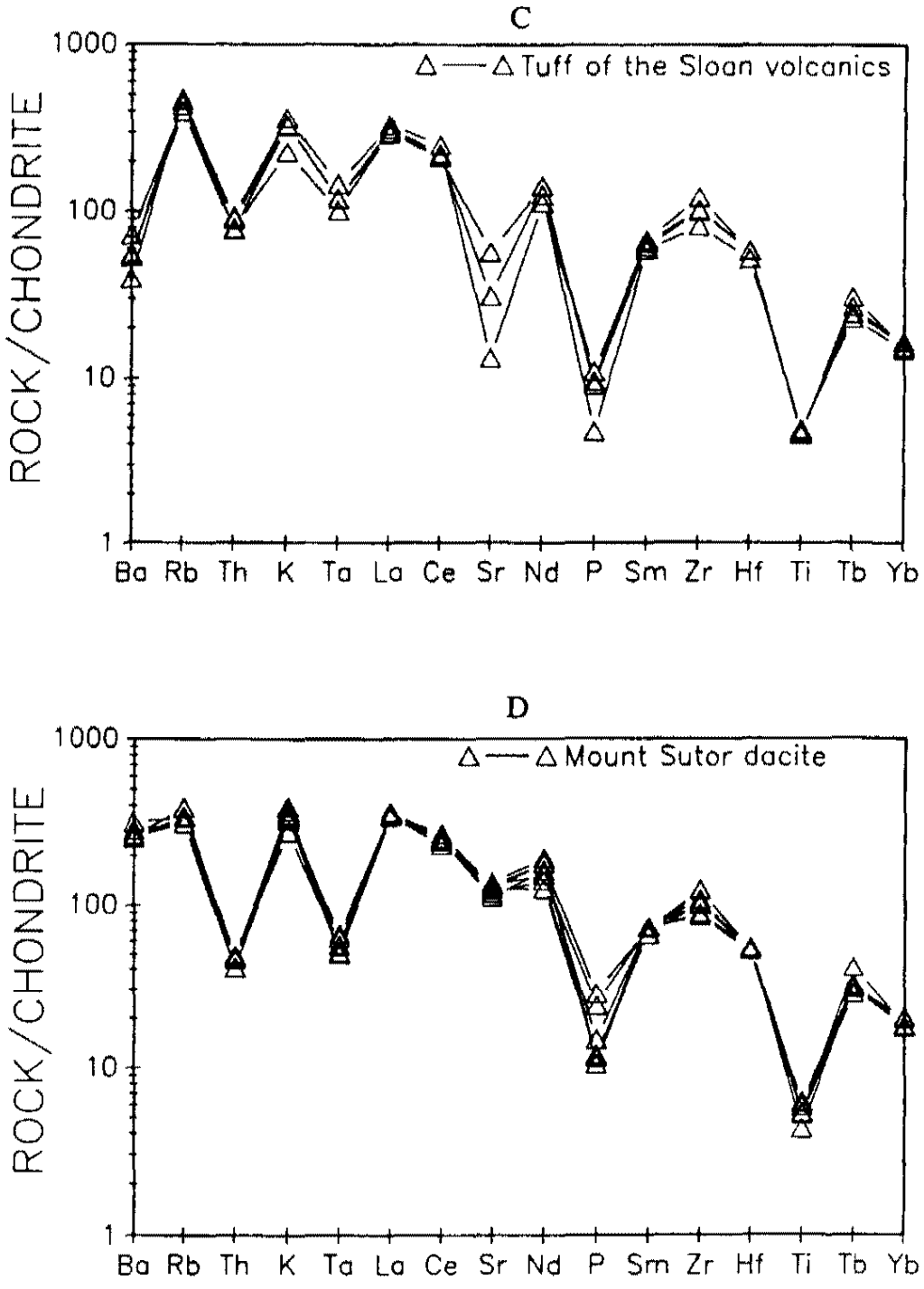

Figure 18: Continued

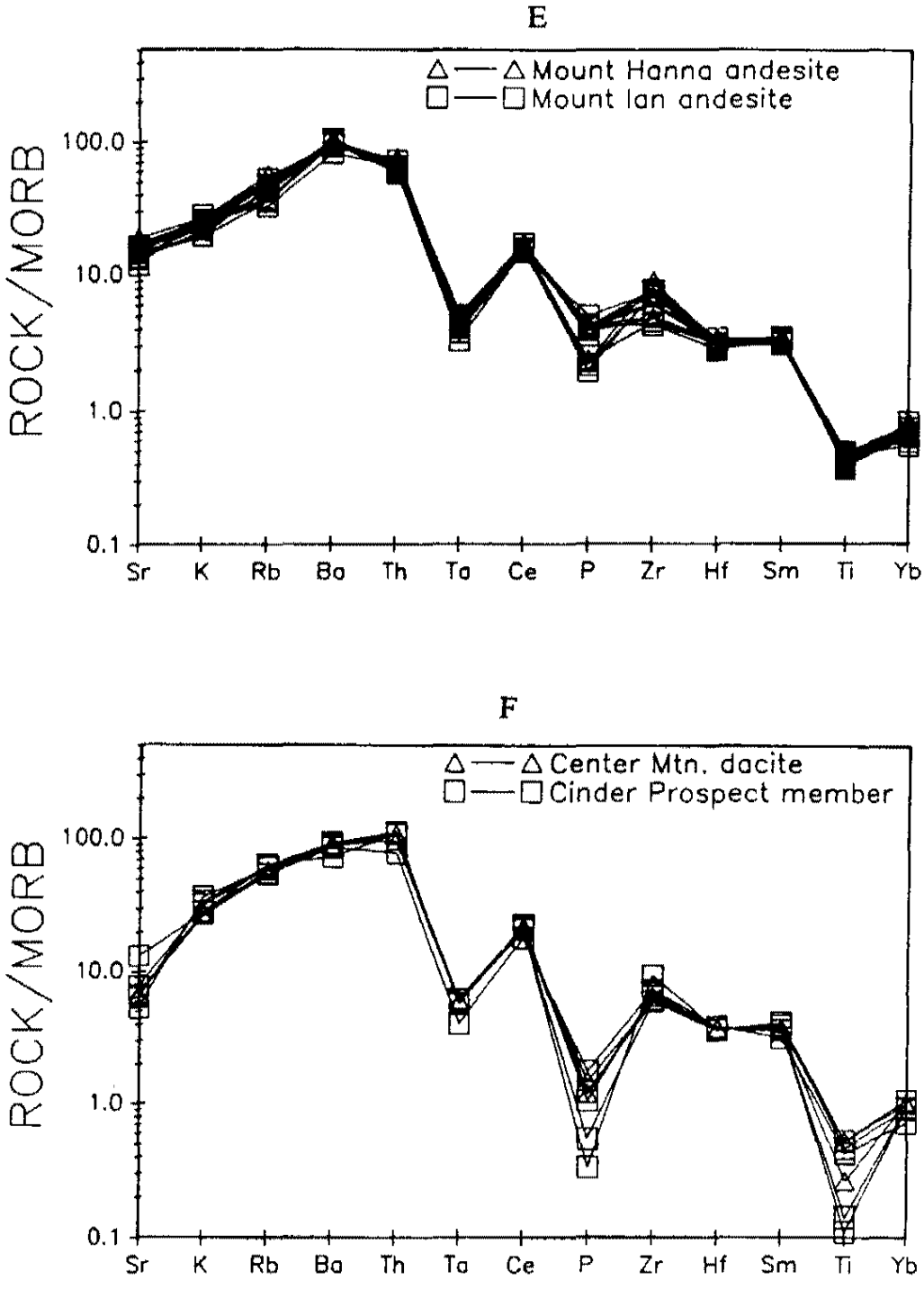

Figure 18: Continued

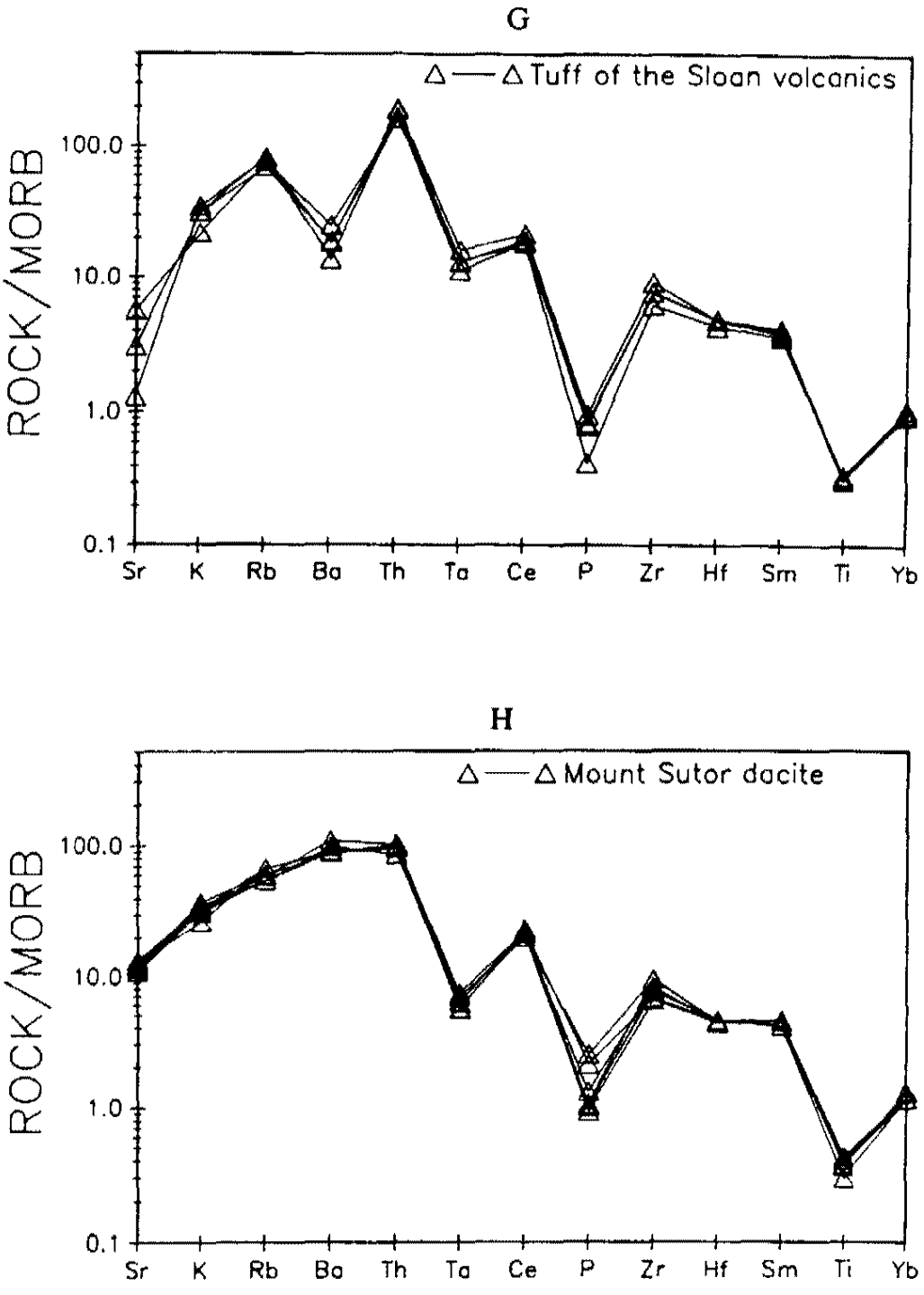

Figure 18: Continued

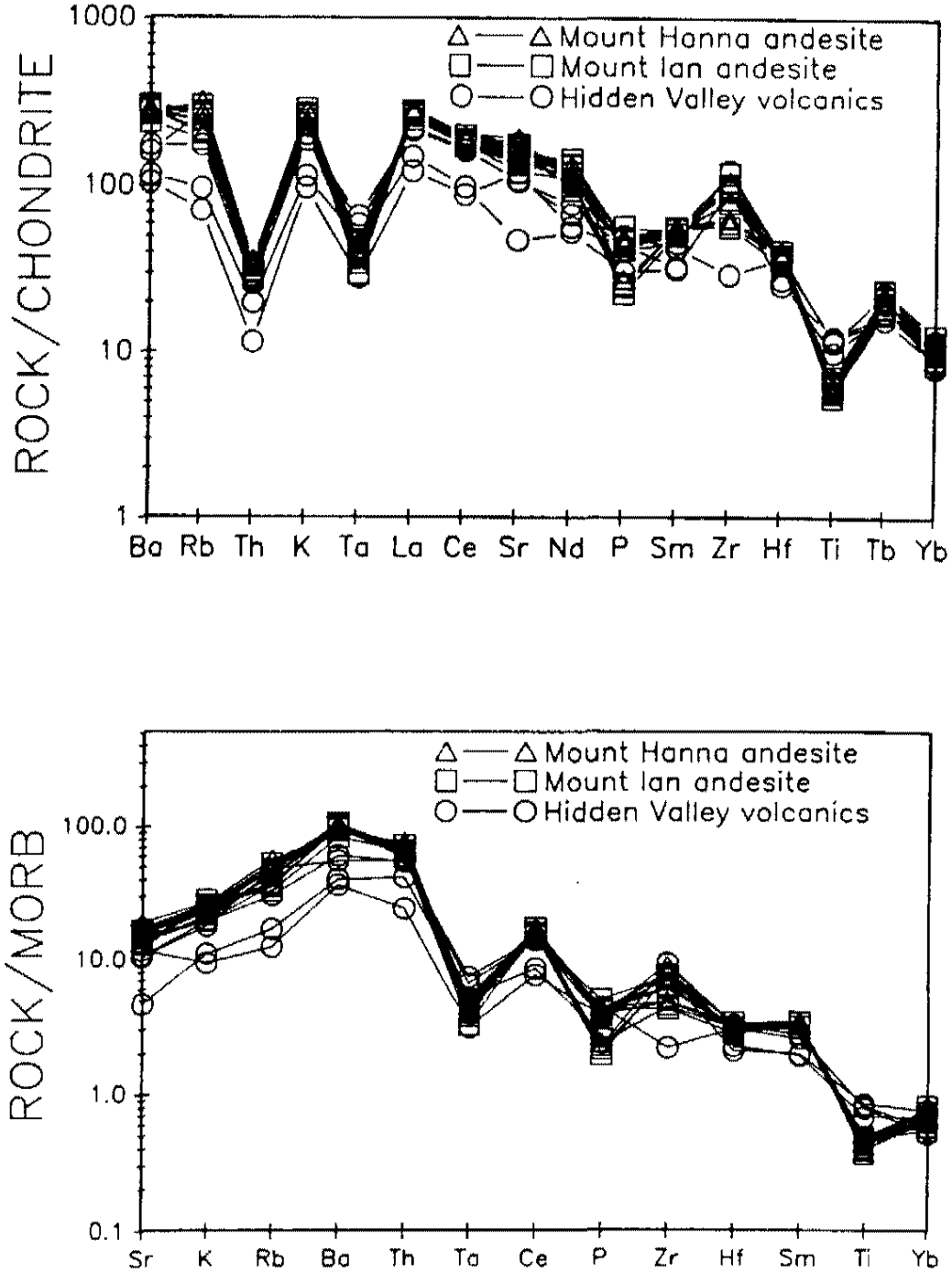

Figure 19: Chondrite and MORB-normalized spider diagrams showing chemical similarities between the Sloan andesites and the Hidden Valley volcanics.

both had a common source.

To determine the regional extent of rocks that share the McCullough Mountain's chemical signature, Tertiary volcanic rocks from the McCullough, Eldorado and River Mountains, Devil Peak, Table Mountain, the White Hills and the Hamblin Cleopatra volcano (Fig. 1) were plotted on spider diagrams. Volcanic rocks with the chemical signature of the McCullough Mountains occur in the McCullough, Eldorado and River Mountains, and the White Hills. There are two other chemically distinct patterns. Felsic volcanic rocks occurring at Table Mountain and Devil Peak in the Spring Range are enriched in Th, Rb and Ta, and depleted in Ba, P and Ti. Basalts of the Hamblin Cleopatra volcano are depleted in Ce, Nd, Sm and La (Figs. 20A-20D).

This type of geochemical analysis suggests that the scale of significant chemical variation of source rocks in the lower crust and mantle in the Las Vegas-Lake Mead area is probably in the tens to hundreds of square kilometers. This analysis also suggests that each source area did not appreciably change chemically over the approximately five Ma represented by rocks exposed in the central McCullough Mountains.

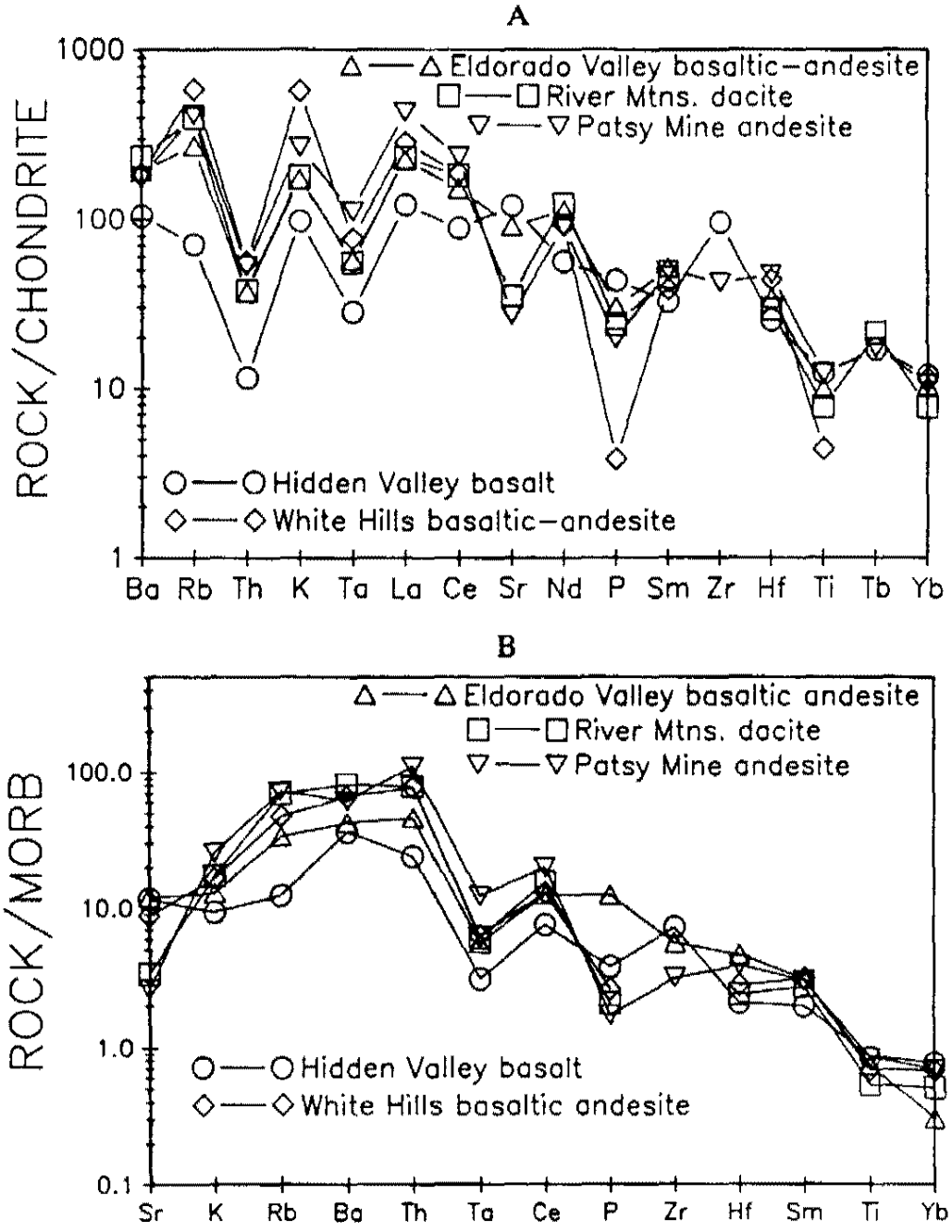

Figure 20: Chondrite and MORB-normalized spider diagrams showing spatial similarities of Tertiary volcanic rocks in the Lake Mead-Las Vegas area. The three chemically distinct groups include rocks from: 1) the McCullough, Eldorado and River Mountains, and the White Hills; 2) the Spring Range (Table Mountain and Devil Peak); 3) the Hamblin Cleopatra volcano.

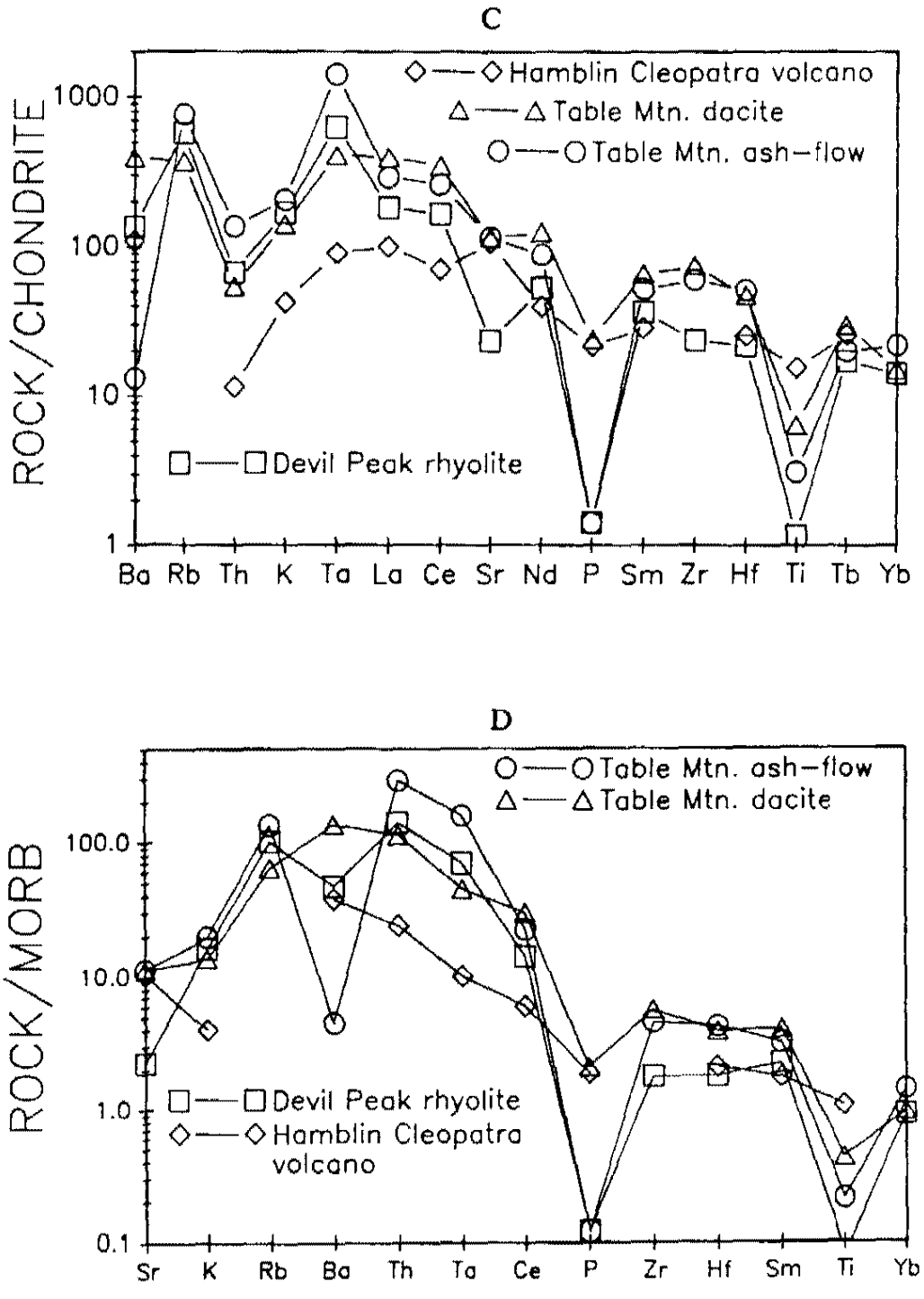

Figure 20: Continued

MAGMA PETROGENESIS

Variations Between Groups of the Sloan Volcanics

Introduction

In this section, three different models for the origin of the Sloan volcanics are introduced and discussed. The models involve magma commingling, crystal fractionation and partial melting. Using petrographic and geochemical evidence, I will show that partial melting of separate sources is responsible for the production of the Sloan volcanics.

Magma Commingling

The production of mid-Miocene intermediate igneous rocks in the Las Vegas-Lake Mead area by mechanisms of magma commingling was documented by Naumann and Smith (1987), Naumann (1987), Larsen (1989) and Larsen and Smith (1991) for the diorite to quartz monzonite of the Wilson Ridge pluton, and by Naumann and Smith (1987) and Naumann (1987) for the andesites and dacites in the northern Black Mountains (Fig.1).

Textural evidence for magma commingling includes: 1) disequilibrium mineral assemblages such as quartz in andesite or olivine in dacite; 2) resorbed, embayed phenocrysts rimmed with glass; 3) plagioclase xenocrysts displaying glass-charged zones (fretted texture); 4) mafic blobs/enclaves in intermediate rocks that show a decrease in phenocryst size toward their margins (Koyaguchi, 1986).

Chemical and textural evidence must be combined to document magma commingling. On chemical plots, rocks formed by magma commingling will plot on a linear variation line between the two end members (Koyaguchi, 1986).

Rocks of the Sloan volcanics do not show petrographic evidence of magma commingling. The Mount Ian andesite, however, contains less than 1% biotite. Biotite may be an equilibrium phase in andesites with SiO_2 greater than 55% (Williams, Turner & Gilbert, 1982), or it may represent a disequilibrium phase that was introduced during magma commingling. Because of the possibility that magma commingling may have contributed to the petrogenesis of the Mount Ian andesite, it was chosen to test magma commingling models for the Sloan volcanics.

Mafic and felsic rocks from the central McCullough Mountains were evaluated as possible end member-magmas for the production of the Mount Ian andesite. A possible mafic end member is the basalt of the Hidden Valley volcanics. Possible felsic end members are the rhyolites of the McCullough Pass volcanics (Schmidt, 1987) and the dacites of the Cinder Prospect member of the Sloan volcanics. A dacite from the Cinder Prospect member of the Sloan volcanics was chosen because it plots on the same linear variation line as the Hidden Valley volcanics and the Mount Ian andesite. The McCullough Pass rhyolites were ruled out because they do not plot on this variation trend.

The computer program XLFRAC (Stormer and Nichols, 1978) (modified by Rob Helvie, 1991) was used to evaluate the possibility that the Mount Ian

Table 4a

Mix model #1: Mixing of Hidden Valley basalt (Mc116) with Cinder Prospect member dacite (Mc121) to produce Mount Ian andesite (Mc77).

Composition	Hidden Valley basalt	Cinder Prospect member dacite	Mount Ian andesite	Model rock	% of dacite added to basalt
SiO2	51.72	69.86	59.28	60.36	69.86
Al2O3	17.05	15.65	17.22	17.53	15.65
Fe2O3	10.44	3.00	7.08	7.21	3.00
CaO	9.35	1.63	4.15	4.23	1.63
MgO	5.15	0.48	1.84	1.87	0.48
Na2O	3.15	3.65	3.62	3.69	3.65
K2O	1.73	5.63	4.41	4.49	5.63
TiO2	1.40	0.11	0.61	0.62	0.11

Above values are in weight percentages Total = 95.35

Sum of the squares of the residuals = 20.04

Table 4b

Mix model #2: Fractionation of olivine clinopyroxene, albite and anorthite from Hidden Valley basalt with addition of Cinder Prospect member dacite to produce Mount Ian andesite. See model #1 for rock compositions.

Phase	Amount added or subtracted from Hidden Valley basalt
Olivine	-2.07
Clinopyroxene	-17.50
Albite	-5.80
Anorthite	-2.00
Cinder Prospect member dacite	68.90

Values are in weight percentages

andesite is a hybrid magma produced by the commingling of the Hidden Valley basalt and dacite of the Cinder Prospect member. Using a mixing model with no fractionation, it is necessary to add 95.35% by volume Cinder Prospect dacite to basalt of the Hidden Valley volcanics (Table 4a). This model is unrealistic for two reasons. First, the sum of the squares of the residuals (R^2) is 20.04. R^2 is the square of the sum of the differences between the observed and calculated weight percentages of each oxide and must be close to 1.00 if the model is to be acceptable at the 99% level of significance. Second, the addition of 95.35% dacite magma to a basalt magma would result in abundant petrographic and field evidence of magma commingling. No mixing textures are evident in The Mount Ian andesite.

Another model was analyzed utilizing the fractionation of olivine, clinopyroxene and plagioclase from Hidden Valley basalt, along with the addition of dacite of the Cinder Prospect member. For this model, it is necessary to add 68.90% dacite to Hidden Valley basalt (Table 4b). The lack of mixing textures suggests that this model is unrealistic.

I suggest, therefore, that magma commingling may be ruled out as a major process in the petrogenesis of the Sloan volcanics.

Fractionation and Partial Melting

If a suite of rocks is produced by fractionation of a common parent, magmas derived by small amounts of fractional crystallization will be enriched in elements compatible with the fractionating phases. Rocks formed by greater

degrees of fractional crystallization will be depleted in these elements. For example, if plagioclase is fractionated, early-forming rocks will be enriched in Ca, Eu and Sr, while later-forming rocks will be depleted in these elements.

A chemical plot of elements compatible with the fractionating phase will display a linear trend with a positive slope. The trend should also display a continuous range of composition with no gaps between rock types. If no fractionation has occurred, rocks will plot in clusters or in vertical or horizontal trends on a compatible element diagram.

Spider plots will also indicate fractionation. If plagioclase has fractionated, a low value or "dip" in the data will occur for elements compatible with this phase. On chondrite-normalized REE diagrams, plagioclase fractionation will result in a Eu anomaly.

Plagioclase and clinopyroxene are common phenocryst phases in rocks of the Sloan volcanics. Fractionation of these phases was evaluated to analyze the relationship between the four rock groups of the Sloan volcanics. On Sr versus Eu, CaO versus Eu (plagioclase compatible), and Sc versus V (clinopyroxene compatible) plots, there are no fractionation trends relating the four rock groups to a common parent (Figs. 16D, 16E & 16I). I conclude, therefore, that the four rock groups of the Sloan volcanics were not produced by fractionation of a common melt. This analysis also suggests that the four groups are not related to each other by a fractionation process.

During partial melting, incompatible elements enter the melt early because

their mineral/liquid distribution coefficients are low. Rocks produced by small amounts of partial melting will be enriched in incompatible elements. Rocks produced by a larger amount of partial melting will be depleted in incompatible elements. On a plot of incompatible elements (Hf versus Th for example), rocks produced by partial melting of a common source will fall on a linear trend with a positive slope, displaying a continuous range of composition. Partial melting of different sources is suggested if data are clustered on incompatible element plots.

The four rock groups of the Sloan volcanics were analyzed to determine whether or not they represent independent partial melts. On incompatible element plots (Hf versus Th and Hf versus Ta), the rocks cluster into the same four chemically distinct groups defined by the major elements (Figs. 16B & 16C). I conclude, therefore, that each rock group evolved by partial melting of a chemically distinct source. The nature of these sources will be discussed in the "Sources for Partial Melting" section.

Variations Within Groups of the Sloan Volcanics

Introduction

In this section, fractionation processes and trends will be evaluated for the andesites, dacites and tuff of the Sloan volcanics. Refer to Figure 16 for trace element diagrams, and Figure 17 for chondrite-normalized REE diagrams.

Andesites

Elements that are compatible with plagioclase (Eu, Sr and Ca) were

plotted to determine if fractionation of this phase occurred in the andesites of the Sloan volcanics. The lack of a positive linear trend on these diagrams for the Mount Hanna andesite suggests that no plagioclase fractionation occurred (Figs. 16D & 16E). A positive linear trend on the Eu versus Sr plot, however, suggests minor plagioclase fractionation in the Mount Ian andesite (Fig. 16D). The lack of a Eu anomaly on the chondrite-normalized REE diagram confirms that plagioclase fractionation was minor (Fig. 17A). No positive linear trends are evident on plots of Cr versus Co and Sc versus V, suggesting no olivine and clinopyroxene fractionation respectively (Figs. 16H & 16I).

Dacites

Dacites and tuffs of the Cinder Prospect member contain phenocrysts of plagioclase and biotite. No plagioclase fractionation trend is apparent on plots of Sr versus Eu and CaO versus Eu (Figs. 16D & 16E). The lack of a Eu anomaly on the chondrite- normalized REE diagram also suggests that plagioclase did not fractionate (Fig. 17B). No biotite fractionation is apparent on a Sr versus Rb (biotite compatible) diagram (Fig. 16F).

An ash-flow tuff in the Cinder Prospect member (sample Mc78) consistently plots outside the Cinder Prospect field on compatible element diagrams. It is approximately 5 weight% lower in SiO_2, 1 weight% higher in CaO and Al_2O_3, and 3.5, 40 and 600 ppm higher in Co, V and Sr respectively than other rocks in its group. On plots of incompatible elements (Th, Ta and Hf), this tuff plots within the field of the Cinder Prospect member (Figs. 16B & 16C).

Fractionation of the tuff before eruption may be responsible for the differences in compatible element abundances.

In the Center Mountain dacite, biotite fractionation is not evident in a plot of Rb versus Sr (Fig. 16F). Chemical plots of CaO versus SiO_2 (Fig. 13D), and the lack of a Eu anomaly on the chondrite-normalized REE diagram (Fig. 17B) indicate that plagioclase did not fractionate.

In the Mount Sutor dacite, chemical plots of CaO versus Eu and Sr versus Eu (Figs. 16D & 16E), and the lack of a Eu anomaly (Fig. 17D) suggest that plagioclase was not fractionated. Plots of Sc versus V and Sr versus Rb indicate no clinopyroxene and biotite fractionation respectively (Figs. 16I & 16F).

The Tuff of the Sloan Volcanics

Chemical plots suggest fractionation of plagioclase, sanidine and clinopyroxene. Plagioclase and sanidine fractionation is suggested by the positive linear trend on a plot of the compatible elements Sr and Eu (Fig. 16D), and by a Eu anomaly on the chondrite-normalized REE diagram (Fig. 17C). Clinopyroxene fractionation is suggested by the positive correlation of the compatible elements Sc and V (Fig. 16I).

Sources for Partial Melting

Introduction

In the previous sections, it was demonstrated that magma commingling and fractionation are not responsible for the production of the four rock groups of the

Sloan volcanics. It was concluded that partial melting of chemically distinct sources was the dominant process. In this section I will propose model source rocks for the Sloan volcanics.

Geochemical modeling was used to explore possible explanations concerning magma petrogenesis. A model is non-unique and must be combined with field and petrographic analyses to be of any merit.

The Pascal computer program MELT was used to evaluate source rock compositions and the amount of partial melting required to produce the andesites and dacites of the Sloan volcanics. MELT uses trace element distribution coefficients (Arth, 1976) and calculates a model rock using the batch melting equation of Shaw (1970). In these models, a critical assumption is the mineralogy and geochemistry of the source rock.

Two source rocks were used in the models. The first is a Precambrian amphibolite exposed in the lower plate of the Saddle Island detachment, Lake Mead (Smith, 1982a, 1984, 1986; Sewall, 1988; Duebendorfer et al., 1990). The amphibolite contains plagioclase (25-40%), actinolite and chlorite. It was assumed that the protolith of the amphibolite was gabbro containing plagioclase and clinopyroxene +/- olivine. Chemistry of the amphibolite (Tables 5a & 5b) is from an unpublished data base (E.I. Smith, University of Nevada, Las Vegas). The Saddle Island amphibolite is a reasonable source rock for the following reasons: 1) it will yield intermediate composition magma upon partial melting; 2) it crops out in the Lake Mead-Las Vegas area; 3) its occurrence in the lower

Table 5a

Melt model #1: Production of Sloan andesite (Mc110)
from 25% partial melting of Saddle Island amphibolite.
All rock compositions are in ppm.

Element	Saddle Island amphibolite composition	Sloan andesite composition	Model Melt composition	Bulk distribution coefficient
Ba	655.00	1800.00	2078.01	0.087
Sr	1396.00	2280.00	1926.18	0.633
Ce	60.07	173.00	169.37	0.140
Nd	31.20	65.50	78.82	0.238
Sm	6.90	10.00	13.17	0.365
Eu	1.81	2.57	3.07	0.454
Yb	1.80	2.53	3.07	0.448
Lu	0.19	0.32	0.34	0.405
Sc	21.45	6.47	13.83	1.735
Cr	113.00	136.00	24.50	5.817
V	291.00	70.60	315.28	0.897
Co	26.30	10.30	29.24	0.866

Mineral modal percentages of source rock:
plagioclase = 30; clinopyroxene = 69; olivine = 1

Table 5b

Melt model #2: Production of Sloan dacite (Mc119)
from 15% partial melting of Saddle Island amphibolite.
All rock compositions are in ppm.

Element	Saddle Island amphibolite composition	Sloan dacite composition	Model Melt composition	Bulk distribution coefficient
Ba	655.00	1780.00	2712.66	0.108
Sr	1396.00	1310.00	1661.51	0.812
Ce	60.07	216.00	224.73	0.138
Nd	31.20	101.00	93.05	0.218
Sm	6.90	14.80	16.13	0.327
Eu	1.81	3.32	3.44	0.442
Yb	1.80	3.84	3.68	0.399
Lu	0.19	0.64	0.42	0.360
Sc	21.45	7.42	14.96	1.510
Cr	113.00	40.20	25.48	5.040
V	291.00	19.20	357.93	0.780
Co	26.30	3.19	34.51	0.720

Mineral modal percentages of source rock:
plagioclase = 40; clinopyroxene = 60

plate of a detachment implies that it probably represents mid-to lower-crustal rocks. The second source is spinel peridotite. Spinel peridotite occurs as xenoliths in alkali basalts in the nearby Fortification Hill field of northwestern Arizona (Wilshire et al., 1988; Nielson and Nakata, in press). Ultramafic xenoliths are also found in the alkali basalt that crops out near the Sloan limestone quarry just to the northwest of Hidden Valley (Plate 1, Appendices A and D). Felsic upper-crustal rocks were not considered as possible source rocks since the amount of partial melting required to produce andesites and dacites is unrealistically high.

Partial Melt Models

Four models were tested. They are:

1) A 25% partial melt of Saddle Island gabbro consisting of 30% plagioclase, 69% clinopyroxene and 1% olivine produces an acceptable model for the production of the Sloan andesites. There is close agreement of the REE concentrations between the model rock and andesite. Concentration of elements compatible with clinopyroxene and olivine (Sc, Cr, V and Co), however, do not match well between the model rock and andesite. Agreement between the model rock and andesite for concentrations of Sr and Ba is very good (Table 5a, Fig. 21).

2) A 15% partial melt of Saddle Island gabbro consisting of 40% plagioclase and 60% clinopyroxene provides a realistic model for the production of the Sloan dacites. With the exception of Lu, there is excellent agreement of all of the REE between the model rock and dacite. There is poor to average

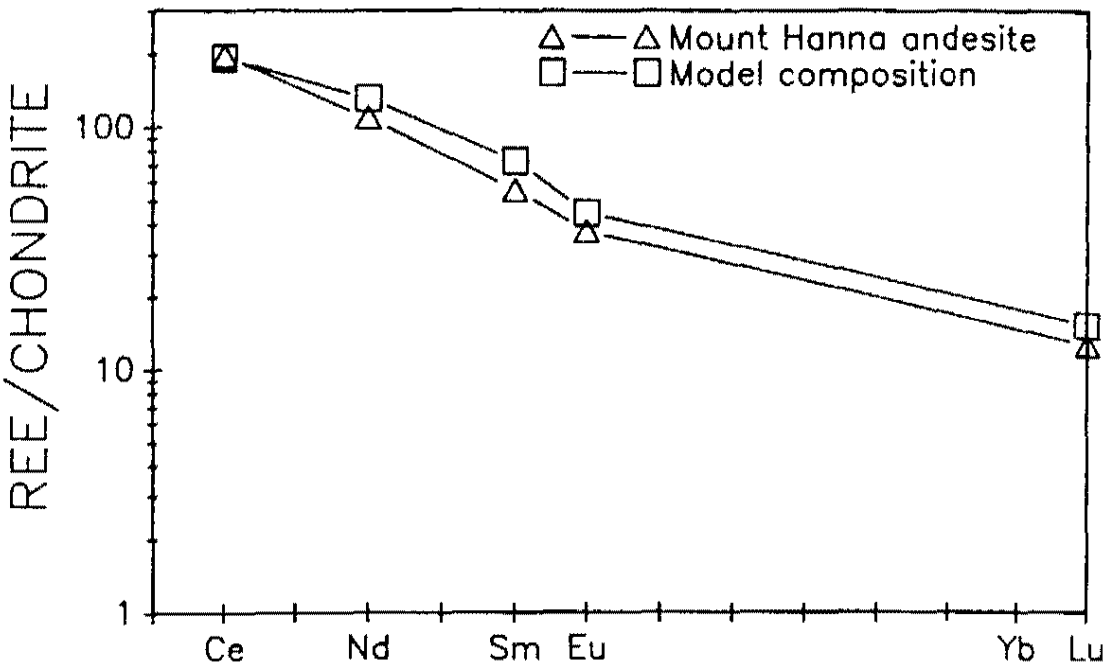

Figure 21: Chondrite-normalized REE diagram showing the chemical similarities between the Sloan andesites (Mc 110) and a 25% partial melt of gabbro.

correspondence between compatible elements (V, Sr and Ba) in the model rock and the dacite (Table 5b, Fig. 22).

3) A 0.5% partial melt of spinel peridotite containing 56.4% olivine, 30.1% orthopyroxene, 10% clinopyroxene and 3.5% spinel, with 2 times chondrite REE concentration did not produce favorable results. The concentrations of Ce, Nd, Sm and Eu in the model rock are lower than the andesite. The concentrations of Yb and Lu in the model rock are higher than the andesite.
(Table 5c, Fig. 23).

4) A 0.5% partial melt of spinel peridotite with the same mineralogy as above, but with concentrations of 10 times chondrite for Ce, Nd and Sm, 3 times chondrite for Eu, and 2 times chondrite for Yb and Lu also does not produce favorable results (Table 5d, Fig. 24). The REE concentration in this model represents a metasomatized mantle that has been enriched in LREE.

Discussion

These models suggest that the Sloan andesites and dacites can be produced from partial melts of a rock similar to the Saddle Island gabbro. It must be kept in mind that using the Saddle Island gabbro as a source rock does not provide a unique solution. The Saddle Island gabbro may have followed a different evolutionary path than the source rocks for the Sloan volcanics. The large amount of variance between the compatible elements may be a reflection of their different petrogenetic histories. Even though these models are non-unique, they constrain the mineralogy and geochemistry of the source rocks for the Sloan

Table 5c

Melt model #3: Production of Sloan andesite (Mc110)
from 0.5% partial melting of peridotite. Rock compositions are in ppm.

Element	Peridotite composition: normalized to chondrite	Sloan andesite composition: normalized to chondrite	Melt composition: normalized to chondrite	Bulk distribution coefficient
Ce	2	196.59	68.47	0.026
Nd	2	109.17	40.06	0.045
Sm	2	55.25	27.71	0.068
Eu	2	37.25	26.22	0.072
Yb	2	12.65	18.52	0.103
Lu	2	9.41	19.39	0.099

Mineral modal percentages of source rock:
olivine = 56.4; orthopyroxene = 30.1;

Table 5d

Melt model #4: Production of Sloan andesite (Mc110)
from 0.5% partial melting of peridotite. Rock compositions are in ppm.

Element	Peridotite composition: normalized to chondrite	Sloan andesite composition: normalized to chondrite	Melt composition: normalized to chondrite	Bulk distribution coefficient
Ce	10	196.59	324.34	0.026
Nd	10	109.17	200.29	0.045
Sm	10	55.25	138.55	0.068
Eu	3	37.25	39.33	0.072
Yb	2	12.65	18.52	0.103
Lu	2	9.41	19.39	0.099

Mineral modal percentages of source rock:
olivine = 56.4; orthopyroxene = 30.1;

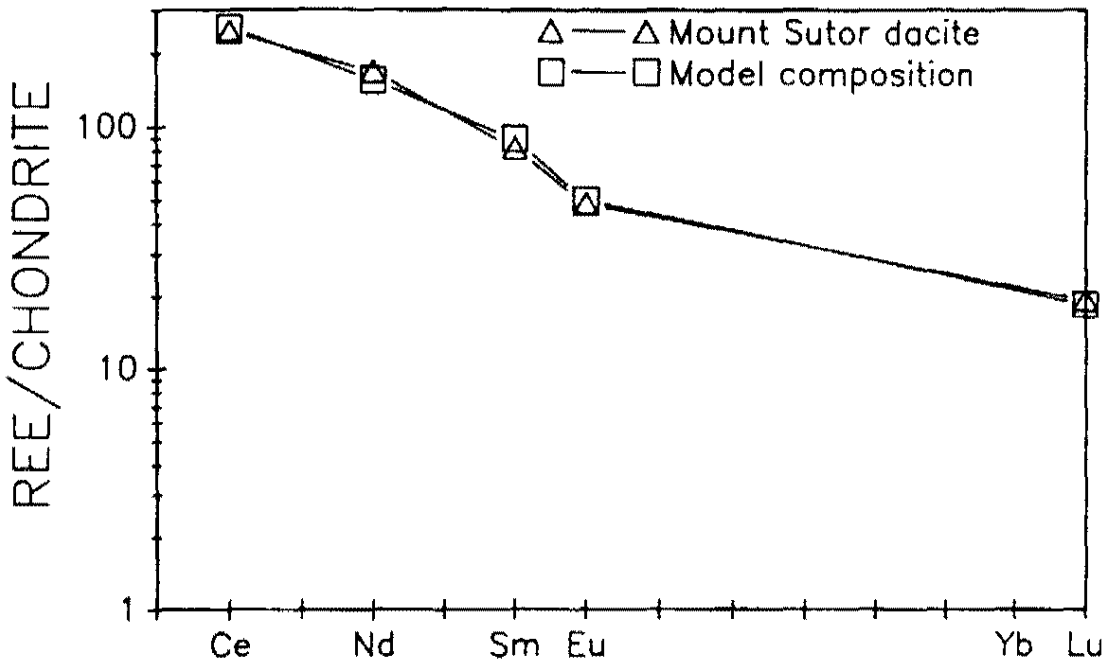

Figure 22: Chondrite-normalized REE diagram showing the chemical similarities between the Sloan dacites (Mc 119) and a 15% partial melt of gabbro.

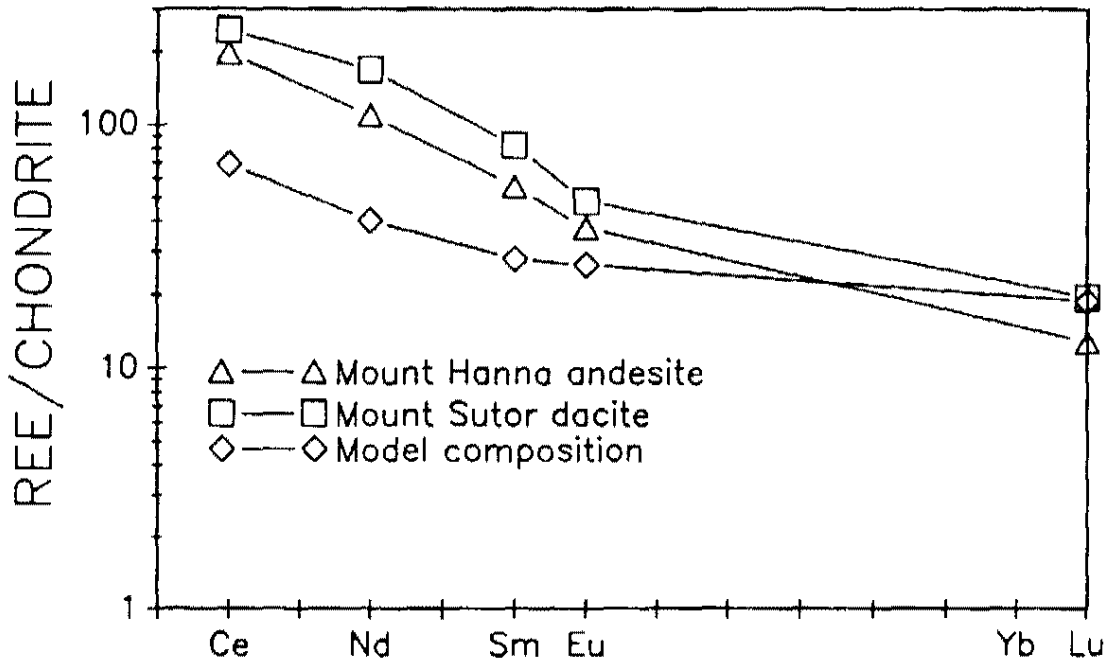

Figure 23: Chondrite normalized REE diagram showing the chemical differences between the Sloan andesites (Mc 110) and dacites (Mc 119), and a 0.5% partial melt of spinel peridotite. Values for the spinel peridotite are two times chondrite concentration.

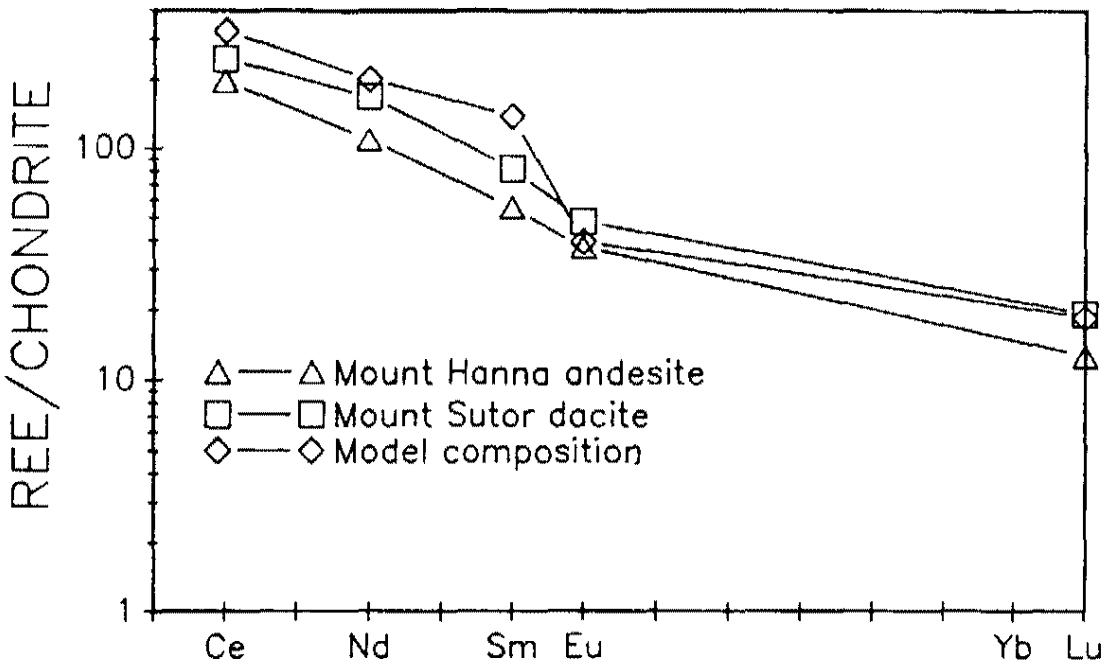

Figure 24: Chondrite-normalized REE diagram showing the chemical differences between the Sloan andesites (Mc 110) and dacites (Mc 119), and a 0.5% partial melt of spinel peridotite. Concentrations used for the spinel peridotote are ten times chondrite for Ce, Nd and Sm, three times chondrite for Eu, and two times chondrite for Yb and Lu.

volcanics.

Crustal Contamination

Geochemistry suggests that rocks of the Sloan volcanics were produced in the mid-to lower-crust by the partial melting of a gabbro. In this section, crustal contamination of rocks of the Sloan volcanics will be evaluated using petrographic and geochemical evidence.

Petrographic evidence for crustal contamination is limited to the Tuff of the Sloan volcanics. The tuffs contain abundant xenoliths, many of them gabbroic.

Sr contents greater than 1,000 ppm rule out large degrees of crustal contamination. Sr contents are normally greater than 1,000 ppm in rocks derived from the lower-crust and mantle. Rocks derived in the upper-crust are enriched in Rb and depleted in Sr (< 1,000 ppm Sr). Crustal contamination, therefore, commonly results in Sr contents less than 1,000 ppm. The high Sr contents in the Mount Hanna and Mount Ian andesites, and the Mount Sutor dacite (> 1,000 ppm) suggests a lack of significant crustal contamination (Appendix B). Volumetrically, these rocks are the dominant lithologies of the Sloan volcanics. In contrast, the dacites and tuffs from the Center Mountain dome complex have Sr contents less than 1,000 ppm (Appendix B). This suggests that residence time in the crust and/or crustal contamination may have played a part in the evolution of these rocks.

THE SLOAN SAG

Evidence for a Sag in Hidden Valley

Introduction

In this section, by using field data, I will demonstrate that there is a structural sag in Hidden Valley.

The Hidden Valley Sag

Even though neither cited evidence, both Hewett (1956) and Longwell (1965) recognized the existence of a semi-circular depression in Hidden Valley. My field mapping has revealed structural evidence for a sag in Hidden Valley. In the northern part of Hidden Valley, the Tuff of Bridge Spring and the Hidden Valley volcanics dip 10°-15° south. Rocks of the Hidden Valley volcanics in the southern part of Hidden Valley dip 20°-30° north. Tuffs and basalts west of Hidden Valley dip about 10° east. East of Hidden Valley, pre-Sloan volcanic rocks dip 10°-30° west (Plate 1).

Additional evidence for a structural depression includes log data from a water well in western Hidden Valley (Plate 1). The drill hole penetrated 700 feet into alluvium, never striking bedrock.

Association to a structural sag may not be the only explanation for the east and west dips about Hidden Valley. The eastward regional dip of the McCullough Mountains (Anderson et al., 1985; Schmidt, 1987) may be responsible for the orientation of pre-Sloan volcanic rocks to the west of Hidden Valley. In

the McCullough Mountains, westward dipping normal faults resulted in eastward stratal tilting of up to 40° (Anderson et al., 1985). An alternate explanation for the westward dips in the northern McCullough Mountains is suggested by the model of Weber and Smith (1987). By using a plot of relatively immobile and incompatible elements (Hf, Ta and Th), Weber and Smith chemically correlated Tertiary plutonic rocks of the Boulder City and Nelson plutons with volcanic rocks of the Eldorado and northern McCullough Mountains (Fig. 2). If their model is correct, the Eldorado and northern McCullough Mountains formed a volcano above the Boulder City and Nelson plutons. Westward dips of volcanic rocks in the northern McCullough Mountains, therefore, may represent the western flank of this stratocone.

Conclusion

The south and north dips of pre-Sloan volcanic rocks to the north and south of Hidden Valley respectively cannot be easily explained by regional trends, and I suggest that they are directly related to the formation of the Sloan sag. Although there are alternative explanations for the east and west dips of pre-Sloan volcanic rocks to the west and east of Hidden Valley respectively, I conclude that the overall inward dips of Pre-Sloan volcanic rocks about Hidden Valley indicates the presence of a structural depression. This conclusion is supported by well-log data.

Classic Caldera, or Volcanotectonic Depression?

Introduction

A physiographic sag filled with and surrounded by volcanic domes and flows is suggestive of a caldera. In this section, evidence for a classic collapse caldera origin for the Sloan sag will be evaluated. Using field evidence, I will show that a classic collapse caldera does not exist in Hidden Valley.

Discussion

Two of the main criteria for the existence of a collapse caldera are: 1) embayed, scalloped and faulted caldera margins with associated slump breccias; 2) an ash-flow tuff related to the caldera (Steven and Lipman, 1976; Steven et al., 1984; Walker, 1984). My initial field mapping concentrated on a search for features suggestive of a classic collapse caldera in Hidden Valley.

The Mount Hanna andesite member of the Sloan volcanics is in direct contact with older basalts of the Hidden Valley volcanics only in the eastern part of the thesis area. In other areas, contacts are covered by alluvium. Careful mapping along this contact demonstrated that it is depositional and is not a fault. In some areas the contact is low-angle and conformable, while in other places it cuts across topography and appears unconformable. (Plate 1). This relationship can be explained by the deposition of the Sloan volcanics on the irregular surface of the Hidden Valley basalt. No slump breccias are found in this, or any other area of Hidden Valley.

Ash-flow tuff occurs in the Center Mountain dome complex and in the western portion of the northern Mount Sutor field. There are also outcrops of ash-flow tuff west of Hidden Valley (Plate 1). Tuff within Hidden Valley is associated with isolated pyroclastic events related to dome formation. Chemical studies demonstrate that the tuff to the west of Hidden Valley is the Tuff of Bridge Spring, a regional ash-flow sheet whose source is unknown. None of the tuff exposures in and around Hidden Valley are associated with a pyroclastic event related to caldera formation.

The lack of slump breccias and an associated ash-flow tuff, argues strongly against a classic collapse caldera origin for the Sloan sag.

Significance of the Mount Hanna Andesite

Introduction

In this section, I will begin to discuss the origin of the Sloan sag by evaluating the significance of the thick pool of Mount Hanna andesite within the depression. High silica lava flows are typically thick and of small areal extent. Walker (1973) reported that rhyolitic lava flows have a median length of 1.1 km, with none longer than 10 km. Felsic to intermediate pyroclastic flows, however, may be very thin and travel greater than 70 km from their source (Henry et al., 1988). Ekren et al. (1984) described extensive "lavalike" rhyolite flows without pyroclastic textures in and adjacent to the Owyhee Mountains and the Owyhee Plateau of southwestern Idaho. Experimental data from one of the Owyhee flows

(the Little Jacks Tuff) suggests that it formed from a dry melt (2% H_2O or less) under pressures as great as 8 kilobars and temperatures of greater than 1,000 °C. Magmas originated from a depth of about 25 km. Similar deposits include the Oligocene Bracks Rhyolite (SiO_2 = 68% to 72%) of the Trans-Pecos volcanic field, Texas, which covers an area of 1,000 km^2 (Henry et al., 1988), and the Middle Proterozoic Yardea Dacite (SiO_2 = 67%) of south Australia, which covers an area of over 12,000 km^2 (Creaser and White, 1991). The Trans-Pecos and Yardea rocks lack pyroclastic textures. Low water content allows devolitilization and fragmentation of magma near the surface. High temperatures produce non-viscous lavas capable of flowing great distances (Henry et al., 1988). If these lavas erupted at lower temperatures and higher water contents, it is reasonable to assume that ash-flow tuffs would have been produced.

Origin of the Mount Hanna Andesite

I propose that the Mount Hanna andesite member of the Sloan volcanics is analogous to a hot, dry ash-flow tuff, similar to the Owyhee, Trans-Pecos and Yardea lavas. Geochemical modeling suggests that the Mount Hanna andesite was produced from partial melting of a gabbroic source at lower-crustal levels (Table 5a, Fig, 21). Sr contents of 1700-2280 ppm for the Mount Hanna andesite suggests a lower-crustal or mantle source for this unit. If these magmas equilibrated at temperatures of 1,000°C (similar to the Owyhee lavas), they originated at a depth of about 25 km, assuming a geothermal gradient of 40°C/km. The aphyric texture of the Mount Hanna andesite (Fig. 25) and the

Figure 25: Microphoto of the Mount Hanna Andesite

lack of fractionation trends on chemical plots (Figs. 16D, 16E, 16H & 16I) suggests that the Mount Hanna andesite rose to the surface quickly, without pausing to substantially cool or fractionate. The high Sr contents also suggest that magma was not significantly contaminated by crustal material, indicating a quick ascent from its source area.

The Mount Hanna andesite erupted from a single vent, creating a large pool (exposed maximum volume of 9 km^3) of andesite lava (Plate 1; cross section C-C'; Fig. 7). The fact that such a large pool of andesite was erupted from a single vent suggests that the magma had a lower viscosity than typical andesite and was capable of flowing greater distances than would be expected of an intermediate composition lava. Its low viscosity may be attributed to high temperature and low gas content.

Sparks and Wilson (1976) proposed that a hot, dry magma will produce an eruptive column that is too dense to mix with the atmosphere. Such a column would consist only of the gas thrust phase, and would be too dense to produce a gaseous convective thrust component. Because of this, Ekren et al. (1984) envisioned lava fountain-type eruptions for the Owyhee rhyolites, as opposed to large Plinian clouds. The Mount Hanna andesite may also have erupted by lava fountaining. Much of this unit is characterized by a mottled, streaky texture consisting of black and red, or black and gray discontinuous patches (Fig.26). This texture may have formed by hot magma rain that produced droplets of magma. Upon hitting the surface, the droplets coalesced, moving away from the

90
89

Figure 26: Photo of the Streaky, Discontinuous Texture of the Mount Hanna Andesite

vent as lava flows.

Duffield (1990) has described similar textures in the Oligocene Taylor Creek Rhyolite of the Mogollon-Datil volcanic field in southwestern New Mexico. He suggests that the streaky "agglunitnated" texture in the rhyolites is a result of lava fountaining. If the magma droplets are hot enough, upon hitting the surface they will coalesce to form homogeneously-textured rocks. Duffield proposes that if the eruptive fountain is high, magma droplets will cool before hitting the surface and not be hot enough to completely coalesce and homogenize. Fluctuating fountain height, therefore, will alternately produce homogeneous and streaky-textured rocks.

Even though the discontinuous streaks in the Mount Hanna andesite are suggestive of a primary volcanic origin, they may also represent highly sheared and attenuated flow foliation. To evaluate the origin of the streaks, I compared their size to the size-frequency distributions of particles produced during lava-fountaining and pyroclastic eruptions. Heiken (1972) determined the mean droplet diameter for a variety of different magma types and eruptive styles. To evaluate if the streaky texture of the Mount Hanna andesite may reflect magma droplets, mean streak diameter was determined. The cross-sectional area of ten streaks from the Mount Hanna andesite (sample Mc115) was measured. Values were adjusted to represent the cross sectional diameter of a sphere. Diameters range from 0.8-6.8 mm, with a mean of 4.08 mm. The mean diameter of the discontinuous streaks in the Mount Hanna andesite is similar to those of magma

droplets produced in the following lava-fountaining events: 1) the basaltic strombolian eruption of Pacaya, Guatemala (6.35 mm); 2) the basaltic phreatomagmatic eruption of Capelinhos, Azores Islands (3.18 mm); 3) the rhyolitic phreatomagmatic eruption of Sugarloaf, San Francisco Mountains, Arizona (3.18 mm) (Heiken, 1972). The correlation of the mean diameter of the discontinuous streaks in the Mount Hanna andesite with recognized lava-fountaining deposits supports a primary origin for the streaks.

Depth of Magma Generation Versus Depth of Eruption

Magma must migrate to shallow crustal levels before devolatilization of gases can occur, resulting in fragmentation and eruption. For magmas with SiO_2 contents comparable to the Sloan andesites and dacites, the level at which gas exsolution and magma fragmentation can occur is approximately 5.4 km (Fisher and Schmincke, 1984). Magmas with H_2O contents of 2% or less may devolatilize and fragment even closer to the surface. The above information suggests that the Mount Hanna andesite resided at these shallower depths long enough only to exsolve gas and fragment before erupting. Exsolution of gases, therefore, probably occurred in the conduit as opposed to within shallow chambers.

Formation of the Sloan Sag

Introduction

I will now consider the formation of the sag, and will suggest that: 1) the Sloan volcanics filled pre-existing grabens and half-grabens bounded by the

McCullough Wash fault system; 2) sagging in Hidden Valley occurred during and/or after the eruption of the Sloan volcanics.

The McCullough Wash Fault System

The McCullough Wash fault is the only major internal structure in the McCullough Mountains. South of Hidden Valley in the South McCullough Wilderness Study Area, this fault places Precambrian basement against rocks of the Hidden Valley volcanics and has at least 600 m of throw. Displacement decreases to the north. North of the wilderness study area, it splays into three northeast striking faults (Anderson et al, 1985). East and west dipping splays of the McCullough Wash fault system produced numerous grabens and half-grabens in the area of the McCullough Pass caldera, just south of Hidden Valley (Schmidt, 1987). These faults display only minor offset. The McCullough Wash fault system probably continues north into Hidden Valley. Most of these faults are covered by alluvium and possibly by domes and flows of the Sloan volcanics. A north-south striking, west-dipping, normal fault on the west side of the ridge just to the north of the McCullough Pass caldera (Plate 1) offsets pre-Sloan volcanic rocks, and may represent the northward projection of the McCullough Wash fault system. I propose that Hidden Valley is cut by a series of grabens and half-grabens bounded by faults of the McCullough Wash fault system. Field mapping has also revealed an en-echelon splay of the McCullough Wash fault in Hidden Valley. The sharp, steep linear escarpment of the Mount Hanna andesite and Mount Sutor dacite in the eastern portion of Hidden Valley is suggestive of a

fault scarp (Plate 1). This type of en-echelon relationship of normal faults is common and has been documented in many areas including the East African rift zone (Morley, 1988 & 1989) and the Dead Horse graben of west Texas (Maler, 1990). The strike of this fault changes from north-south to northwest-southeast in the area of the Mount Sutor stock (Plate 1). Rocks of the Mount Hanna andesite and Mount Sutor dacite are offset by this fault suggesting that it was active after eruption of these units. The McCullough Wash fault system does not appear to extend farther to the north of Hidden Valley, and its displacement decreases to the south. Based on mapping done by Schmidt (1987) along the south rim of Hidden Valley, faults may be spaced every 300 m. Accumulated displacement on buried and exposed faults in Hidden Valley is estimated to be at least 2.25 km.

Sagging and Tectonic Control

Faults of the McCullough Wash system strike north-south. If subsidence was controlled entirely by these faults, north-south oriented grabens would have formed in Hidden Valley. This is the case in the northern segment of the McCullough Pass caldera south of Hidden Valley (Schmidt, 1987). Subsidence was accommodated by faults of the McCullough Wash system, resulting in a north-south trending graben. In the case of the Sloan sag, however, contacts cut across these north-south striking structures. I propose, therefore, that sagging in Hidden Valley resulted from rejuvenation on the McCullough Wash fault system in the east and northeast, and sagging into emptied magma chambers in the west.

Summary of Events

A scenario for the formation of the Sloan sag is described below (refer to Figure 27).

1) Before the eruption of the Sloan volcanics, Hidden Valley consisted of a series of grabens and half grabens, bounded by the north-south striking McCullough Wash fault system.

2) The Mount Hanna andesite and rocks of the Center Mountain dome complex were the first members of the Sloan volcanics to erupt. The Mount Hanna andesite was generated at depths as great as 25 km by partial melting of gabbro, rising to the surface and erupting quickly in a lava-fountaining event. Eruption of this unit caused sagging by reactivating faults of the McCullough Wash system in eastern Hidden Valley. Fault movement produced a surface sag over the emptied chamber. Unlike other units of the Sloan volcanics which were emitted from numerous vents and domes, the Mount Hanna andesite erupted from a single vent resulting in a pool of andesite with a maximum exposed volume of 9 km^3.

3) Volcanic dome formation is represented by the rocks of the Center Mountain dome complex. Ash-flow tuffs of the Cinder Prospect member and the Tuff of the Sloan volcanics represent the early stages of pyroclastic and phreatomagmatic activity, reflecting tuff ring formation. The tuff ring was intruded by the Center Mountain dacite. The Mount Ian andesite intruded rocks of the Center Mountain dome complex, resulting in the formation of platy,

96
95

Figure 27: Formation Sequence of the Sloan Sag

foliated andesite domes, many of which overlie tuff rings. The Mount Sutor dacite erupted from numerous vents and domes resulting in two large pools of viscous biotite dacite.

Subsidence into shallow chambers occurred during and/or after the eruption of these units. Sagging caused renewed movement on a splay of the McCullough Wash fault system, offsetting rocks of the Mount Hanna andesite and the Mount Sutor dacite in the northeast part of Hidden Valley.

CONCLUSIONS

Important conclusions of this thesis are:

1) A volcanotectonic depression in Hidden Valley resulted from the eruption of the Sloan volcanics.

2) Sagging was accommodated by a combination of displacement on splays of the McCullough Wash fault system in eastern and northeastern Hidden Valley, and sagging into evacuated magma chambers in the western part of the valley.

3) The rocks of the Sloan volcanics belong to four magma groups, each of which were produced by partial melting of chemically distinct sources.

4) Partial melting of a crustal source similar to the Saddle Island amphibolite produced the andesites and dacites of the Hidden Valley volcanics.

5) Except for rocks of the Center Mountain dome complex, magmas rose through the crust rapidly without experiencing significant crystal fractionation or crustal contamination.

6) The Mount Hanna andesite member of the Sloan volcanics erupted a large pool (approximately 9 km^3) of lava from a single vent. This unit may have been emplaced as a hot (1,000 °C), dry (2% H_2O or less) analog of an ash-flow tuff in a lava-fountaining event. If this magma had erupted at lower temperatures and higher water contents, a plinian-style eruption probably would have occurred, resulting in an ash-flow tuff.

FUTURE WORK

As in any research project, unanswered questions and problems arise that cannot be answered due to time and/or financial constraints. The following is a list of projects that may provide important information about the McCullough Mountains and the southern Basin-and-Range.

1) The $^{40}Ar/^{39}Ar$ date of the Tuff of Bridge Spring is the only reliable date yet obtained from the north-central McCullough Mountains. $^{40}Ar/^{39}Ar$ dates on rocks stratigraphically above and below this unit will help constrain the absolute age and timing of eruption of the volcanic units.

2) The exotic trace mineral assemblage in the lower-most rhyolite tuff of the Tuff of the Sloan volcanics (sample Mc59a) is intriguing. Even though this tuff contains monazite, allanite, epidote, zircon and sphene, its incompatible trace element concentration is not higher than the other tuffs from this unit. A detailed study of mineral chemistry is required to understand the geochemistry of this unit.

3) Detailed geologic mapping has never been done north of Hidden Valley. Work in the northern McCullough Mountains will test the Weber and Smith (1987) hypothesis that a stratocone exists in this area.

4) Geochemistry suggests that volcanic rocks from the White Hills, and the River, Eldorado and McCullough Mountains have similar sources. A geochemical study of igneous rocks from a larger part of the southern Basin-and-Range may help us understand the scale of heterogeneity of crustal and mantle sources.

5) The hot, dry, fountaining-eruption mechanism of the Mount Hanna

andesite is unique. Such an eruptive mechanism may be the crux to understanding the large areal extent of some felsic-to-intermediate lavas. Unless they erupt as ash-flow tuffs, intermediate-to-felsic lavas usually form short, thick deposits. The discontinuous, streaky texture displayed in the Mount Hanna andesite and the Taylor Creek rhyolites may be indicative of a lava-fountaining mechanism. Detailed mapping of the Mount Hanna andesite field along with petrographic and geochemical studies are needed to help us further understand what may be a significant eruptive mechanism.

REFERENCES CITED

Anderson, R.E., 1971, Thin-skinned distension in Tertiary rocks of south-eastern Nevada: Geological Society of America Bulletin, v. 82, p. 42-58.

Anderson, R.E., 1977, Geologic map of the Boulder City 15 minute quadrangle, Clark County, Nevada: U.S. Geological Survey Geologic Quadrangle Map GQ-1394.

Anderson, J.L., Young, E.D., Clarke, S.H., Orrell, S.E., Winn, M., Schmidt, C.S., Weber, M.E. and Smith, E.I., 1985, The geology of the McCullough Range Wilderness Area, Clark County, Nevada: Technical Report, University of Southern California, Los Angeles, 46 pp.

Arth, J.G., 1976, Behavior of the trace elements during magmatic processes; A summary of theoretical models and their applications: U.S. Geological Survey Journal of Research, v. 4, no. 1, p. 41-47.

Bingler, E.C. and Bonham, H.F. Jr., 1972, Reconnaissance geologic map of the McCullough Range and adjacent areas, Clark County, Nevada: Nevada Bureau of Mines and Geology, Special Map 45.

Carr, M.D., 1983, Geometry and structural history of the Mesozoic thrust belt in the Goodsprings district, southern Spring Mountains, Nevada: Geological Society of America Bulletin, v. 94, p. 1185-1198.

Cascadden, T.E., 1991, Styles of volcanism and extensional tectonics in the eastern Basin-and-Range province: northern White Hills, Arizona: Unpublished Masters Thesis, University of Nevada, Las Vegas, 156 pp.

Cole, J.W., 1979, Structure, petrology, and genesis of Cenozoic volcanism, Taupo volcanic zone, New Zealand. A review: New Zealand Journal Geol. Geophysics, v. 22, p. 631-657.

Creaser, R.A. and White, A.J.R., 1991, Yardea Dacite--large-volume, high-temperature felsic volcanism from the Middle Proterozoic of south Australia: Geology, v. 19, p. 48-51.

De Witt, E, Anderson, J.L., Barton, H.N., Jachens, R.C., Podwysocki, M.H., Brickley, D.W. and Close, T.J., 1989, Mineral resources of the South McCullough Mountains Wilderness Study Area, Clark County, Nevada: U.S. Geological Survey Bulletin 1730-C, 24 pp.

Damon, P.E., 1971, The relationship between late Cenozoic volcanism and tectonism and orogenic-epeirogenic periodicity: in Conference on Late Cenozoic Glacial Ages, Turekian, K.K., editor, John Wiley and Sons, New York, p. 15-35.

Duebendorfer, E.M., Sewall, A.J. and Smith, E.I., 1990, The Saddle Island detachment; An evolving shear zone in the Lake Mead area, Nevada: Geological Society of America Memoir 176, p. 77-97.

Duebendorfer, E.M. and Wallin, E.T., 1991, Basin development and syntectonic sedimentation associated with kinematically coupled strike-slip and detachment faulting, southern Nevada: Geology, v. 19, p. 87-90.

Duffield, W.A., 1990, Eruptive fountains of silicic magma and their possible effects on the tin content of fountain-fed lavas, Taylor Creek Rhyolite, New Mexico: in Stein, H.J. and Hannah, J.L., eds., Ore-bearing granite systems; Petrogenesis and mineralizing processes: Geological Society of America Special Paper 246, p. 251-261.

Ekren, E.B., McIntyre, D.H. and Bennet, E.H., 1984, High-temperature, large-volume lavalike ash-flow tuffs without calderas in southwestern Idaho: Geological Survey Professional Paper 1272, 73 pp.

Feuerbach, D.L., 1986, Geology of the Wilson Ridge pluton; a mid-Miocene quartz monzonite intrusion in the northern Black Mountains, Mojave County, Arizona and Clark County, Nevada: Unpublished Masters Thesis, University of Nevada, Las Vegas, 79 p.

Fisher, R.V. and Schminke, H.V., 1984, Pyroclastic Rocks, Springer-Verlag, New York, 472 p.

Goddard, E.N., Trask, P.D., De Ford, R.K., Rove, O.N., Singewald Jr, J.T. and Overbeck, R.M., 1970, Rock-color chart: The Geological Society of America, Boulder, Colorado.

Glazner, A.F., 1990, Recycling of continental crust in Miocene volcanic rocks from the Mojave Block, southern California: Geological Society of America Memoir 174.

Grindley, G.W., 1965, The geology, structure, and exploitation of the Wairakei geothermal field: New Zealand Geological Survey Bulletin 75.

Heiken, G., 1972, Morphology and petrography of volcanic ashes: Geological Society of America Bulletin, v. 83, p. 1961-1988.

Henry, C.D. and Price, J.G., 1986, The Van Horn Mountains Caldera, Trans-Pecos Texas: Bureau of Economic Geology, University of Texas at Austin, Report of Investigations No. 151, 46 pp.

Henry, C.D., Price, J.G., Rubin, J.N., Parker, D.F., Wolff, J.A., Self, S., Franklin, R. and Barker, D.S., 1988, Widespread, lavalike silicic volcanic rocks of Trans-Pecos, Texas: Geology, v. 16, p. 509-512.

Hewett, D.F., 1956, Geology and mineral resources of the Ivanpah Quadrangle, California and Nevada: U.S. Geological Survey Professional Paper 275, 172 pp.

Irvine, T.N. and Baragar, W.R.A., 1971, A guide to the chemical classification of the common volcanic rocks: Canadian Journal of Earth Sciences, v. 8, p. 523-548.

Kohl, M.S., 1978, Tertiary volcanic rocks of the Jean-Sloan area, Clark County, Nevada and their possible relationship to carnotite occurrences in caliches: Unpublished Masters Thesis, University of California, Los Angeles, 117 pp.

Koyaguchi, T., 1986, Textural and compositional evidence for magma mixing and its mechanism, Abu volcano group, southwestern Japan: Contributions to Mineralogy and Petrology, v. 93, p. 33-45.

Larsen, L.L., 1989, The origin of the Wilson Ridge Pluton and its enclaves, northwest Arizona: implications for the generation of a calc-alkaline intermediate pluton in an extensional environment: Unpublished Masters Thesis, University of Nevada, Las Vegas, 81 pp.

Larsen, L.L. and Smith, E.I., 1990, Mafic enclaves in the Wilson Ridge pluton, northwestern Arizona: implications for the generation of a calc-alkaline intermediate pluton in an extensional environment: Journal of Geophysical Research, v. 95, no. B11, p. 17,693-17,716.

Lipman, P.W., 1984, The roots of ash-flow calderas: windows into granitic batholiths: Journal of Geophysical Research, v. 89, p. 8801-8841.

Longwell, C.R., Pampeyan, E.H., Bower, B. and Roberts, R.J., 1965, Geology and mineral deposits of Clark County, Nevada: Nevada Bureau of Mines and Geology Bulletin 62, 218 pp.

Maler, M.O., 1990, Dead Horse graben: A west Texas accommodation zone: Tectonics, v. 9, no. 6, p. 1357-1368.

McMillan, N.J. and Dungan, M.A., 1986, Magma mixing as a petrogenetic process in the development of the Taos Plateau volcanic Field, New Mexico: Journal of Geophysical Research, v. 91, no. B6, p. 6029-6045.

Mills, J.G., 1985, The geology and geochemistry of volcanic and plutonic rocks in the Hoover Dam 7.5 minute quadrangle, Clark County, Nevada and Mojave County, Arizona: Unpublished Master's Thesis, University of Nevada, Las Vegas, 119 p.

Morley, C.K., 1988, Variable extension in Lake Tanganyika: Tectonics, v. 7, no. 4, p. 785-801.

Morley, C.K., 1989, Extension, detachments, and sedimentation in continental rifts (with particular reference to east Africa): Tectonics, v. 8, no. 6, p. 1175-1192.

Naumann, T.R., 1987, Geology of the central Boulder Canyon Quadrangle, Clark County, Nevada: Unpublished Master's Thesis, University of Nevada, Las Vegas, 68 pp.

Naumann, T.R. and Smith, E.I., 1987, Evidence for magma mixing in Mid-Tertiary volcanic rocks, Lake Mead region, southern Nevada: Geological Society of America Abstracts with Programs, v. 19, p. 435-436.

Nielson, J.E. and Nakata, J.K., (manuscript in review), Geology and origin of mafic dikes, and their megacryst-xenolith inclusions, Black Canyon, Arizona.

Nielson, R.L. and Dungan, M.A., 1985, The petrology and geochemistry of the Ocate volcanic field, north-central New Mexico: Geological Society of America Bulletin, v. 96, p. 296-312.

Novak, S.W and Bacon, C.R., 1986, Pliocene rocks of the Coso Range, Inyo County, California: U.S. Geological Survey Professional Paper 1383, 44 p.

Pearce, J.A., 1983, The role of sub-continental lithosphere in magma genesis at destructive plate margins: in Continental basalts and mantle xenoliths, Hawkesworth, C.J and Narry, M.J., editors, Nantwich: Shiva.

Schmidt, C.S., 1987, A Mid-Miocene caldera in the central McCullough Mountains, Clark County, Nevada: Unpublished Masters Thesis, University of Nevada, Las Vegas, 78 pp.

Sewall, A.J., 1988, Structure and geochemistry of the upper plate of the Saddle Island detachment, Lake Mead, Nevada: Unpublished Masters Thesis, University of Nevada, Las Vegas, 84 pp.

Shaw, D.M., 1970, Trace element fractionation during anatexis: Geochim. Cosmochim. Acta, v. 34, p. 237-243.

Smith, E.I., 1973, Mono Craters, California: A new interpretation of the eruptive sequence: Geological of America Bulletin, v. 84, p. 2685-2690.

Smith, E.I., 1982, Geology and geochemistry of the volcanic rocks in the River Mountains, Clark County, Nevada and comparisons with volcanic rocks in nearby areas: in Frost, E.G. and Martin, D.L., eds, Mesozoic - Cenozoic tectonic evolution of the Colorado River region, California, Arizona, Nevada: Dan Diego, California, Cordilleran Publishers, p. 41-54.

Smith, E.I., 1984, Geological map of the Boulder Beach Quadrangle, Nevada: Nevada Bureau of Mines and Geology Map 81, scale 1:24,000.

Smith, E.I., 1986, Geology of the River, Eldorado, and McCullough Ranges, Clark County, Nevada: in Rowland, S.M., ed., Field guide to the geology of Nevada, Las Vegas: Las Vegas, Nevada, p. 22-64.

Smith, E.I., Schmidt, C.S. and Mills, J.G., 1988, Mid-Tertiary volcanoes in the Lake Mead area of southern Nevada and Northwestern Arizona: in Weide, D.L. and Faber, M.L., eds, This extended land: Geological journeys in the southern Basin-and-Range: Field trip guidebook, Geological Society of America, Cordilleran section meeting, Las Vegas, Nevada, p. 107-122.

Smith, E.I., Feuerbach, D.L., Naumann, T.R. and Mills, J.G., 1990, Mid-Miocene volcanic and plutonic rocks in the Lake Mead area of Nevada and Arizona; Production of intermediate volcanic rocks in an extensional environment: Geological Society of America Memoir 174, p. 169-194.

Smith, E.I., Feuerbach, D.L. and Duebendorfer, E.M., 1991, Magmatism, extensional tectonics and sedimentation in the Lake Mead area, Nevada and Arizona: a new model: Geological Society of America Abstracts With Programs, Cordilleran Section, v. 23, no. 2, p. 99.

Smith, R.L. and Bailey, R.A., 1968, Resurgent cauldrons, in Coats, R.R., and others, eds., Studies in volcanology: Geological Society of America Memoir 116, p. 613-662.

Sparks, R.J. and Wilson, L., 1976, A model for the formation of ignimbrites by gravitational column collapse: Journal of the Geological Society of London, v. 132, p. 441-451.

Steven, T.A., 1981, Three Creeks caldera, southern Pavant Range, Utah: Brigham Young University Geol. Stud., v. 28, p 1-7.

Steven, T.A. and Lipman, P.W., 1976, Calderas of the San Jaun Volcanic Field, southwestern Colorado: U.S. Geological Survey Professional Paper 958, 35 pp.

Steven, T.A., Rowley, P.D. and Cunningham, C.G., 1984, Calderas of the Marysvale Volcanic Field, west central Utah: Journal of Geophysical Research, v. 89, p. 8751-8764.

Stormer, J.C. and Nichols, J., 1978, XLFRAC: A program for the interactive testing of magmatic differentiation models: Computers and Geoscience, v. 4, p. 143-159.

Thompson, R.N., Morrison, M.A., Hendry, G.L. and Parry, S.J., 1984, An assessment of the relative roles of crust and mantle in magma genesis: Phil. Trans. R. Soc. London, A310, p. 541-590.

Walker, G.P.L., 1973, Lengths of lava flows: Royal Society of London Philosophical Transactions, ser. A, v. 274, p. 286-302.

Walker, G.P.L., 1984, Downsag calderas, ring faults, caldera sizes, and incremental caldera growth: Journal of Geophysical Research, v. 89, p. 8407-8416.

Walker, J.D., Beaufait, M.S. and Zelt, F.B., Geology of the Devil Peak area, Spring Mountains, Nevada: Geological Society of America Abstracts With Programs, Cordilleran Section, v. 13, no. 2, p. 112.

Weber, M.E., and Smith, E.I., 1987, Structural and geochemical constraints on the reassembly of disrupted Mid-Miocene volcanoes in the Lake Mead-Eldorado Valley area of southern Nevada: Geology, v. 15, p. 553-556.

Wernicke, B., Axen, G.J. and Snow, J.K., 1988, Basin-and-Range extensional tectonics at the latitude of Las Vegas, Nevada: Geological Society of America Bulletin, v. 100, p. 1738-1757.

Williams, H., Turner, F.J. and Gilbert, C.M., 1982, Petrography: An introduction to the study of rocks in thin sections, W.H. Freeman and Company, New York, p. 139-142.

Wilshire, H.G., Meyer, C.E., Nakata, J.K., Calk, L.C., Shervais, J.W., Nielson, J.E. and Schwarzman, E.C., 1988, Mafic and ultramafic xenoliths from volcanic rocks of the western United States: U.S. Geological Survey Professional Paper 1443, 179 pp.

Wood, C.A., 1984, Calderas: a planetary perspective: Journal of Geophysical Research, V. 89, p. 8391-8406.

APPENDIX A: SAMPLE LOCATION AND PETROGRAPHY

Colors are from the Geological Society of America rock-color chart.

TUFF OF BRIDGE SPRING

Sample number: Mc53
Location: NW 1/4, Sec 31, T23S, R61E, Sloan, Nev. 7 1/2' quad: tuff that underlies Thvb in the NE part of the thesis area.
Rock name: Welded dacitic ash-flow tuff
Description: Pyroclastic, eutaxitic and hypocrystalline consisting of fragmented phenocrysts of subhedral, oscillatory sanidine up to 3 mm (24.2%), subhedral, oscillatory plagioclase up to 2.5 mm (3.4%), sub-euhedral, hematized biotite up to 2 mm (3.4%), an-subhedral clinopyroxene up to 1 mm (0.8%), anhedral, oscillatory quartz up to 1 mm (0.6%), sub-euhedral sphene up to 0.5 mm (0.4%), Fe-Ti oxides up to 0.5 mm (0.2%) and trace zircon. Pumice fiamme (9.6%) are devitrified, rarely spherulitic and up to several cm long. Basaltic and granodioritic rock fragments (1.2%) are up to 1 cm. The pale red-colored groundmass (56.2%) consists of devitrified glass and glass shards. Shards wrap around phenocrysts and lithic fragments.

Sample number: Mc60
Location: NW 1/4, Sec 32, T24S, R60E, Jean, Nev. 7 1/2' quad: collected near the intersection of Las Vegas Blvd. and the dirt entrance road to Jean Lake.
Rock Name: Moderately welded dacitic ash-flow tuff
Description: Pyroclastic and hypocrystalline consisting of fragmented phenocrysts of subhedral, oscillatory sanidine up to 2 mm (7.5%), subhedral, oscillatory plagioclase up to 1 mm (1.5%), anhedral quartz up to 0.5 mm (0.8%), subhedral, oxidized biotite up to 1.5 mm (0.6%), an-subhedral clinopyroxene up to 0.5 mm (0.2%), sub-euhedral sphene < 0.5 mm (0.4%), trace Fe-Ti oxides up to 0.5 mm and trace zircon. Flattened, devitrified pumice (2.2%) is up to 1 cm in length. Basaltic, gabbroic and granodioritic rock fragments (0.8%) are up to 1 cm. The pale grayish pink-colored groundmass (86%) consists of devitrified glass and glass shards. Shards wrap around phenocrysts and lithic fragments.

Sample number: Mc62
Location: SE 1/4, Sec 31, T24S, R60E, Jean, Nev. 7 1/2' quad: collected approximately 1 mile S-SE from where the railroad tracks cross under Las Vegas Blvd.
Rock name: Welded dacitic ash-flow tuff

Description: Pyroclastic, eutaxitic and hypocrystalline consisting of fragmented phenocrysts of subhedral, oscillatory sanidine up to 2 mm (4.2%), subhedral, oscillatory plagioclase up to 2 mm (2.8%), anhedral, oscillatory quartz up to 1 mm (1.2%), sub-euhedral, oxidized biotite up to 2 mm (1.0%), Fe-Ti oxides up to 0.5 mm (0.4%), subhedral clinopyroxene up to 2 mm (0.4%), sub-euhedral sphene < 0.5 mm (0.6%) and trace zircon. Pumice fiamme (1.4%) are devitrified and up to 2 cm. Basaltic and granitic rock fragments (1.2%) are up to several cm. The pale red-colored groundmass (86.8%) consists of devitrified glass and glass shards. Shards wrap around phenocrysts and lithic fragments.

Sample: Mc64b
Location: SW 1/4, Sec 2, T24S, R60E, Sloan, Nev. 7 1/2′ quad: collected from the southernmost Tbs exposure west of I-15.
Rock name: Non-welded rhyolitic ash-flow tuff
Description: Pyroclastic and hypocrystalline consisting of fragmented phenocrysts of subhedral, oscillatory sanidine up to 3 mm (6.0%), subhedral, oxidized biotite up to 1 mm (1.8%), anhedral, oscillatory quartz up to 1 mm (1.0%), subhedral, oscillatory plagioclase up to 1 mm (0.8%), an-subhedral clinopyroxene up to 0.5 mm (0.2%), sub-euhedral sphene up to 0.5 mm (0.2%), Fe-Ti oxides up to 0.5 mm (trace) and trace zircon. Spongy devitrified pumice (2.2%) is up to 2 cm. Basaltic rock fragments (1.8%) are up to several cm. The grayish pink-colored groundmass (86%) consists of devitrified glass and glass shards. Shards wrap around phenocrysts and lithic fragments.

Sample number: Mc66
Location: SE 1/4, Sec 35, T23S, R60E, Sloan, Nev. 7 1/2′ quad: collected from the small Tbs exposure surrounded by Thvb: approximately 1,000′ west of the railroad tracks.
Rock name: Partially-welded dacitic ash-flow tuff
Description: Pyroclastic and hypocrystalline consisting of fragmented phenocrysts of subhedral, oscillatory sanidine up to 3 mm (5.4%), subhedral, oxidized biotite up to 1 mm (1.6%), anhedral, oscillatory quartz up to 1 mm (1.0%), subhedral, oscillatory plagioclase up to 1.5 mm (1.2%), an-subhedral clinopyroxene up to 1 mm (0.8%), sub-euhedral sphene up to 0.5 mm (0.4%), Fe-Ti oxides up to 0.5 mm (0.2%) and trace zircon. Flattened devitrified pumice (3.4%) is up to 3 cm long. Basaltic, granodioritic and gabbroic rock fragments (3.0%) are up to several cm. The pale pink-colored groundmass (83.0%) consists of devitrified glass and glass shards. Shards wrap around phenocrysts and lithic fragments.

Sample number: Mc67
Location: NW 1/4, Sec 35, T23S, R60E, Sloan, Nev. 7 1/2' quad: collected approximately 1 mile west of the cinder outcrop in the NW portion of the Tscp.
Rock name: Welded rhyolitic ash-flow tuff
Description: Pyroclastic, eutaxitic and hypocrystalline consisting of fragmented phenocrysts of subhedral, oscillatory sanidine up to 3 mm (10.4%), subhedral, oscillatory plagioclase up to 1 mm (2.0%), anhedral, oscillatory quartz up to 1 mm (0.8%), Fe-Ti oxides up to 0.5 mm, an-subhedral clinopyroxene up to 0.5 mm and trace sphene & zircon (< 0.5 mm). Pumice fiamme are not present in the thin section, and occur only rarely in hand specimens. Basaltic, granodioritic and gabbroic rock fragments (7.2%) are up to 1 cm. The light brownish gray-colored groundmass (79.0%) consists of devitrified glass and glass shards. Shards wrap around phenocrysts and lithic fragments. Approximately 1% of the rock has been replaced by calcite.

Sample number: Mc68
Location: SW 1/4, Sec 36, T23S, R60E, Sloan, Nev. 7 1/2' quad: collected from the Tbs exposure between the railroad tracks and I-15.
Rock name: Welded rhyolitic ash-flow tuff
Description: Pyroclastic, eutaxitic and hypocrystalline consisting of fragmented phenocrysts of an-subhedral, oscillatory sanidine up to 2 mm, (4.8%), an-euhedral, oscillatory plagioclase up to 2 mm (1.4%), sub-euhedral, oxidized biotite up to 1 mm (1.4%), an-subhedral clinopyroxene up to 0.5 mm (0.8%), anhedral, oscillatory quartz up to 1 mm (0.4%), Fe-Ti oxides up to 0.5 mm (0.4%), sub-euhedral sphene up to 0.5 mm (trace) and trace zircon. Devitrified and commonly spherulitic pumice fiamme (11.4%) are up to several cm. Basaltic and gabbroic rock fragments (9.6%) are up to 1 cm. The light brownish gray-colored groundmass (69.8%) consists of devitrified glass and glass shards. Shards wrap around phenocrysts and lithic fragments.

Sample number: Mc69
Location: SW 1/4, Sec 24, T23S, R60E, Sloan, Nev. 7 1/2' quad: collected from the northernmost Tbs exposure in the mapped area west of I-15.
Rock name: Welded rhyolitic ash-flow tuff
Description: Pyroclastic, eutaxitic and hypocrystalline consisting of fragmented phenocrysts of subhedral, oscillatory sanidine up to 2 mm (7.0%), subhedral, oscillatory plagioclase up to 1 mm (5.0%), anhedral, oscillatory quartz up to 1 mm (1.2%), Fe-Ti oxides up to 0.5 mm (0.6%), sub-euhedral sphene < 0.5 mm (0.6%), subhedral, oxidized, subhedral biotite up to 2 mm (0.4%), an-subhedral clinopyroxene up to 3 mm (0.4%) and trace zircon. Devitrified pumice fiamme (0.2%) are up to several cm. Basaltic

and gabbroic rock fragments (1.0%) are up to 1 cm. The grayish red-colored groundmass (83.6%) consists of devitrified glass and glass shards. Shards wrap around phenocrysts and lithic fragments. Fractures are coated with calcite.

Sample number: Mc71
Location: NW 1/4, Sec 24, T23S, R60E, Sloan, Nev. 7 1/2' quad: collected approximately 1,000' N-NW of benchmark 2936 on the railroad tracks
Rock name: Welded rhyolitic ash-flow tuff
Description: Pyroclastic, eutaxitic and hypocrystalline consisting of fragmented phenocrysts of subhedral, oscillatory sanidine up to 2 mm (10.6%), subhedral, oscillatory plagioclase up to 1 mm (3.0%), subhedral, oxidized biotite up to 1.5 mm (1.6%), anhedral, oscillatory quartz up to 1 mm (1.4%), an-subhedral clinopyroxene up to 1 mm (1.6%), sub-euhedral sphene < 0.5 mm (0.4%), trace Fe-Ti oxides up to 0.5 mm and trace zircon. Devitrified pumice fiamme (12.0%) are up to several cm. Basaltic and gabbroic rock fragments (2.0%) are up to 1 cm. The grayish red-colored groundmass (67.4%) consists of devitrified glass and glass shards. Shards wrap around phenocrysts and lithic fragments. Fractures are coated with calcite.

HIDDEN VALLEY VOLCANICS

Sample number: Mc1
Location: SE 1/4, Sec 26, Hidden Valley, Nev. 7 1/2' quad:collected approximately 800' south of the cattle guard on the western entrance road to Hidden Valley.
Rock name: Vesicular, pyroxene olivine basalt
Description: Vesicular, aphanitic and hypocrystalline with phenocrysts of an-subhedral, iddingsitized olivine up to 1.5 mm (0.6%) and an-subhedral clinopyroxene up to 0.5 mm (0.3) in a black-colored, vesicular (11.0%) groundmass consisting of microlites of sub-euhedral plagioclase (44.3%), subhedral, iddingsitized olivine (14.0%), an-subhedral clinopyroxene (12.0%), Fe-Ti oxides (0.3%) and moderately devitrified glass (17.3%). Vesicles are coated with calcite.

Sample number: Mc3a
Location: NE 1/4, Sec 35, T24S, R60E, Hidden Valley, Nev. 7 1/2' quad: collected from the NW corner of the N-S trending Thvb ridge south of the western entrance road to Hidden Valley.
Rock name: Vesicular, pyroxene basalt
Description: Vesicular, aphanitic and hypocrystalline with phenocrysts of embayed, resorbed, an-euhedral clinopyroxene up to 1.5 mm (1.0%), commonly in glomerocrysts. The grayish red-colored, vesicular (8.2%) groundmass

consists of microlites of sub-euhedral, oscillatory plagioclase (55.0%), an-subhedral clinopyroxene (19.0%), granular hematite (13.4%: replacing clinopyroxene), Fe-Ti oxides (2.6%) and glass (0.8%). Vesicles are coated with calcite.

↕ space

Sample number: Mc35

Location: NW 1/4, Sec 23, T24S, R61E, Hidden Valley, Nev. 7 1/2' quad: collected from the isolated Thvb outcrop in the southern portion of the Tsh dome field: on the southern side of the entrance to the major drainage separating Tss from Tsh.

Rock name: Vesicular, pyroxene olivine basalt

Description: Porphyritic, vesicular and hypocrystalline with phenocrysts of subhedral, iddingsitized olivine up to 2 mm (9.8%), subhedral, pitted, embayed and oscillatory plagioclase up to 1 mm (2.2%) and subhedral clinopyroxene up to 0.5 mm (0.8%). Quartz xenocrysts are up to 4 mm and rimmed with glass and cryptocrystalline clinopyroxene(?) (0.6%). The medium dark gray-colored, vesicular (2.6%) groundmass consists of microlites of sub-euhedral, oscillatory plagioclase (58.4%), subhedral clinopyroxene (9.2%), subhedral, iddingsitized olivine (9.8%), subhedral clinopyroxene (9.2%), Fe-Ti oxides (6.2%) and glass (0.4%). Vesicles are coated with calcite.

Sample number: Mc37

Location: SE 1/4, Sec 22, T24S, R61E, Hidden Valley, Nev. 7 1/2' quad: collected 2100' south of sample Mc35.

Rock name: Vesicular, pyroxene olivine basalt

Description: Porphyritic, vesicular and hypocrystalline with phenocrysts of sub-euhedral, iddingsitized olivine up to 2 mm (7.6%), sub-euhedral, pitted and embayed clinopyroxene up to 1 mm (1.4%) and subhedral, pitted, embayed and oscillatory plagioclase up to 2 mm (1.0%). Quartz xenocrysts are up to 5 mm and rimmed with glass (6.0%). The medium dark gray-colored, vesicular (1.2%) groundmass consists of microlites of sub-euhedral, oscillatory plagioclase (57.0%), subhedral, iddingsitized olivine (8.2%), sub-euhedral clinopyroxene (11.6%), Fe-Ti oxides (6.2%) and glass (0.8%).

Sample number: Mc40b

Location: E 1/4, Sec 27, T24S, R61E, Hidden Valley, Nev. 7 1/2' quad: collected from the small isolated Thvb outcrop on the W border of the Tsh dome complex.

Rock name: Vesicular, pyroxene olivine basalt

Description: Porphyritic, vesicular and hypocrystalline with commonly pitted and embayed phenocrysts of an-subhedral, iddingsitized olivine up to 1 mm (6.3%) and sub-euhedral, oscillatory plagioclase up to 1 mm (3.3%).

Quartz xenocrysts are up to 5 mm and rimmed with glass and fine-grained clinopyroxene (2.6%). The vesicular (9.3%), brownish black-colored groundmass consists of microlites of sub-euhedral, oscillatory plagioclase (58.3%), an-subhedral clinopyroxene (7.3%), an-subhedral, iddingsitized olivine (7.3%), Fe-Ti oxides (2.0%) and glass.

Sample number: Mc42
Location: SW 1/4, Sec 26, T24S, R61E, Hidden Valley, Nev. 7 1/2' quad: collected from the small isolated Thvb outcrop on the NE side of major drainage on the SW Tsh dome complex border.
Rock name: Vesicular, olivine pyroxene basalt
Description: Vesicular, porphyritic and holocrystalline with commonly pitted and embayed phenocrysts of an-euhedral, mildly iddingsitized olivine up to 2 mm (5.6%), an-subhedral, up to 1 mm, commonly glomerocrystic clinopyroxene (4.0%) and sub-euhedral, oscillatory plagioclase up to 1 mm (1.0%). Quartz xenocrysts are up to 5 mm and rimmed with glass (< 1%). The vesicular (3.6%), black-colored groundmass consists of microlites of sub-euhedral, oscillatory plagioclase (62%), an-subhedral clinopyroxene (11.6%), an-euhedral, iddingsitized olivine (5.3%) and Fe-Ti oxides (6.6%).

Sample number: Mc43
Location: NW 1/4, Sec 34, T24S, R61E, Hidden Valley, Nev. 7 1/2' quad: collected from the east side of the N-S trending Thvb ridge in the south-central part of the mapped area.
Rock name: Vesicular, olivine pyroxene basalt
Description: Vesicular, porphyritic and hypocrystalline with commonly pitted and embayed phenocrysts of an-subhedral, up to 1 mm, commonly glomerocrystic clinopyroxene (10.0%), an-subhedral, iddingsitized, up to 1 mm, commonly glomerocrystic olivine (6%) and sub-euhedral, oscillatory plagioclase up to 1 mm (1.0%). The vesicular (3.4%) grayish black-colored groundmass consists of microlites of sub-euhedral, oscillatory plagioclase (58.9%), an-subhedral clinopyroxene (8.8%), an-subhedral, iddingsitized olivine (5.4%), Fe-Ti oxides (3.6%) and glass (3.0%). Vesicles are commonly coated with calcite.

Sample number: Mc47
Location: E 1/4, Sec 30, T23S, R61E, Sloan, Nev. 7 1/2' quad: collected from the isolated Thvb outlier just west of the Pzcu outcrop in the NW portion of the mapped area.
Rock name: Vesicular, olivine pyroxene basalt
Description: Porphyritic, vesicular and holocrystalline with commonly pitted and embayed phenocrysts of an-subhedral, up to 1 mm, commonly glomerocrystic clinopyroxene (10.8%), subhedral, oxidized phlogopite up to 2 mm (3.6%), anhedral, up to 1 mm, commonly glomerocrystic plagioclase

up to 1 mm, (0.4%) and an-subhedral, iddingsitized olivine up to 1 mm (0.4%). The vesicular (8.2%), dark gray-colored groundmass consists of microlites of sub-euhedral, oscillatory plagioclase (50.2%), Fe-Ti oxides (10.4%), an-subhedral clinopyroxene (7.4%), granular hematite (probably replaced phlogopite, 6.4%) and subhedral, iddingsitized olivine (2.2%). Vesicles are commonly coated or filled with calcite and/or quartz.

Sample number: Mc48
Location: SE 1/4, Sec 30, T23S, R61E, Sloan, Nev. 7 1/2′ quad: collected from the northern part of the Thvb exposure in the NW part of the mapped area.
Rock name: Vesicular, olivine pyroxene basalt
Description: Porphyritic, vesicular and holocrystalline with commonly pitted and embayed phenocrysts of subhedral, oxidized phlogopite up to 2 mm (4.8%), subhedral, up to 1.5 mm, commonly glomerocrystic with olivine, clinopyroxene (4.6%) and subhedral, up to 1 mm, commonly glomerocrystic with clinopyroxene, olivine (1.2%). The vesicular (10.4%), brownish black-colored groundmass consists of microlites of subhedral, oscillatory plagioclase (58.6%), subhedral clinopyroxene (7.2%), Fe-Ti oxides (7.2%) and an-euhedral, iddingsitized olivine (6.0%). Vesicles are commonly coated with calcite.

Sample number: Mc87
Location: SE 1/4, Sec 28, T24S, R61E, Hidden Valley, Nev. 7 1/2′ quad: collected on the west side of the N-S trending Thvb ridge in the S-central part of the mapped area.
Rock name: Pyroxene olivine basalt
Description: Aphanitic, trachytic and hypocrystalline with pitted, embayed, oscillatory, fritted sub-euhedral plagioclase phenocrysts up to 1 mm (0.8%). The brownish black-colored groundmass consists of sub-parallel microlites of sub-euhedral, oscillatory plagioclase (72.4%), an-subhedral, iddingsitized olivine (17.4%), an-subhedral clinopyroxene (8.0%), Fe-Ti oxides (0.4%) and glass (1.0%).

Sample number: Mc108
Location: Collected from the basaltic dike in the Thvb on the eastern escarpment of the McCullough's, approximately 3,000′ S-SE of peak 3912.
Rock name: Vesicular, olivine pyroxene basaltic dike
Description: Vesicular, porphyritic and holocrystalline consisting of phenocrysts of subhedral, oscillatory plagioclase up to 3 mm (13.2%), subhedral, embayed clinopyroxene up to 1 mm (1.6%), an-subhedral, iddingsitized olivine up to 1 mm (1.4%) and Fe-Ti oxides up to 0.5 mm (0.5%). The vesicular (18.2%), medium dark gray-colored groundmass consists of microlites of sub-euhedral, oscillatory plagioclase (16.8%), subhedral clinopyroxene

(3.8%), an-subhedral, iddingsitized olivine (1.4%), granular hematite (0.2%) and Fe-Ti oxides (0.3%).

Sample number: W-hvb
Location: NW 1/4, Sec 36, T23S, R60E, Sloan, Nev. 7 1/2' quad: collected from the northernmost Thvb exposure associated with Tbs on the west side of I-15.
Rock name: Weakly vesicular, olivine pyroxene basalt
Description: Weakly vesicular, porphyritic and hypocrystalline consisting of commonly pitted and embayed phenocrysts of an-subhedral, oscillatory plagioclase up to 5 mm (18.4%), an-subhedral, iddingsitized olivine up to 5 mm (11.4%), an-subhedral clinopyroxene up to 5 mm (9.6%) and Fe-Ti oxides up to 0.5 mm (0.5%). Approximately 10% of the clinopyroxene, olivine and plagioclase phenocrysts occur in glomerocrysts with each other. The weakly vesicular (1.6%), black-colored groundmass consists of microlites of sub-euhedral, oscillatory plagioclase (30.2%), an-subhedral clinopyroxene (5.6%), an-subhedral, iddingsitized olivine (1.4%), Fe-Ti oxides (0.5%) and devitrified glass (20.8%). Vesicles are coated with calcite.

MT. HANNA ANDESITE

Sample number: Mc31b
Location: SE 1/4, Sec 14, T24S, R61E, Sloan SE, Nev. 7 1/2' quad: collected at the southernmost Tss/Tsh contact.
Rock name: Andesite
Description: Fine-grained, trachytic and hypocrystalline consisting of sub-parallel, sub-euhedral plagioclase laths (< 0.5 mm) with subordinate interstitial devitrified glass, Fe-Ti oxides and cryptocrystalline, high birefringent minerals. Trace, subhedral, pitted, embayed, zoned and oscillatory plagioclase phenocrsyts (up to 1 mm) occur. The groundmass is very dusky red with moderate red-colored streaks.

Sample number: Mc110
Location: T24S, R62E, Sloan SE, Nev. 7 1/2' quad: collected on peak 3912 near the Tsh/Thvb contact on the eastern escarpment of the McCullough's.
Rock name: Andesite
Description: Fine-grained, trachytic and hypocrystalline consisting of sub-parallel, sub-euhedral plagioclase laths (<0.5 mm) with subordinate interstitial devitrified glass and Fe-Ti oxides. Trace, subhedral, pitted, embayed, zoned and oscillatory plagioclase phenocrysts up to 1 mm occur. The slide also contains a subhedral, oxidized, 3 mm biotite phenocryst. The weakly vesicular (< 1.0%) groundmass is black.

Sample number: Mc112
Location: 800′ east, 2400′ north of the SE corner of Sec 12, T24S, R61E, Sloan SE, Nev. 7 1/2′ quad: collected near entrance to the major drainage in the northern part of the Tsh dome complex.
Rock name: Andesite
Description: Fine-grained, trachytic and hypocrystalline consisting of sub-parallel, sub-euhedral plagioclase laths (< 0.5 mm) with subordinate interstitial devitrified glass and Fe-Ti oxides. Trace, subhedral, pitted, embayed, zoned and oscillatory plagioclase phenocrysts up to 1 mm occur. The weakly vesicular (< 1%), groundmass is dark gray with medium light gray-colored streaks.

Sample number: Mc115
Location: NW 1/4, Sec 36, T24S, R61E, Sloan SE, Nev. 7 1/2′ quad: collected on the ridge just to the SE of the major Tsh vent area.
Rock name: Andesite
Description: Fine-grained, massive and hypocrystalline consisting of sub-euhedral plagioclase laths (< 0.5 mm) with subordinate interstitial partially devitrified glass, granular hematite and Fe-Ti oxides. The slide contains two pitted, embayed, sub-euhedral plagioclase xenocrysts (1.5 mm). The groundmass is black with grayish red-colored streaks.

CINDER PROSPECT MEMBER

Sample number: Mc25
Location: SW 1/4, Sec 5, T24S, R61E, Sloan, Nev. 7 1/2′ quad: dacite underlying Tsi on south-facing hillside one mile east of the Mt. Ian vent.
Rock name: Dacite
Description: Glomeroporphyritic: glomerocrysts form approximately 2% of the rock and consist of commonly pitted and embayed phenocrysts of zoned, oscillatory, sub-euhedral plagioclase up to 2 mm and subordinate sub-euhedral, oxidized biotite up to 2 mm. Individual phenocrysts form approximately 2% of the rock and consist of the same minerals found in the glomerocrysts. The medium gray-colored groundmass consists of microlites of plagioclase with trace biotite, Fe-Ti oxides, zircon and glass. Approximately 40% of the groundmass has been replaced by calcite.

Sample number: Mc78
Location: SE 1/4, Sec 6, T24S, R61E, Sloan, Nev. 7 1/2′ quad: vitrophyre on the ridge approximately 1,750′ SE of the Mt. Ian Tsi vent center
Rock name: Dacite vitrophyre
Description: Porphyritic and hypohyaline with commonly fragmented, pitted and embayed phenocrysts of sub-euhedral, oscillatory and seriate up to 2 mm plagioclase (12.0%), sub-euhedral, oxidized and seriate up to 2 mm biotite

(3.8%), sub-euhedral, oscillatory and seriate up to 2 mm sanidine (3.4%), Fe-Ti oxides seriate up to 0.5 mm (0.4) and trace zircon. Basaltic, gabbroic and granodioritic rock fragments (5.6%) are up to 1 cm. The mottled dark reddish brown and black-colored groundmass (74.6) consists of devitrified glass and glass shards.

Sample number: Mc79
Location: NE 1/4, Sec 6, T24S, R61E, Sloan, Nev. 7 1/2′ quad: glassy, resistant vitrophyre that crops out in the NE part of Tscp.
Rock name: Rhyolite vitrophyre
Description: Porphyritic and hypohyaline with commonly fragmented, pitted and embayed phenocrysts of subhedral, oscillatory and seriate up to 1 mm plagioclase (17.4%), subhedral, oscillatory and seriate up to 1 mm sanidine (3.8%), sub-euhedral, oxidized and seriate up to 2 mm biotite (3.6%), Fe-Ti oxides seriate up to 0.5 mm (1.2%), trace sub-euhedral clinopyroxene up to 0.5 mm and trace zircon. Trace basaltic rock fragments are up to 1 mm. The mottled dark reddish brown and black-colored groundmass (74.0%) consists of devitrified glass and glass shards with trace granular hematite.

Sample number: Mc121
Location: SW 1/4, Sec 31, T23S, R61E, Sloan, Nev. 7 1/2′ quad: dacite that lies stratigraphically immediately below Tts.
Rock name: Biotite dacite
Description: Glomeroporphyritic: glomerocrysts form approximately 4% of the rock and consist of commonly pitted and embayed phenocrysts of zoned, oscillatory, subhedral plagioclase up to 2 mm with subordinate subhedral hematized biotite up to 2 mm. Individual phenocrysts form approximately 6% of the rock and consist of the same minerals found in the glomerocrysts and trace Fe-Ti oxides up to 0.5 mm. The light brownnish gray-colored groundmass consists of microlites of plagioclase with trace hematized biotite, Fe-Ti oxides and glass. Approximately 1% of the groundmass has been replaced by calcite.

Sample number: Mc125
Location: S 1/4, Sec 31, T23S, R61E, Sloan, Nev. 7 1/2′ quad: dacite from the Cinder Prospect Member, below the Sloan Tuff.
Rock name: Biotite dacite
Description: Glomeroporphyritic: glomerocrysts form approximately 6% of the rock and consist of commonly pitted and embayed phenocrysts of zoned, oscillatory, subhedral plagioclase up to 3 mm with subordinate Fe-Ti oxides up to 0.5 mm and subhedral biotite up to 3 mm that ranges from unaltered to totally replaced by red and black Fe oxides. Individual phenocrysts form approximately 5% of the rock and consist of the same minerals found in the glomerocrysts. The medium light gray-colored groundmass consists of

microlites of plagioclase with subordinate oxidized biotite, trace zircon and glass. Approximately 5% of the groundmass has been replaced by calcite.

TUFF OF THE SLOAN VOLCANICS

Sample number: Mc59a
Location: SW 1/4, Sec 31, T24S, R61E, Sloan, Nev. quad: collected from the bottom cooling unit in the drainage at station 59 in the Tsc dome complex.
Rock name: Welded rhyolitic ash-flow tuff
Description: Pyroclastic, eutaxitic and hypocrystalline consisting of fragmented phenocrysts of subhedral sanidine up to 3 mm (21.2%), subhedral, zoned and oscillatory plagioclase up to 2 mm (4.8%), sub-euhedral, oxidized biotite up to 1.5 mm (0.4%), Fe-Ti oxides up to 0.5 mm (< 1%), sub-euhedral sphene (< 0.5 mm, 0.2%) and trace amounts of clinopyroxene, monazite, epidote, allanite, and zircon (each < 0.5 mm). Pumice fiamme (9%) are up to several cm long, devitrified and rarely spherulitic. Basaltic and gabbroic rock fragments (3.8%) are up to 1 cm. The grayish red-colored groundmass (60.6%) consists of devitrified glass shards that wrap around phenocrysts and lithic fragments.

Sample number: Mc59b
Location: SW 1/4, Sec 31, T24S, R61E, Sloan, Nev. quad: collected from the middle cooling unit in the drainage at station 59 in the Tsc dome complex.
Rock name: Non-welded dacitic ash-flow tuff
Description: Pyroclastic and hypocrystalline consisting of fragmented phenocrysts of an-subhedral, oscillatory sanidine up to 2.5 mm (4.8%), subhedral, oscillatory plagioclase up to 1.5 mm (2.0%), subhedral, oxidized biotite up to 1 mm (0.8%), an-subhedral clinopyroxene up to 0.5 mm (0.2%), sub-euhedral sphene up to 0.5 mm (0.2%), Fe-Ti oxides up to 0.5 mm (< 1%) and trace zircon. Spongy, devitrified, rarely spherulitic pumice (2.2%) is up to 1 cm. Basaltic and gabbroic rock fragments (13.2%) are up to 1 cm. The very light gray- colored groundmass (76.4%) consists of devitrified, axiolitic glass shards that wrap around phenocrysts and lithic fragments.

Sample number: Mc59c
Location: SW 1/4, Sec 31, T24S, R61E, Sloan, Nev. quad: collected from the top cooling unit in the drainage at station 59 in the Tsc dome complex.
Rock name: Welded dacitic ash-flow tuff
Description: Pyroclastic, eutaxitic and hypocrystalline consisting of fragmented phenocrysts of subhedral, oscillatory sanidine up to 4 mm (8.6%), subhedral, oscillatory plagioclase up to 1 mm (2.4%), Fe-Ti oxides up to 0.5 mm (1.4%), anhedral quartz < 0.5 mm (0.4%), an-subhedral clinopyroxene up to 0.5 (1.4%), subhedral, oxidized biotite up to 2 mm (0.4%) and trace zircon. Pumice fiamme (11.6%) are up to several cm

long. Basaltic and gabbroic rock fragments (21.2%) are up to 2 cm. The pale red-colored groundmass (52.6%) consists of blocky shaped, slightly devitrified glass shards.

Sample number: Mc73
Location: NW 1/4, Sec 6, T24S, R61E, Sloan, Nev. 7 1/2′ quad: collected in drainage just west of the Sta. 59 tuffs.
Rock name: Non-welded rhyolitic ash-flow tuff
Description: Pyroclastic and hypocrystalline consisting of fragmented phenocrysts of subhedral, oscillatory sanidine up to 3 mm (10.0%), anhedral quartz up to 1 mm (1.8%), an-subhedral, oscillatory plagioclase up to 3 mm (3.4%), subhedral, oxidized biotite up to 1 mm (0.6%), Fe-Ti oxides up to 0.5 mm (0.2%), trace, an-subhedral, hematized clinopyroxene up to 0.5 mm and trace amounts of sphene and zircon (sub-euhedral, < 0.5 mm). Spongy, devitrified pumice (1.6%) is up to 1 cm. Basaltic, gabbroic and granodioritic rock fragments (4.6%) are up to 1 cm. The grayish pink-colored groundmass (77.8%) consists of devitrified, weakly axiolitic glass shards, interstitial glass and < 1% yellow Fe oxides.

CENTER MTN. DACITE

Sample number: Mc59d
Location: N 1/2, Sec 6, T23S, R61E, Sloan, Nev. 7 1/2′ quad: dacite that lies stratigraphically immediately above Tts.
Rock name: Biotite dacite
Description: Glomeroporphyritic: glomerocrysts form approximately 3% of the rock and consist of commonly pitted and embayed phenocrysts of subhedral plagioclase up to 2 mm with subordinate Fe-Ti oxides and sub-euhedral, oxidized biotite up to 2 mm. Phenocrysts form approximately 3% of the rock and consist of the same minerals found in the glomerocrysts. The medium light gray-colored groundmass consists of microlites of plagioclase with subordinate hematized biotite, Fe-Ti oxides and glass. Approximately 5% of the groundmass has been replaced by calcite.

Sample number: Mc130
Location: SW 1/4, Sec 31, T23S, R60E, Sloan, Nev. 7 1/2′ quad: dacite overlying Tscp in the NW section of the Center Mtn. dome complex.
Rock name: Biotite dacite
Description: Holocrystalline, and porphyritic with phenocrysts of sub-euhedral, zoned and oscillatory plagioclase up to 2 mm (4.4%), sub-euhedral, oxidized biotite up to 5 mm (1.2%) and sub-euhedral Fe-Ti oxides < 0.5 mm (0.4%). The medium gray-colored groundmass consists of microlites of plagioclase with subordinate oxidized biotite, Fe-Ti oxides and pyroxene(?), and secondary calcite (5%).

Sample number: Mc131
Location: SW 1/4, Sec 6, T24S, R61E, Sloan, Nev. 7 1/2' quad: dacite overlying Tscp in the southern part of the Center Mtn. dome complex.
Rock name: Biotite dacite
Description: Holocrystalline, porphyritic and trachytic with sub-parallel phenocrysts of sub-euhedral, zoned and oscillatory plagioclase up to 2 mm (7.2%), sub-euhedral, oxidized biotite up to 3 mm (1.6%) and sub-euhedral Fe-Ti oxides < 0.5 mm (0.4%). The medium light gray-colored groundmass consists of microlites of plagioclase with subordinate oxidized biotite, Fe-Ti oxides and pyroxene(?), and secondary calcite (1.2%).

MT. IAN ANDESITE

Sample number: Mc93
Location: SW 1/4, Sec 5, T24S, R61E, Sloan, Nev. 7 1/2' quad: andesite that overlies dacite on the hill 1 mile east of Mt. Ian: stratigraphically above Mc25 biotite dacite.
Rock name: Andesite
Description: Fine-grained and hypocrystalline consisting of commonly pitted and embayed phenocrysts of sub-euhedral, zoned and oscillatory plagioclase up to 1 mm (5.2%), subhedral iddingsitized olivine up to 0.5 mm (0.4%), sub-euhedral, commonly oxidized subhedral biotite up to 1 mm (0.4%), Fe-Ti oxides up to 1 mm and trace subhedral orthopyroxene up to 0.5 mm. The orthopyroxene commonly occurs in glomerocrysts with plagioclase and Fe-Ti oxides. The medium dark gray- colored, weakly vesicular groundmass consists of microlites of plagioclase with trace biotite, olivine, Fe-Ti oxides and glass. Vesicles are coated with calcite.

Sample number: Mc94
Location: N 1/4, Sec 5, T24S, R61E, Sloan, Nev. 7 1/2' quad: from the hilltop 1 mile east of the Tuff of the Sloan Volcanics at station 59.
Rock name: Andesite
Description: Vesicular, fine-grained and hypocrystalline consisting of commonly pitted and embayed phenocrysts of zoned, oscillatory, sub-euhedral plagioclase up to 0.5 mm (2.4%), Fe-Ti oxides up to 0.25 mm (4%), subhedral, iddingsitized olivine up to 0.5 mm (0.4%) and trace subhedral oxidized biotite up to 0.5 mm. The vesicular (9.6%), grayish red-colored groundmass consists of microlites of plagioclase (72.8%), iddingsitized olivine (3.0%) and glass (0.6%). 7.0% of the groundmass has been replaced by hematite. Vesicles are coated with calcite.

Sample number: Mc95a
Location: NE 1/4, Sec 5, T24S, R61E, Sloan, Nev. 7 1/2' quad: massive andesite from hill 3346 just west of the major drainage separating Tsi from Tss.

Rock name: Andesite

Description: Fine-grained and hypocrystalline consisting of commonly pitted and embayed phenocrysts of zoned, oscillatory, sub-euhedral plagioclase up to 1 mm (5.6%), an-subhedral chloritized(?) and oxidized biotite up to 1 mm (10.4%) and subhedral orthopyroxene up to 0.5 mm (trace) that commonly occurs in glomerocrysts with plagioclase and Fe-Ti oxides. The black-colored groundmass consists of microlites of plagioclase (74.0%), clinopyroxene (0.2%), iddingsitized olivine (0.6%), Fe-Ti oxides (4.6%), zircon (trace) and devitrified glass (4.6%).

Sample number: Mc95b

Location: NE 1/4, Sec 5, T24S, R61E, Sloan, Nev. 7 1/2' quad: platy andesite from hill 3346 just west of the major drainage separating Tsi from Tss: lies stratigraphically below the more massive Mc95a andesite.

Rock name: Andesite

Description: Fine-grained and hypocrystalline consisting of commonly pitted and embayed phenocrysts of zoned, oscillatory, sub-euhedral plagioclase up to 1 mm (4.0%), sub-euhedral oxidized biotite up to 2 mm (0.4%), Fe-Ti oxides up to 0.5 mm (0.2%) and subhedral orthopyroxene up to 0.5 mm (trace) that commonly occurs in glomerocrysts with plagioclase and Fe-Ti oxides. The dusky brown-colored, weakly vesicular (0.4%) groundmass consists of microlites of plagioclase (68.4%), iddingsitized olivine (3.0%), Fe-Ti oxides (4.0%), biotite (trace) and devitrified glass (19.8%). The slide contains a granodiorite xenolith 1.5 mm by 1 mm. Vesicles are coated with calcite.

Sample number: Mc97

Location: NW 1/4, Sec 4, T23S, R61E, Sloan, Nev. 7 1/2' quad: collected from the Tsi ridge-top in the NW part of the northern Tss dacite dome complex.

Rock name: Andesite

Description: Fine-grained, weakly vesicular and hypocrystalline consisting of commonly pitted and embayed phenocrysts of zoned, oscillatory, sub-euhedral plagioclase up to 1 mm (4.4%), an-subhedral, iddingsitized olivine up to 0.5 mm (2.0%), subhedral, oxidized biotite up to 0.5 mm (trace), Fe-Ti oxides up to 0.5 mm (2.0%) and subhedral orthopyroxene up to 0.5 mm (0.2%) that commonly occurs in glomerocrysts with Fe-Ti oxides. The black-colored, weakly vesicular (1.8%) groundmass consists of microlites of plagioclase (57.0), iddingsitized olivine (2.2%), clinopyroxene (0.2%), Fe-Ti oxides (0.6%) and devitrified glass (29.4%).

Sample number: Mc98

Location: SE 1/4, Sec 6, T24S, R61E, Sloan, Nev. 7 1/2' quad: collected from the Tsi dome in the SE part of the Tsc dome complex.

Rock name: Andesite

Description: Fine-grained, weakly vesicular and hypocrystalline consisting of commonly pitted and embayed phenocrysts of zoned, oscillatory, sub-euhedral plagioclase up to 0.5 mm (4.6%), an-subhedral, iddingsitized olivine up to 0.5 mm (0.5%), Fe-Ti oxides up to 0.5 mm (2.0%) and sub-euhedral, oxidized biotite up to 0.5 mm (trace). The medium dark gray-colored, weakly vesicular (0.8%) groundmass consists of microlites of plagioclase (79.0%), iddingsitized olivine (4.1%), Fe-Ti oxides (3.4%) and devitrified glass (1.8%). Sericite (3.8%) is replacing plagioclase. The vesicles are coated with calcite.

Sample number: Mc120a
Location: S 1/4, Sec 6, T24S, R61E, Sloan, Nev. 7 1/2' quad: andesite collected from the Mt. Ian vent.
Rock name: Andesite
Description: Fine-grained and hypocrystalline consisting of commonly pitted and embayed phenocrysts of zoned, oscillatory, sub-euhedral, seriate plagioclase up to 1 mm (31.8%), sub-euhedral orthopyroxene up to 0.5 mm (1.2%), Fe-Ti oxides up to 0.5 mm (1.5%) and subhedral, oxidized biotite up to 0.5 mm (0.2%). The grayish black-colored groundmass consists of microlites of plagioclase (50%), orthopyroxene (trace), biotite (0.6%), Fe-Ti oxides (2.1%) and devitrified glass (9.8%). Veins of fine to medium-grained quartz forms 2% of the rock.

Sample number: Mc129
Location: NE 1/4, Sec 4, T24S, R61E, Sloan, Nev. 7 1/2' quad: andesite that underlies Tss on the east side of drainage in the NW part of the northern Tss dome complex.
Rock name: Andesite
Description: Fine-grained, weakly vesicular and hypocrystalline consisting of commonly pitted and embayed phenocrysts of zoned, oscillatory, sub-euhedral, seriate plagioclase up to 2 mm (30.8%), sub-euhedral, iddingsitized olivine up to 0.5 mm (0.2%), Fe-Ti oxides up to 0.5 mm (0.2%) and sub-euhedral orthopyroxene up to 0.5 mm (trace). The weakly vesicular (1.0%), dark gray-colored groundmass consists of microlites of plagioclase (49%), iddingsitized olivine (0.6%) and Fe-Ti oxides (0.8%). Vesicles are coated with calcite.

MT. SUTOR DACITE

Sample number: Mc9
Location: E 1/2, Sec 26, T24S, R60E, Hidden Valley, Nev. 7 1/2' quad: at the Tss/Thvb contact near the western entrance road to Hidden Valley.
Rock name: Biotite dacite

Description: Glomeroporphyritic: glomerocrysts form approximately 10% of the rock and are composed of commonly pitted and embayed phenocrysts of zoned, oscillatory, sub-euhedral plagioclase up to 3 mm with subordinate sub-euhedral biotite up to 3 mm and Fe-Ti oxides up to 0.5 mm. Individual phenocrysts form approximately 2% of the rock and consist of the same minerals found in the glomerocrysts, but many are not pitted and embayed. The medium gray-colored groundmass consists of microlites of plagioclase with trace biotite and Fe-Ti oxides, devitrified glass, and < 1% vesicles. Vesicles and fractures are coated with secondary calcite.

Sample number: Mc16
Location: SW 1/4, Sec 14, T24S, R60E, Hidden Valley, Nev. 7 1/2' quad: near the Tss/Pzcu contact on the western margin of the southern dacite dome complex.
Rock name: Biotite dacite
Description: Glomeroporphyritic: glomerocrysts form approximately 7% of the rock and are composed of commonly pitted and embayed phenocrysts of zoned, oscillatory, sub-euhedral plagioclase up to 3 mm with subordinate an-subhedral orthopyroxene up to 1 mm and Fe-Ti oxides up to 0.5 mm. Individual phenocrysts form approximately 5% of the rock and consist of the same minerals found in the glomerocrysts, plus an-subhedral pitted and embayed, oxidized biotite (1.4%). Many of the individual phenocrysts do not show the disequilibrium textures displayed in the glomerocrysts. The mottled medium gray and medium dark gray-colored groundmass consists of microlites of plagioclase with trace biotite, orthopyroxene and glass.

Sample number: Mc19
Location: NE 1/4, Sec 13, T24S, R60E, Hidden Valley, Nev. 7 1/2' quad: from the NW portion of the southern dacite dome complex.
Rock name: Vesicular biotite dacite
Description: Glomeroporphyritic: glomerocrysts form approximately 2% of the rock and are composed of commonly pitted and embayed phenocrysts of zoned, oscillatory, sub-euhedral plagioclase up to 2 mm with subordinate subhedral orthopyroxene up to 1 mm, subhedral biotite < 0.5 mm and Fe-Ti oxides up to 0.5 mm. Individual phenocrysts form 9.8% of the rock and consist of the same minerals found in the glomerocrysts, plus sub-euhedral, pitted and embayed, oxidized biotite (2.2%) up to 1 mm. The vesicular (11.8%) black-colored groundmass consists of microlites of plagioclase with trace biotite, Fe-Ti oxides, iddingsitized olivine, and glass. Vesicles and fractures are coated with secondary calcite.

Sample number: Mc21
Location: N 1/2, Sec 20, T24S, R61E, Hidden Valley, Nev. 7 1/2' quad: isolated outlier near the eastern margin of the southern dacite dome complex.

Rock name: Vesicular biotite dacite

Description: Glomeroporphyritic: glomerocrysts form approximately 15% of the rock and are composed of commonly pitted and embayed phenocrysts of zoned, oscillatory, sub-euhedral plagioclase up to 3 mm with subordinate subhedral biotite up to 3 mm and Fe-Ti oxides up to 0.5 mm. Individual phenocrysts form approximately 3.5% of the rock and consist of the same minerals found in the glomerocrysts. The vesicular (3.8%) dark gray-colored groundmass consists of microlites of plagioclase with trace biotite, clinopyroxene, olivine and glass.

Sample number: Mc 27

Location: SW 1/4, Sec 10, T24S, R61E, Hidden Valley, Nev. 7 1/2′ quad: on NW side of the entrance to the major drainage near the hypabyssal phase Tss.

Rock name: Biotite dacite

Description: Glomeroporphyritic: glomerocrysts for approximately 18% of the rock and are composed of commonly pitted and embayed phenocrysts of zoned, oscillatory, sub-euhedral plagioclase up to 4 mm, with subordinate Fe-Ti oxides up to 0.5 mm, sub-euhedral biotite up to 4 mm, and subhedral clinopyroxene up to 2 mm that is commonly rimmed with black Fe oxides. Individual phenocrysts form approximately 4.5% of the rock and consist of the same minerals found in the glomerocrysts, plus < 1% anhedral hornblende up to 0.5 mm that is rimmed with black Fe oxides. The dark gray- colored weakly vesicular (1.2%) groundmass consists of microlites of plagioclase with trace biotite and glass.Vesicles are coated with secondary calcite.

Sample number: Mc28

Location: N 1/4, Sec 10, T24S, R61E, Hidden Valley, Nev. 7 1/2′ quad: isolated outlier in the mouth of the major drainage near hypabyssal phase Tss.

Rock name: Biotite dacite

Description: Glomeroporphyritic: glomerocrysts for approximately 10% of the rock and are composed of commonly pitted and embayed phenocrysts of zoned, oscillatory, sub-euhedral plagioclase up to 2 mm, and subordinate subhedral clinopyroxene up to 1 mm and oxidized biotite up to 3 mm. Individual phenocrysts form approximately 2% of the rock and consist of the same minerals found in the glomerocrysts. The medium gray-colored groundmass consists of microlites of plagioclase with trace Fe-Ti oxides and glass. Calcite has replaced approximately 5% of the groundmass.

Sample number: Mc31a

Location: SE 1/4, Sec 14, T24S, R61E, Sloan SE, Nev. 7 1/2′ quad: at the southernmost Tss/Tsh contact.

Rock name: Biotite dacite

Description: Glomeroporphyritic: glomerocrysts form approximately 7% of the rock and are composed of commonly pitted and embayed phenocrysts of zoned, oscillatory, sub-euhedral plagioclase up to 2 mm, and subordinate subhedral, oxidized biotite up to 3 mm, an-subhedral clinopyroxene up to 1 mm, Fe-Ti oxides up to 0.5 mm and trace anhedral orthopyroxene up to 0.5 mm. Individual phenocrysts form approximately 5% of the rock and consist of the same minerals found in the glomerocrysts. The dark gray-colored groundmass consists of microlites of plagioclase with trace biotite and Fe-Ti oxides and glass. Fractures are rarely coated with calcite.

Sample number: Mc91a
Location: NW 1/4, Sec 19, T24S, R61E, Hidden Valley, Nev. 7 1/2' quad: dacite vent center in the east-central part of the southern dacite dome complex.
Rock name: Biotite dacite
Description: Glomeroporphyritic: glomerocrysts form approximately 5% of the rock and are composed of commonly pitted and embayed phenocrysts of zoned, oscillatory, subhedral plagioclase up to 3 mm and subordinate sub-euhedral hematized biotite up to 4 mm, and Fe-Ti oxides up to 0.5 mm. Individual phenocrysts form approximately 1.6% of the rock and consist of the same minerals found in the glomerocrysts. The dark greenish gray-colored groundmass consists of microlites of plagioclase with trace zircon and glass.

Sample number: Mc92
Location: NW 1/4, Sec 19, T24S, R61E, Hidden Valley, Nev. 7 1/2' quad: on hilltop 3957 just NW of the vent area at station 91.
Rock name: Vesicular biotite dacite
Description: Glomeroporphyritic: glomerocrysts form approximately 5.5% of the rock and are composed of commonly pitted and embayed phenocrysts of zoned, oscillatory, sub-euhedral plagioclase and subordinate sub-euhedral, oxidized biotite up to 2 mm, subhedral orthopyroxene up to 1 mm, and Fe-Ti oxides up to 0.5 mm. Individual phenocrysts form approximately 5.5% of the rock and consist of the same minerals found in the glomerocrysts. Biotite is rare in glomerocrysts and more abundant as individual phenocrysts. The slide contains < 1% granodiorite (?) xenoliths up to 1 cm. The vesicular (3%) medium dark gray-colored groundmass consists of microlites of plagioclase with trace biotite, orthopyroxene, Fe-Ti oxides and glass. Vesicles are coated with secondary calcite.

Sample number: Mc96
Location: W 1/2, Sec 4, T24S, R61E, Sloan, Nev. 7 1/2' quad: collected on the west-facing slope of hill 3490 in the northern Tss dome complex.
Rock name: Biotite dacite

Description: Glomeroporphyritic: glomerocrysts form approximately 7.5% of the rock and are composed of commonly pitted and embayed phenocrysts of zoned, oscillatory, sub-euhedral plagioclase up to 3 mm and subordinate sub-euhedral, oxidized biotite up to 3 mm, rare an-subhedral clinopyroxene up to 0.5 mm, and Fe-Ti oxides up to 0.5 mm. Individual phenocrysts form approximately 5.5% of the rock and consist of the same minerals found in the glomerocrysts. There is, however, a higher percentage of individual clinopyroxene phenocrysts (an-subhedral, up to 2 mm). The slide contains a 2 mm by 0.5 mm xenocryst of fine-to medium-grained clinopyroxene and orthopyroxene with interstitial glass. The weakly vesicular (1%) dark gray-colored groundmass consists of microlites of plagioclase with trace biotite and glass.

Sample number: Mc100
Location: SW 1/4, Sec 17, T24S, R61E, Hidden Valley, Nev. 7 1/2 quad: from hilltop 3650 in the NE part of the southern dacite dome complex.
Rock name: Biotite dacite
Description: Glomeroporphyritic: glomerocrysts form approximately 11% of the rock and are composed of commonly pitted and embayed phenocrysts of zoned, oscillatory, sub-euhedral plagioclase up to 2 mm and subordinate an-subhedral, oxidized biotite up to 2 mm, an-subhedral clinopyroxene up to 5 mm and Fe-Ti oxides up to 0.5 mm. Individual phenocrysts form approximately 4% of the rock and consist of the same minerals found in the glomerocrysts. The weakly vesicular (< 1%) brownish gray-colored groundmass consists of microlites of plagioclase with trace Fe-Ti oxides and glass. Vesicles are coated with secondary calcite.

Sample number: Mc118
Location: E 1/2, Sec 3, T24S, R61E, Sloan NE, Nev. 7 1/2′ quad: hypabyssal dacite near the NW Tss hypabyssal/volcanic contact.
Rock name: Hypabyssal biotite dacite
Description: Holocrystalline, glomeroporphyritic: glomerocrysts form approximately 13% of the rock and consist of commonly pitted and embayed phenocrysts of zoned, oscillatory, sub-euhedral plagioclase up to 3 mm, subordinate subhedral, oxidized biotite up to 3 mm, and < 1% subhedral clinopyroxene up to 1.5 mm that is rimmed with fine-grained black Fe oxides. Individual phenocrysts form approximately 6% of the rock and consist of the same minerals found in the glomerocrysts. The medium gray-colored, fine-grained groundmass consists of plagioclase (80%, subhedral, < 0.5 mm), biotite (3.8%, subhedral, < 0.5 mm), and trace Fe-Ti oxides (< 0.5 mm).

Sample number: Mc119
Location: NW 1/4, Sec 11, T24S, R61E, Sloan NE, Nev. 7 1/2' quad: Hypabyssal dacite near the SE Tss hypabyssal/volcanic contact.
Rock name: Hypabyssal biotite dacite
Description: Holocrystalline, glomeroporphyritic: glomerocrysts form approximately 12% of the rock and consist of commonly pitted and embayed phenocrysts of zoned, oscillatory, sub-euhedral plagioclase up to 3 mm, subordinate, oxidized biotite up to 2 mm, and < 1% subhedral clinopyroxene that is rimmed by fine-grained black Fe oxides. Individual phenocrysts form approximately 3% of the rock and consist of the same minerals found in the glomerocrysts. The medium gray- colored, fine-grainecd groundmass consists of plagioclase (80.4%, subhedral, < 0.5 mm), biotite (0.6%, subhedral, < 0.5 mm), and trace Fe-Ti oxides (< 0.5 mm). < 1% of the groundmass has been replaced by calcite.

Sample number: Mc128
Location: SE 1/4, Sec 24, T24S, R60E, Hidden Valley, Nev. 7 1/2' quad: from the central part of the southern dacite dome complex.Rock name: Vesicular biotite dacite
Description: Glomeroporphyritic: glomerocrysts form approximately 3% of the rock and consist of commonly pitted and embayed phenocrysts of zoned, oscillatory sub-euhedral plagioclase up to 5 mm and subordinate sub-euhedral, oxidized biotite up to 4 mm, and Fe-Ti oxides up to 0.5 mm. Individual phenocrysts form approximately 3% of the rock and consist of the same minerals found in the glomerocrysts. The brownish gray-colored vesicular (3.6%) groundmass consists of plagioclase microlites and trace glass.

ALKALI BASALT

Sample number: Mc124
Location: SE 1/4, Sec 13, T23S, R60E, Sloan, Nev. 7 1/2' quad: alkali basalt exposure at the Sloan Limestone quarry.
Rock name: Weakly vesicular alkali basalt
Description: Trachytic, holocrystalline and aphanitic with ultramafic nodules and Precambrian crust xenoliths up to several cm (< 1%). The weakly vesicular (0.2%), black-colored groundmass consists of sub-parallel microlites of sub-euhedral, oscillatory plagioclase (56%), subhedral clinopyroxene (21.2%), an-subhedral, iddingsitized olivine (20.4%) and Fe-Ti oxides (2.2%).

APPENDIX B: CHEMISTRY TABLES

Tuff of Bridge Spring								
Sample No.	ET-1	YT	92	R	T	V	M63	M105
SiO2	72.59	70.03	69.01	68.51	67.73	66.65	66.81	66.10
AL2O3	14.29	13.43	14.69	14.52	15.44	14.41	15.06	16.10
Fe2O3	1.78	1.88	2.17	1.97	2.83	2.04	2.52	2.50
CaO	1.38	1.15	1.43	1.90	1.65	2.31	1.6	1.70
MgO	0.35	0.46	0.48	0.30	0.44	0.32	0.71	1.30
Na2O	4.19	3.47	4.20	3.94	4.46	4.22	4.33	4.70
K2O	5.29	4.82	5.12	5.71	4.93	4.97	5.92	6.30
TiO2	0.34	0.35	0.41	0.40	0.53	0.39	0.43	0.40
MnO	0.07	0.08	0.06	0.05	0.06	0.07	0.09	0.10
P2O5	0.06	0.06	0.14	0.09	0.16	0.12	0.02	0.20
LOI	0.98	4.77	0.93	1.72	1.22	2.03	2.57	0.40
TOTAL	101.32	100.50	98.64	99.11	99.45	97.53	100.06	99.80
Trace elements in ppm								
La							121.0	104.0
Ce							191.0	155.0
Nd								70.00
Sm							11.00	10.00
Eu							1.71	1.85
Tb							0.80	0.91
Yb							3.12	1.21
Lu							0.45	0.34
U	8.50	12.00	8.20	7.30	5.20	5.90		
Th							32.22	25.00
Cr	21.40	17.90			21.80	18.30		
Hf							11.05	10.00
Ba							909.7	1332
Rb	248.0	480.0	217.0	217.0	159.0	179.0	157.0	143.0
Sr	214.0	402.0	233.0	197.0	563.0	365.0	264.0	1015
Sc								
Ta							2.30	1.84
Cd								
Zr	330.0	344.0	118.0	389.0	422.0	350.0		414.0
Y		66.20	51.00	58.00	41.00	42.00		
Nb								
Co								
Ti								
V								
Mg#	0.14	0.17	0.16	0.12	0.12	0.12	0.19	0.31

Tuff of Bridge Spring: continued								
Sample No.	Mc53	Mc60	Mc61	Mc62	Mc64a	Mc64b	Mc65	Mc66
SiO2	64.65	63.90	66.47	67.27	65.09	66.69	69.54	66.69
AL2O3	15.66	14.77	14.92	13.95	13.72	13.72	14.40	14.48
Fe2O3	3.95	3.55	3.47	2.72	3.11	3.11	3.31	3.16
CaO	2.43	3.24	1.72	2.36	5.66	0.65	0.63	4.12
MgO	0.97	1.05	0.86	0.58	1.42	1.00	1.02	0.84
Na2O	4.33	4.09	4.33	3.97	3.35	3.86	3.94	3.74
K2O	6.03	5.67	6.17	5.99	4.69	6.40	4.64	5.77
TiO2	0.53	0.45	0.47	0.35	0.42	0.42	0.45	0.43
MnO	0.15	0.15	0.15	0.15	0.15	0.15	0.15	0.15
P2O5	0.18	0.16	0.16	0.10	0.40	0.13	0.27	0.33
LOI	1.27	1.97	1.14	2.04	1.48	0.65	4.11	3.00
TOTAL	100.06	99.00	99.87	99.48	99.49	96.78	102.46	102.71
Trace elements in ppm								
La	118.0	93.20	91.50	92.10		96.30		
Ce	204.0	170.0	167.0	184.0		181.0		
Nd	73.40	64.00	75.20	55.30		67.30		
Sm	9.67	8.33	11.30	11.10		11.50		
Eu	1.78	1.70	1.33	1.01		1.11		
Tb	0.93	0.86	1.41	1.10		1.06		
Yb	2.87	3.14	3.92	3.50		3.76		
Lu	0.42	0.41	0.48	0.60		0.58		
U	6.26	5.42	6.36	10.90		8.86		
Th	28.60	27.30	35.80	44.30		44.60		
Cr	32.00	45.30	35.20	9.94		15.50		
Hf	10.30	10.10	9.78	10.60		11.10		
Ba	818.0	927.0	390.0	170.0		296.0		
Rb	121.0	127.0	160.0	172.0		170.0		
Sr	502.0	781.0				389.0		
Sc	4.67	4.21	3.89	3.23		3.63		
Ta	1.74	1.86	2.40	2.71		2.70		
Cd								
Zr	578.0	483.0	826.0	553.0		577.0		
Y								
Nb		64.00						
Co	4.17	3.68	3.41	1.96		2.84		
Ti	2980	2790	2260	2430		2100		
V	39.7	35.3	44.6	23.3		29.5		
Mg#	0.17	0.2	0.18	0.15	0.28	0.19	0.21	0.22

	Tuff of Bridge Spring: continued				Hidden Valley volcanics			
Sample No.	Mc67	Mc68	Mc69	Mc71	65	66	68	125
SiO2	68.12	65.46	68.40	69.27	46.94	50.18	52.05	51.61
AL2O3	14.60	14.32	14.46	14.88	16.87	15.11	16.04	16.69
Fe2O3	2.91	3.19	3.07	2.93	9.64	8.94	7.86	9.18
CaO	1.69	3.43	1.61	0.65	11.01	9.97	8.80	8.90
MgO	0.61	0.66	0.53	0.40	7.23	7.19	5.92	5.82
Na2O	4.38	4.10	4.33	4.44	2.69	2.61	2.69	2.75
K2O	5.94	5.82	5.85	6.15	1.38	1.72	3.01	1.79
TiO2	0.39	0.42	0.40	0.41	1.54	1.35	1.31	1.73
MnO	0.15	0.14	0.15	0.15	0.13	0.14	0.13	0.14
P2O5	0.11	0.13	0.09	0.09	0.81	0.61	0.78	0.50
LOI	1.38	2.56	1.33	0.56	1.11	2.35	3.01	0.70
TOTAL	100.29	100.23	100.22	99.93	99.35	100.17	101.60	99.81
Trace elements in ppm								
La	94.50	91.70	93.40	101.0				
Ce	173.0	177.0	184.0	188.0				
Nd	79.80	63.70	57.00	80.90				
Sm	12.80	11.80	12.10	13.70				
Eu	1.14	1.22	1.22	1.17				
Tb	1.16	1.17	1.27	1.26				
Yb	3.62	3.36	3.56	3.77				
Lu	0.56	0.54	0.49	0.63				
U	8.66	7.23	8.47	8.42				
Th	39.30	39.40	41.90	42.00				
Cr	11.70	20.90	10.40	11.20				
Hf	10.00	10.10	11.00	11.30				
Ba		303.0						
Rb	155.0	165.0	179.0	173.0	22.30	22.00	65.20	29.70
Sr	219.0	200.0	168.0	196.0	940.0	828.0	1170.0	622.0
Sc	3.16	3.85	3.39	3.25				
Ta	2.44	2.36	2.56	2.76				
Cd								
Zr	455.0	544.0	603.0	663.0	218.0	223.0	317.0	235.0
Y					17.70	18.10	25.10	23.40
Nb								
Co	1.96	3.90	2.45	1.93				
Ti	2270	1890	2780	2220				
V	23.6	31.0	30.0	34.3				
Mg#	0.15	0.15	0.13	0.1	0.39	0.41	0.39	0.35

Hidden Valley volcanics: continued							
Sample No.	M24	M27	M35	M57	M58	Mc87	Mc108
SiO2	58.72	58.70	55.86	59.42	59.65	55.19	57.61
AL2O3	17.85	15.80	16.30	17.59	17.49	16.02	16.14
Fe2O3	7.14	5.11	8.47	5.41	5.55	8.98	7.74
CaO	5.25	4.49	7.49	4.00	4.03	7.06	5.54
MgO	2.00	2.53	4.33	1.80	1.80	5.12	3.29
Na2O	4.35	3.63	4.29	3.69	3.64	3.62	3.47
K2O	3.95	5.29	1.89	5.22	5.22	2.36	3.63
TiO2	0.71	0.82	0.95	0.55	0.55	1.08	1.18
MnO	0.06	0.09	0.08	0.35	0.12	0.17	0.16
P2O5	0.77	0.35	0.20	0.12	0.34	0.64	1.05
LOI	0.82	1.29	1.35	0.35	0.76	0.06	1.35
TOTAL	101.62	98.10	101.21	98.50	99.15	100.30	101.16
Trace elements in ppm							
La	97.80	102.0	26.23	99.43	98.04	48.60	69.70
Ce	182.3	168.6	42.04	167.8	166.9	85.20	139.0
Nd	68.83	74.76	23.89	76.63		32.80	42.00
Sm	14.24	13.05	4.29	12.83	12.60	6.37	8.52
Eu	3.50	2.73	1.58	2.84	2.78	1.57	2.34
Tb	1.48	1.47	1.59	1.53	1.46	0.91	0.82
Yb	2.85	2.84	1.41	2.93	2.85	2.36	1.93
Lu	0.56	0.40	0.39	0.45	0.46	0.34	0.36
U							1.10
Th	12.54	20.19	6.39	13.69	13.50	8.28	10.80
Cr						220.0	61.20
Hf	6.99	9.43	4.26	7.61	7.62	5.46	7.31
Ba	2440.0	1620.0	654.9	2203.0	1897.0	802.0	1200.0
Rb	97.85	118.5	43.64	98.16	99.95	33.80	60.60
Sr	1741.0	745.0	455.2	1468.0	1157.0	556.0	1280.0
Sc						19.70	12.80
Ta	0.70	1.42	0.54	0.86	0.85	0.94	1.18
Cd							
Zr		390.00		367.80	234.10		199.00
Y							
Nb							
Co						27.6	19.5
Ti						6130	7410
V						135	149
Mg#	0.19	0.30	0.30	0.22	0.22	0.33	0.27

	Hidden Valley volcanics: continued		Mount Hanna andesite					
Sample No.	Mc109	Mc116	Mc110	Mc111	Mc112	Mc113	Mc114	Mc115
SiO2	57.96	51.00	60.15	60.74	60.15	59.75	60.93	59.37
AL2O3	16.18	16.81	17.31	17.07	17.05	17.00	17.10	16.73
Fe2O3	8.07	10.29	6.51	6.79	6.73	6.90	6.53	6.61
CaO	5.72	9.22	3.88	3.98	4.08	4.06	3.84	4.10
MgO	3.38	5.08	1.87	1.72	1.62	1.84	1.61	1.81
Na2O	3.35	3.11	3.46	3.53	3.62	3.75	3.68	3.87
K2O	3.47	1.71	4.45	4.52	4.40	4.23	4.36	4.31
TiO2	1.15	1.38	0.60	0.61	0.62	0.59	0.57	0.57
MnO	0.16	0.17	0.16	0.16	0.16	0.16	0.16	0.15
P2O5	0.87	0.91	0.93	1.02	0.94	0.57	1.02	0.93
LOI	0.62	0.28	0.66	0.59	0.32	0.62	0.48	0.45
TOTAL	100.93	99.96	99.98	100.73	99.69	99.47	100.28	98.90
Trace elements in ppm								
La	72.30	40.00	89.10	89.10	89.70	90.00	94.80	91.40
Ce	143.0	76.20	173.0	170.0	172.0	163.0	171.0	171.0
Nd	48.60	35.30	65.50	74.80	57.60	82.50	72.20	69.80
Sm	9.12	6.56	10.00	10.60	9.96	10.90	11.50	10.90
Eu	2.42	1.84	2.57	2.51	2.71	2.45	2.57	2.62
Tb	1.18	0.88	1.09	1.08	0.95	1.17	1.02	0.94
Yb	1.78	2.60	2.53	2.65	2.37	2.61	2.78	2.46
Lu	0.31	0.41	0.32	0.29	0.32	0.42	0.43	0.43
U		1.13	1.99	3.22	2.90	2.59	3.81	2.40
Th	11.10	4.81	15.00	13.60	14.70	13.40	14.30	14.00
Cr	101.0	184.0	136.0	132.0	94.00	72.60	105.0	108.0
Hf	7.74	5.03	8.04	7.74	7.90	7.41	7.93	7.62
Ba	1100.0	724.0	1800	1990	1840	1990	1930	2020
Rb	95.80	24.90	112.0	95.20	85.30	71.60	85.70	94.90
Sr	1250.0	1410	2280	1920	2110	1830	1610	1700
Sc	13.60	24.90	6.47	6.20	6.65	6.15	5.99	6.35
Ta	1.32	0.56	0.88	0.75	0.79	0.92	0.83	0.84
Cd								
Zr	843.00	658.0	725.0	560.0	722.0	402.0	438.0	430.0
Y								
Nb								
Co	21.7	28.2	10.3	9.98	10.9	9.79	9.11	10.0
Ti	7100	7630	3950	3780	4480	4420	3610	3430
V	150	203	70.6	81.3	88.8	79.7	70.2	79.9
Mg#	0.26	0.30	0.20	0.18	0.17	0.19	0.17	0.19

Cinder Prospect member							
Sample No.	Mc59e	Mc78	Mc79	Mc117a	Mc121	Mc125	Mc126
SiO2	66.37	61.31	67.25	67.67	69.88	68.74	69.70
AL2O3	15.25	16.63	15.30	15.53	15.65	15.35	15.45
Fe2O3	3.36	5.71	3.30	3.45	3.00	3.05	3.11
CaO	2.08	3.39	1.10	2.07	1.63	1.67	1.21
MgO	0.99	1.38	0.55	0.55	0.48	0.40	0.44
Na2O	3.96	4.03	3.85	4.39	3.65	3.85	3.69
K2O	5.27	4.63	5.58	5.69	5.63	5.56	5.48
TiO2	0.16	0.45	0.13	0.11	0.11	0.10	0.10
MnO	0.16	0.16	0.16	0.17	0.16	0.17	0.16
P2O5	0.13	0.42	0.08	0.29	0.25	0.24	0.25
LOI	2.47	0.14	2.47	1.12	0.83	0.99	2.93
TOTAL	100.19	98.25	99.76	101.04	101.27	100.12	102.52
Trace elements in ppm							
La	116.0	88.40	123.0	121.0	129.0		
Ce	210.0	182.0	216.0	227.0	222.0		
Nd	83.50	60.10	77.90	88.20	101.00		
Sm	11.70	10.30	11.90	12.80	13.50		
Eu	2.45	2.86	2.55	2.46	2.47		
Tb	1.33	1.00	1.23	1.02	1.20		
Yb	3.09	2.41	3.16	3.05	3.57		
Lu	0.47	0.27	0.44	0.45	0.52		
U	4.92	3.08	5.12	5.77	4.98		
Th	21.70	15.50	21.50	22.40	21.90		
Cr	38.40	79.60	32.10	43.80			
Hf	8.67	9.07	8.61	8.53	8.60		
Ba	1450	1700	1840	1850	1780		
Rb	127.0	108.0	125.0	120.0	121.0		
Sr	801.0	1580	764.0	925.0	638.0		
Sc	4.82	5.41	4.76	5.00	4.55		
Ta	1.02	0.72	1.10	1.03	1.09		
Cd							
Zr	534.0	652.0	837.0	532.0	619.0		
Y							
Nb							
Co	1.22	6.6	0.82	1.02	0.73		
Ti	1020	3770	1230	4151	4637		
V	15.2	58.7					
Mg#	0.20	0.17	0.13	0.12	0.12	0.10	0.11

	Tuff of the Sloan volcanics				Center Mountain dacite			
Sample No.	Mc59a	Mc59b	Mc59c	Mc73	Mc59d	Mc120b	Mc130	Mc131
SiO2	69.76	64.87	64.26	68.58	68.06	67.67	68.43	68.06
AL2O3	15.08	15.09	15.12	14.56	15.94	15.67	15.52	15.48
Fe2O3	3.34	3.95	4.42	3.10	3.58	4.11	3.07	3.09
CaO	0.59	1.37	1.64	0.69	2.15	1.56	1.64	1.57
MgO	0.77	1.73	1.71	1.07	0.51	0.63	0.38	0.44
Na2O	4.32	3.73	3.92	4.62	3.75	3.70	3.51	3.86
K2O	5.91	5.90	4.56	5.84	5.47	5.37	5.65	5.73
TiO2	0.45	0.63	0.64	0.48	0.15	0.20	0.11	0.10
MnO	0.15	0.15	0.15	0.15	0.16	0.17	0.16	0.16
P2O5	0.10	0.19	0.20	0.23	0.28	0.35	0.21	0.16
LOI	0.61	1.30	2.99	0.82	1.04	0.85	1.03	1.10
TOTAL	101.08	98.91	99.62	100.14	101.09	100.28	99.71	99.75
Trace elements in ppm								
La	95.40	103.0	98.40	109.0	118.0	114.0		
Ce	183.0	192.0	185.0	216.0	217.0	206.0		
Nd	78.70	89.20	90.00	70.90	85.80	101.0		
Sm	11.90	13.20	12.50	13.70	12.20	12.00		
Eu	1.31	1.52	1.79	1.41	2.37	2.52		
Tb	1.19	1.60	1.40	1.27	1.10	0.94		
Yb	3.24	3.31	3.39	3.62	3.34	3.39		
Lu	0.55	0.50	0.44	0.57	0.48	0.46		
U	7.08	6.03	6.04	6.70	4.68	4.19		
Th	37.50	32.30	33.00	38.90	21.40	19.20		
Cr	58.70	47.80	66.40	21.60	31.00	27.70		
Hf	10.40	11.70	11.60	11.60	8.77	8.92		
Ba	271.0	380.0	497.0	366.0	1700	1810		
Rb	165.0	139.0	151.0	162.0	115.0	108.0	131.53	
Sr		364.0	670.0	155.0	784.0	800.0	535.83	
Sc	3.65	5.55	6.18	4.17	5.28	5.03		
Ta	2.38	2.36	2.02	2.91	1.08	1.05		
Cd								
Zr	560.0	701.0	693.0	833.0	577.0	540.0	347.44	
Y							12.16	
Nb								
Co	2.73	5.89	7.98	3.24	1.23	1.92		
Ti	3039	2820	2899	2950	4662	2300		
V	26.7	37.8	52.8	31.5	15.8	16.1		
Mg#	0.17	0.27	0.25	0.23	0.11	0.12		0.11

	Mount Ian andesite							
Sample No.	Mc72	Mc77	Mc83b	Mc84	Mc93	Mc94	Mc95a	Mc95b
SiO2	57.85	59.28	58.93	59.26	60.22	58.12	58.24	58.94
AL2O3	16.72	17.22	16.90	16.83	17.32	16.71	17.18	16.89
Fe2O3	7.14	7.08	6.56	6.82	7.87	7.34	6.97	7.76
CaO	4.24	4.15	3.93	4.00	4.31	4.22	4.36	4.09
MgO	1.81	1.84	1.91	1.54	1.94	1.95	2.13	1.56
Na2O	3.74	3.62	3.91	3.80	3.64	3.65	3.77	3.51
K2O	4.16	4.41	4.29	4.25	4.18	4.19	4.10	4.41
TiO2	0.60	0.61	0.59	0.62	0.66	0.63	0.64	0.64
MnO	0.16	0.16	0.16	0.16	0.16	0.16	0.16	0.16
P2O5	0.97	1.02	0.47	0.86	1.00	0.98	0.54	0.85
LOI	0.66	1.04	0.74	0.73	0.25	0.33	1.18	0.72
TOTAL	98.05	100.43	98.39	98.87	101.55	98.28	99.27	99.53
Trace elements in ppm								
La	86.70	85.60	88.20	92.20	86.30	88.40	89.20	
Ce	155.0	152.0	153.0	172.0	156.0	155.0	164.0	
Nd	81.70	73.70	69.10	74.70	82.60	89.40	69.00	
Sm	11.40	11.40	10.40	11.20	11.20	11.10	11.10	
Eu	2.56	2.52	2.37	2.73	2.76	2.68	2.83	
Tb	1.22	1.03	0.89	1.23	1.11	0.98	0.92	
Yb	2.51	1.88	2.16	2.78	2.34	2.22	2.26	
Lu	0.36	0.36	0.34	0.33	0.34	0.36	0.27	
U	2.66	3.79	1.72	3.54	3.43	4.66	2.28	
Th	13.00	11.60	12.80	14.20	12.80	11.80	12.80	
Cr	60.70	82.50	85.10	38.40	80.00	40.10	87.20	
Hf	6.96	6.73	7.08	8.06	7.25	7.26	7.60	
Ba	1970	1930	1650	1970	1990	2090	2070	
Rb	91.70	71.30	65.50	105.0	71.40	95.30	97.60	
Sr	1640	1580	1430	1790	1980	1810	2070	
Sc	5.75	5.67	5.68	6.36	6.20	5.90	6.13	
Ta	0.74	0.89	0.83	0.85	0.73	0.59	0.94	
Cd								
Zr	637.0	387.0	679.0	675.0	689.0	543.0	808.0	
Y								
Nb								
Co	10.4	10.5	9.25	10.3	11.4	10.4	10.9	
Ti	4130	4110	3540	3300	3970	4370	3790	
V	77.7	96.4	81.2	75.1	88.2	85	79.7	
Mg#	0.18	0.18	0.20	0.16	0.17	0.19	0.21	0.15

	Mount Ian andesite: continued			Mount Sutor dacite			
Sample No.	Mc97	Mc98	Mc120a	Mc21	Mc83a	Mc85	Mc96
SiO2	58.03	58.07	58.73	61.91	62.41	63.03	62.91
AL2O3	17.21	17.18	17.20	16.09	16.51	16.25	16.19
Fe2O3	7.19	7.14	7.77	5.71	5.48	5.85	5.14
CaO	4.30	4.43	4.17	3.13	2.45	3.20	2.44
MgO	1.92	2.16	1.72	1.34	1.16	1.15	1.20
Na2O	3.87	3.86	3.82	3.49	3.68	3.46	3.53
K2O	4.22	4.44	4.14	5.75	5.84	4.69	5.68
TiO2	0.64	0.69	0.62	0.39	0.43	0.58	0.43
MnO	0.16	0.16	0.16	0.17	0.16	0.16	0.16
P2O5	0.52	0.54	1.19	0.24	0.24	0.59	0.22
LOI	0.34	1.05	0.15	1.93	0.70	0.44	1.02
TOTAL	98.40	99.72	99.67	99.13	99.06	99.40	98.73
Trace elements in ppm							
La	85.60		81.40	118.0	115.0	111.0	119.0
Ce	159.0		149.0	220.0	219.0	199.0	210.0
Nd	59.00		62.60	112.0	87.80	112.0	120.0
Sm	11.20		10.40	14.70	13.30	14.50	14.60
Eu	2.77		2.46	3.34	3.41	3.30	3.22
Tb	1.12		0.98	1.46	1.61	1.60	2.11
Yb	2.18		2.01	4.43	3.88	3.91	3.92
Lu	0.40		0.40	0.60	0.53	0.56	0.65
U	2.86		2.94	4.75	2.57	3.63	3.67
Th	12.60		12.00	20.30	20.30	17.00	19.40
Cr	160.0		76.10	8.99	61.60	18.30	57.60
Hf	7.29		6.95	10.70	10.80	10.40	10.30
Ba	1900		1900	2180	1780	1950	1830
Rb	75.30		85.90	118.0	135.0	109.0	109.0
Sr	1990		1880	1480	1380	1530	1600
Sc	6.04		5.85	6.73	6.73	7.80	6.69
Ta	0.76		0.68	1.32	0.99	1.24	1.01
Cd							
Zr	645.0		670.0	681.0	697.0	833.0	580.0
Y							
Nb							
Co	11.2		10.6	2.76	3.30	3.56	2.82
Ti	3890		4330	3220	2630	3820	3220
V	88.3		79.2	24.2	24.4	34.6	23.8
Mg#	0.19	0.21	0.16	0.17	0.15	0.14	0.17

	Mount Sutor dacite: continued				Alkali basalt
Sample No.	Mc100	Mc118	Mc119	Mc128	Mc124
SiO2	61.67	62.29	64.96	66.55	51.04
AL2O3	16.19	16.43	16.44	15.84	14.92
Fe2O3	5.14	5.71	5.51	3.85	8.70
CaO	2.44	2.99	2.98	1.98	8.80
MgO	1.24	1.04	1.14	0.69	7.71
Na2O	3.84	3.56	3.64	3.53	3.32
K2O	5.51	5.17	5.27	5.33	2.56
TiO2	0.49	0.48	0.43	0.25	0.96
MnO	0.17	0.17	0.17	0.16	0.16
P2O5	0.25	0.50	0.31	0.35	1.13
LOI	0.50	0.74	0.64	1.83	1.19
TOTAL	97.44	99.08	101.49	100.36	100.49
Trace elements in ppm					
La	112.0	114.0	116.0		
Ce	215.0	231.0	216.0		
Nd	78.30	95.00	101.0		
Sm	13.20	14.50	14.80		
Eu	3.56	3.44	3.32		
Tb	1.60	1.67	1.57		
Yb	4.31	3.92	3.84		
Lu	0.54	0.57	0.64		
U	4.21	3.65	4.87		
Th	19.10	19.60	19.10		
Cr	80.80	29.80	40.20		
Hf	10.60	10.70	10.30		
Ba	1760	1800	1780		
Rb	120.0	135.0	109.0		
Sr	1460	1560	1310		
Sc	7.50	8.04	7.42		
Ta	0.99	1.10	1.13		
Cd					
Zr	844.0	602.0	732.0		
Y					
Nb					
Co	3.01	3.41	3.19		
Ti	3300	3790	3590		
V	32.0	23.1	19.2		
Mg#	0.17	0.14	0.15	0.13	0.43

APPENDIX C: CIPW NORMS

	Tuff of Bridge Spring														
Sample No.	ET-1	YT	92	R	T	V	M63	M105	Mc53	Mc60	Mc61	Mc62	Mc64a	Mc64b	Mc65
Q	25	28	21	20	18	18	15	9	10	11	13	17	17	19	20
or	31	28	30	34	29	29	35	37	36	34	36	35	28	38	28
ab	35	29	36	33	38	36	37	40	37	35	37	34	28	33	36
an	5	5	6	5	7	6	4	4	5	5	3	3	9	2	2
C	0	1	0	0	0	0	0	0	0	0	0	0	0	1	2
di	2	0	0	3	0	4	3	2	5	8	4	6	12	0	0
hy	1	2	3	0	3	0	2	4	3	1	3	0	0	4	5
wo	0	0	0	0	0	0	0	0	0	0	0	0	1	0	0
mt	1	1	1	1	2	1	1	1	2	2	2	1	2	2	2
il	1	1	1	1	1	1	1	1	1	1	1	1	1	1	1
ap	0	0	0	0	0	0	0	0	0	0	0	0	1	0	0
ol	0	0	0	0	0	0	0	0	0	0	0	0	0	0	0
hem	0	0	0	0	0	0	0	0	0	0	0	0	0	0	0

	Tuff of Bridge Spring: continued					Hidden Valley volcanics									
Sample No.	Mc66	Mc67	Mc68	Mc69	Mc71	65	66	68	125	M24	M27	M35	M57	M58	Mc87
Q	15	16	13	17	17	0	0	0	2	7	7	5	8	16	2
or	34	35	34	35	36	8	10	18	11	23	32	11	31	36	14
ab	32	37	35	37	38	22	22	23	23	37	32	36	31	38	31
an	6	3	3	3	3	30	24	23	28	18	12	20	16	4	20
C	0	0	0	0	0	0	0	0	0	0	0	0	0	0	0
di	9	4	8	4	0	16	17	13	10	1	5	10	0	2	8
hy	0	2	0	2	3	0	14	14	16	5	4	6	5	1	17
wo	1	0	1	0	0	0	0	0	0	0	0	0	0	0	0
mt	2	2	2	2	2	4	4	4	5	0	0	0	0	0	4
il	2	1	1	1	1	3	3	2	3	0	0	0	0	0	2
ap	1	0	0	0	0	2	1	2	1	2	1	0	1	0	1
ol	0	0	0	0	0	13	2	0	0	0	0	0	0	0	0
hem	0	0	0	0	0	0	0	0	0	7	5	8	6	3	0

	H. V. volcanics: cont.			Mount Hanna andesite						Cinder Prospect member		
Sample No.	Mc108	Mc109	Mc116	Mc110	Mc111	Mc112	Mc113	Mc114	Mc115	Mc59e	Mc78	Mc79
Q	8	13	0	12	12	10	9	12	9	16	10	19
or	21	21	10	26	27	26	25	26	25	31	27	33
ab	29	29	26	29	30	31	32	31	33	34	34	33
an	18	18	27	13	13	14	16	12	14	8	14	5
C	0	0	0	2	2	1	0	2	0	0	0	1
di	2	2	11	0	0	0	0	0	0	1	0	0
hy	13	8	17	11	11	13	11	10	11	5	8	4
wo	0	0	0	0	0	0	0	0	0	0	0	0
mt	4	4	4	3	3	2	3	3	3	2	3	2
il	2	2	3	1	1	0	1	1	1	0	1	0
ap	2	3	2	2	2	2	1	2	2	0	1	0
ol	0	0	0	0	0	0	0	0	0	0	0	0
hem	0	0	0	0	0	0	0	0	0	0	0	0

	Cinder Prospect member: cont.				Tuff of the Sloan volcanics				Center Mountain dacite			
Sample No.	Mc117a	Mc121	Mc125	Mc126	Mc59a	Mc59b	Mc59c	Mc73	Mc59d	Mc120b	Mc130	Mc131
Q	15	22	20	23	17	14	17	12	19	21	22	19
or	34	33	33	32	35	35	27	35	32	32	33	34
ab	37	31	33	31	37	32	33	41	33	31	30	33
an	6	6	7	4	2	6	7	1	9	5	7	7
C	0	1	1	2	1	1	1	0	0	2	1	0
di	2	0	0	0	0	0	0	2	0	0	0	0
hy	4	4	4	4	8	7	8	5	5	5	4	4
wo	0	0	0	0	0	0	0	0	0	0	0	0
mt	2	2	2	2	0	2	2	2	2	2	2	2
il	0	0	0	0	1	1	1	1	0	0	0	0
ap	1	1	1	1	0	0	0	0	1	1	0	0
ol	0	0	0	0	0	0	0	0	0	0	0	0
hem	0	0	0	0	0	0	0	0	0	0	0	0

	Mount Ian andesite										
Sample No.	Mc72	Mc77	Mc83b	Mc84	Mc93	Mc94	Mc95a	Mc95b	Mc97	Mc98	Mc120a
Q	8	3	7	6	3	4	7	8	5	5	9
or	25	26	25	25	25	25	24	26	25	26	24
ab	32	33	33	33	31	32	32	30	34	33	32
an	15	15	16	16	16	17	18	13	17	16	13
C	1	0	0	0	0	0	0	1	0	0	2
di	0	2	0	1	2	1	0	0	1	2	0
hy	12	11	11	11	12	13	12	12	11	11	13
wo	0	0	0	0	0	0	0	0	0	0	0
mt	3	3	3	3	3	3	3	3	3	3	3
il	1	1	1	1	1	1	1	1	1	1	1
ap	2	1	1	1	1	1	1	2	1	1	3
ol	0	0	0	0	0	0	0	0	0	0	0
hem	0	0	0	0	0	0	0	0	0	0	0

	Mount Sutor dacite								Alkali basalt
Sample No.	Mc21	Mc83a	Mc85	Mc96	Mc100	Mc118	Mc119	Mc128	Mc124
Q	10	10	16	12	9	13	14	20	0
or	34	35	28	34	33	31	31	32	15
ab	30	31	29	30	32	30	31	33	28
an	11	11	12	11	12	12	13	7	18
C	0	0	1	0	0	1	0	1	0
di	2	0	0	0	1	0	0	0	15
hy	6	8	8	7	7	8	8	4	2
wo	0	0	0	0	0	0	0	0	0
mt	3	3	3	3	3	3	3	2	4
il	1	1	1	1	1	1	1	0	2
ap	1	1	1	1	1	1	1	1	3
ol	0	0	0	0	0	0	0	0	14
hem	0	0	0	0	0	0	0	0	0

APPENDIX D: ROCK MODES

	Tuff of Bridge Spring									Hidden Valley volcanics				
Sample number	Mc53	Mc60	Mc62	Mc64b	Mc66	Mc67	Mc68	Mc69	Mc71	Mc1	Mc3a	Mc35	Mc37	Mc40b
Plagioclase	3.4	1.5	2.8	0.8	1.2	2.0	1.4	5.0	3.0			2.2	1.0	3.3
Olivine										0.6		9.8	7.6	6.3
Biotite	3.4	0.6	1.0	1.8	1.6		1.4	0.4	1.6					
Orthopyroxene														
Clinopyroxene	0.8	0.2	0.4	0.2	0.8	0.2	0.8	0.4	1.6	0.3	1.0	0.8	1.4	
Fe-Ti oxides	0.2	Trace	Trace	Trace	Trace	Trace	0.4	0.6	Trace					
Groundmass	56.2	86.0	87.2	86.0	83.0	79.4	69.8	83.6	67.4	88.1	90.8	84.0	82.8	78.5
Sanidine	24.2	7.5	4.2	6.0	5.4	10.4	4.8	7.0	10.6					
Phlogopite														
Zircon	Trace	Trace	Trace	Trace	Trace	Trace	Trace	Trace	Trace					
Sphene	0.4	0.4	0.6	0.2	0.4	Trace	Trace	0.6	0.4					
Hornblende														
Monazite														
Epidote														
Allanite														
Quartz	0.6	0.8	1.2	1.0	1.0	0.8	0.4	1.2	1.4			0.6	6.0	2.6
Calcite						Trace								
Pumice	9.6	2.2	1.4	2.2	3.4	Trace	11.4	0.2	12.0					
Rock xenoliths	1.2	0.8	1.2	1.8	3.0	7.2	9.6	1.0	2.0					
Vesicles										11.0	8.2	2.6	1.2	9.3

	Hidden Valley volcanics: continued							Mount Hanna andesite				Cinder Prospect member		
Sample number	Mc42	Mc43	Mc47	Mc48	Mc87	Mc108	W-Hvb	Mc31b	Mc110	Mc112	Mc115	Mc25	Mc78	Mc79
Plagioclase	1.0	1.0	0.4		1.8	13.2	18.4	Trace	Trace	Trace	Trace	3.6	10.4	17.4
Olivine		6.0	0.4	1.2		1.4	11.4							
Biotite												0.4	4.0	3.6
Orthopyroxene														
Clinopyroxene	4.0	10.0	10.8	4.6		1.6	9.6							Trace
Fe-Ti oxides							0.5					0.8		1.2
Groundmass	91.4	79.6	76.6	79.0	98.2	65.6	58.5	100.0	100.0	100.0	100.0	69.4	85.2	74.0
Sanidine														3.8
Phlogopite			3.6	4.8										
Zircon												Trace		Trace
Sphene														
Hornblende														
Monazite														
Epidote														
Allanite														
Quartz														
Calcite												25.8		
Pumice														
Rock xenoliths														Trace
Vesicles	3.6	3.4	8.2	10.4		18.2	1.6						0.4	

	Cinder Prospect member: cont.		Tuff of the Sloan volcanics				Center Mtn. dacite			Mount Sutor dacite				
Sample number	Mc121	Mc125	Mc59a	Mc59b	Mc59c	Mc73	Mc59d	Mc130	Mc131	Mc9	Mc116	Mc19	Mc21	Mc27
Plagioclase	8.2	6.6	4.8	2.0	2.4	3.4	4.0	4.4	7.2	7.4	8.8	7.2	13.6	13.0
Olivine														
Biotite	1.8	3.6	0.4	0.8	0.4	0.6	1.4	1.2	1.6	3.2	1.4	2.2	3.4	5.4
Orthopyroxene											1.6	1.2		
Clinopyroxene			Trace	0.4	1.4	Trace							Trace	2.0
Fe-Ti oxides		0.4			1.4	0.2		0.4		0.8	0.4	1.2	1.0	1.6
Groundmass	83.6	84.0	60.6	76.6	52.6	77.8	94.6	89.0	88.6	88.0	87.8	76.4	78.2	76.4
Sanidine			21.2	4.8	8.6	10.0								
Phlogopite														
Zircon		Trace	Trace	Trace		Trace				Trace				
Sphene			0.2	Trace		Trace								
Hornblende														0.4
Monazite			Trace											
Epidote			Trace											
Allanite			Trace											
Quartz					0.4	1.8								
Calcite	6.4	5.4						5.0	1.2					
Pumice			9.0	2.2	11.6	1.6								
Rock xenoliths			3.8	13.2	21.2	4.6								
Vesicles									1.4	0.6		11.8	3.8	1.2

Mount Sutor dacite: continued									
Sample number	Mc28	Mc31a	Mc91a	Mc92	Mc96	Mc100	Mc118	Mc119	Mc128
Plagioclase	14.8	8.6	4.2	6.8	8.8	11.0	11.4	7.4	3.0
Olivine									
Biotite	3.2	2.6	2.0	1.8	3.6	3.2	5.4	9.4	2.6
Orthopyroxene				1.7					
Clinopyroxene	Trace	0.4			0.4	0.6	Trace		
Fe-Ti oxides	1.4		0.4	0.8	0.6			0.8	Trace
Groundmass	80.6	87.6	93.4	88.9	82.6	81.4	83.2	81.0	90.8
Sanidine									
Phlogopite									
Zircon			Trace						
Sphene									
Hornblende									
Monazite									
Epidote									
Allanite									
Quartz									
Calcite		0.8						1.4	
Pumice									
Rock xenoliths									
Vesicles					4.0	3.8			3.6